Fall 2008

Synthesis and properties of poly(itaconic acid)

Ming Cao
University of New Hampshire, Durham

NOTE TO USERS

SYNTHESIS AND PROPERITES OF POLY(ITACONIC ACID)

BY

Ming Cao

Bachelor of Engineering, East China University of Science and Technology (China),

2005

THESIS

Submitted to the University of New Hampshire

In Partial Fulfillment of

The Requirement for the Degree of

Master of Science

In

Materials Science

September, 2008

This thesis has been examined and approved.

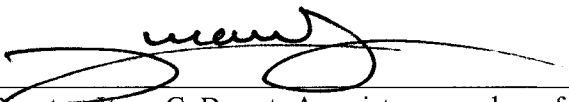

Thesis Director, Yvon G. Durant, Associate research professor of Materials Science

Donald C. Sundberg, Professor of Materials Science

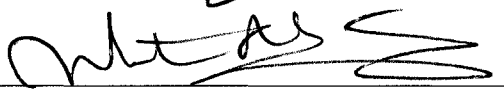

Weihua Ming, Associate research professor of Materials Science

8/14/2008

Date

ACKNOWLEDGEMENTS

I should thank my advisor professor Yvon Durant for his excellent advice and support on research. The research projects I did at the Nanostructured Polymers Research Center under his supervision made me improve much of my research skills. I sincerely appreciated that he provided me the great opportunities to work on these exciting research projects.

I was lucky to take the courses that Professor Don Sundberg taught at UNH. With these courses, I built a solid background in polymer, which really helped me to overcome the challenges I met in my research. He is one of the best professors I have ever met. Professor Weihua Ming helped me correcting several ideas in project.

I want to thank all the NPRC members, Zac, John, Pooja, Brian, Mousoumi, Diana, Marine, Anne, Prashant for his help on analysis of NMR, Zakaria for his help on GPC. I enjoy their friendship and working with them.

We thank the Environmental Protection Agency and the New England Green Chemistry Consortium for their financial support.

FORWARD

志之所趋，

无远弗届；

穷山距海，

不能限也。

志之所向，

无坚不入；

锐兵精甲，

不能御也。

《格言联壁》

TABLE OF CONTENTS

LIST OF FIGURES

LIST OF TABLES

SYNTHESIS AND PROPERTIES OF POLY(ITACONIC ACID)

by

Ming Cao

University of New Hampshire, September, 2008

Abstract: Previously, itaconic acid (IA) was known to be at best a difficult monomer to be polymerized. Here we report effective conditions for an easy polymerization of itaconic acid to high conversion and high molecular weight. tert-Butyl Hydroperoxide (tBHP) was used as an efficient initiator for solution polymerization of IA. Conversions higher than 90% can be reached in less than 1hr. Molecular weights of poly(itaconic acid) have been analyzed in GPC. The structure of PIA was studied by ^{1}H-NMR, ^{13}C-NMR. The initiator concentration dependence and monomer concentration effect have been investigated.

Based on the polymerization process of itaconic acid, a simple process to prepare biodegradable non-starch superabsorbents from renewable resource was developed. The hydrogel was prepared by free-radical polymerization of half neutralized itaconic acid in aqueous solution using tetra(ethylene glycol) diacrylate (tEGDA) as crosslinker. Biodegradation of polyitaconic acid and polyitaconic superabsorbent were studied by Biological Oxygen Demand (BOD) measurement.

Keywords: polyitaconic acid; polymerization; tert-Butyl Hydroperoxide; molecular weight; molecular structure; superabsorbent; swelling capacity; biodegradation

CHAPTER I

REVIEW

1.1 Itaconic acid

Itaconic acid (IA), called methylenesuccinic acid, is one of the three acids obtained by the distillation of citric acid. [1] Citric acid is a natural preservative acting as an antioxidant. It is an important intermediate in the citric acid cycle of metabolism. [2, 3] The other two acids formed from the distillation are citraconic acid and mesaconic acid which are two isomers of itaconic acid. In this thesis, we provide evidence for the transition between these three acids during heating.

In 1837, Itaconic acid was discovered by Baup as a thermal decomposition product of citric acid. [4] In 1932, the biosynthesis by fungi from carbohydrates was first reported by Kinoshita who isolated itaconic acid from the growth medium of an osmophilic fungus, Aspergillus itaconicus. [2, 3] In 1952, C.E. Schildknecht reported that itaconic acid can not homopolymerize. This conclusion has been later proved wrong. In 1966, the prominent developments in itaconic acid production (batch fermentation, free suspended biomass) took place, so that the large scale production of low cost IA was made possible. [5]

There are two carboxylic groups in the itaconic acid molecule, which has structure similarities with acrylic acid. The melting point of IA was reported to be around 165°C. Acidified IA can be dissolved in alcohol, water and acetone. Until now, the applications of itaconic acid have been limited to its monomer, copolymer and oligomer.[6, 7] There is no commercial application for the homopolymer of itaconic acid because of the difficulty to prepare it. IA monomer and its ester have been used

as additive for producing cation exchange resin. IA itself can be used as fragrance agent. Mixture of IA and aromatic diamine are good additive for lubricant, herbicide. [8] 1% to 5% itaconic acid and styrene copolymer are used for carpet coating and bookcover. IA improves properties such as water proof and anticorrosion. [9] Itaconic acid is used as a third co-monomer in acrylonitrile fiber. It helps the fibers to absorbe dyes. Acrylic acid and itaconic acid copolymer emulsion are excellent adhesive for fiber products. [10] Also, teeth adhesives made from acrylic acid and itaconic acid have good compression resistance. [11] Copolymer of acrylic acid and itaconic acid can also be used as detergent. Lens or artificial gems made with itaconic acid copolymer have special luster. [12]

1.2 Existing process for polyitaconic acid

The polymerization of itaconic acid has been studied previously by a number of researchers. Most of the research on itaconic acid has been focused on copolymers such as poly(acrylic acid-co-itaconic acid),[13-17] poly(itaconic acid-co-acrylamide),[15, 17-20] poly(acrylonitrile-co-itaconic acid)[13, 21-25], etc. Only few homopolymerization processes for IA has been reported in the past.

The solution polymerization of acidified itaconic acid has been reported. The first homopolymerization of polyitaconic acid was described by Marvel and Shepherd in 1959.[26, 27] The conversion was 35% achieved in 68 hours at 50°C in acid conditions [28, 29] using persulfate initiation. Seigou Kawaguchi repeated the experiment by Marvel and Shepherd at 60°C for 3 days, and the conversion was 10%. [26, 27] Evangelia Grespos, etc. [30] described a polymerization process for acidified itaconic acid using $K_2S_2O_8$ as initiator at 25°C for 4 days, 50% conversion was reached. The structure of PIA was analyzed by ^{13}NMR. David Stawski, etc. [31]

described another process for acidified IA with persulphate ammonium as initiator at 60°C for 30 hrs. Conversion was 16%.

In the recent years, the solution polymerization process has been improved. High conversion can be reached in polymerization of neutralized itaconic acid. In the paper written by Nakamoto, Ogo and Imoto,[32] they described radical polymerization of itaconic acid in various solvents under high pressure with about 50% of monomer remaining in the product. US patent No. 5,223,592 describes a high conversion polymerization process using neutralized itaconic acid with a large amount of sodium persulfate to obtain an oligomer with molecular weight of about 2000 g/mol. Swift and Graham [33] described a high conversion polymerization process with 50 wt% hydrogen peroxide of the total monomer. US patent No. 5,336,744 described a 100% conversion polymerization process with large quantity of hydrogen peroxide with metal salts as redox initator system. The molecular weights of the final polyitaconic acid are less than 2000g/mol.

Alternatively, polyitaconic acid can be obtained from polyitaconate esters or polyitaconic acid anhydride. US patent No. 2,294,226 describes the polymerization of dimethyl itaconate as the dipotassium salt by refluxing it with alcoholic potassium hydroxide, and subsequently hydrolyzing it to produce polyitaconic acid. Stefan Polowinski and David Stawski obtained polyitaconic acid anhydride (PIAn) at 60°C in 16 hrs with AIBN as initiator. Then they obtained PIA by hydrolysizing the PIAn. The conversion for PIAn or PIA was not reported. Kenji Yokota did the same experiment, and the conversion for PIAn was 70%.

Anti Y. Sankhe used atom transfer radical polymerization (ATRP) [34] to prepared PIA layer with initiator molecules of 4-(chloromethyl)-benzoylchloride.

1.3 Decarboxylation of itaconic acid during preparation

In the early studies on the polyitaconic acid, IR absorptions [35-40] showed that a series of chain transfer reactions took place during polymerization and that decarboxylation occurred when drying dramatically. In addition, the evolution of CO_2 [28, 29, 41-43] was observed during both the polymerization and drying, which proved that a complex polymer chain structure of the product was being formed. It was used to explain the low yield of the product and the need for extended polymerization times to reach a certain molecular weight and conversion.

1.4 Itaconate superabsorbent

In order to produce superabsorbents (SAPs) from itaconic acid, two major difficulties need to be overcome. Itaconic acid is a very sluggish monomer to be polymerized because of the steric hindrance in the molecule blocking the attack of radical. Now, even though there are several processes of polymerization of itaconic acid reported, two major problems obviously block the possibility to prepare superabsorbent from itaconic acid. 1. Low conversion, and 2. Low molecular weight. Low crosslink density polyitaconic acid can be prepared only if these two difficulties in polymerization of linear PIA are overcome. No attempts at making itaconic superabsorbent has been reported before.

1.5 Existing Commercial Superabsorbent

Before superabsorbents were invented, cotton, paper and sponge were used as absorbent materials[44]. They can absorb up to 20 times their own weight of liquid, with poor retention under pressure. Superabsorbents can overcome these problems.

Superabsorbents [45-52] are low crosslink density polymers which can absorb

and hold water hundreds of times under load.

There are many applications for superabsorbents [53-61]. They can be wrapped inside the communication cables and used to absorb the water from the atmosphere, so that they will protect the communication cables. SAPs are used in food absorption pads to absorb blood, in order to keep the food package clean. Above 90% superabsorbent are used in baby diapers. All the commercial superabsorbents have the problem of lower absorbency rate compared with traditional absorbent materials, so it requires other traditional absorbent materials to be combined in the product to increase the absorbency rate. For example, fluffy pulp was combined with SAP beads for absorbent layer in the diapers[46-48, 62, 63].

There are two problems for the superabsorbent we currently use.[62, 64-70] Most products containing superabsorbents, such as baby diapers and feminine napkins, are disposable. More than 95% of superabsorbents are made from polyacrylic acid, which are not biodegradable. 1.5-2.0% of total landfill solid waste in the US is attributed to disposable diapers, which obviously increases the burden on the environment. Moreover, Polyacrylic acid is derived from petroleum. Petroleum will be exhausted one day.

1.5.1 Acrylate Superabsorbent

The majority of commercial superabsorbents are made from polyacrylic acid. Nowadays, Polysodium acrylate is the most economical superabsorbent for commercial applications. The industrial process for producing acrylate superabsorbent is relatively simple. However, acrylate superabsorbent can only be applied to water or low concentration water solution. The absorbency of ionic superabsorbent is sensitive

to ions present in the water solutions. The swelling capacity of this kind of absorbents decreases rapidly with the ion concentration in water. The swelling rate is slower than the traditional absorbent materials such as cotton and paper.

To overcome the shortcoming of acrylate absorbents, non-ionic absorbents such as crosslinked polyvinyl alcohol [71] have been produced. The absorbency rates (the speed at with the superabsorbent absorb liquid) of these absorbents are relatively high, and is independent to the ion concentration in solution, but the absorbency capabilities are much lower than acrylate absorbents.

1.5.2. Superabsorbent from natural sources

Also, superabsorbents can be made from grafted natural macromoleculars such as starch and cellulose. The advantages of these superabsorbents is their biodegradablility. However, their applications are limited due to their high cost associated with a complex production process.

Starch - acrylonitrile graft copolymer[50, 72-74] was the first superabsorbent in the world. The absorbents ratio can reach up to 3000 times. The swelling capacity can be increased by grafting different acrylic monomer such as methacrylic acid and acrylamide.

Grafted cellulose can be used to improve the absorbency of synthetic fibers. The swelling rate can reach hundreds of times, which is relatively low.

1.5.3 Synthetic process of existing Superabsorbent

In general, polyacrylate superabsorbents are prepared by radical polymerization with in a solution or inverse suspension polymerization process.

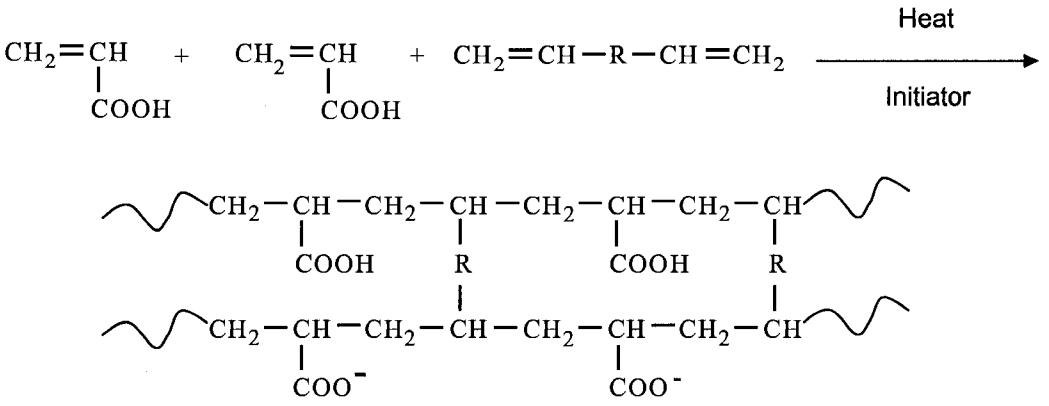

Figure 1 General Polymerization Process of acrylate superabsorbents. R represents the group between the two functional double bonds

Figure 1 shows the general polymerization process of acrylate superabsorbents. Water soluble initiate such as KPS, H_2O_2 and redox initiators such as H_2O_2-ferrous sulphate, KPS -sodium bisulphate are used. Temperature of reaction is between 20 and 80°C. In order to get a high molecular weight, a lower temperature is required. The ratio of neutralization is between 60 and 90%, If higher than 90%, then it is difficult to obtain a crosslinked polymer.

1.5.4. Physics of Superabsorbent

The superabsorbent swells in water according to the following steps: the charged groups of the polymer form hydrogen bonds with the water from the surroundings. The electrostatic repulsion between charged groups provides more room for water to come in. The driving forces for the liquid mobility are the Gibbs-Donnan effect (Osmotic pressure experiment with semi-permeable membrane, it is the behavior of charged particles near a semi-permeable membrane to fail to evenly distribute across the two sides of the membrane) [75] and the free energy of mixing of the solvent and polymer. The equilibrium is achieved when the ionic and dissociation effect is balanced by the elastic response of the network.

The chemical potential [76, 77] is the combination of the three contribution $\Pi=\pi_{mix}+\pi_{net}+\pi_{ion}$

Where π_{mix} is the free energy of mixing andπ_{net} is the elastic response andπ_{ion} is the free energy of ion effect

1.5.5 Swelling properties model from Flory's theory

The relation between swelling ratio Q and crosslinker density can be derived from Flory's solution theory and Flory's elasticity gel theory.[78-80]

In the swelling process, the free energy change of the system can be considered as two parts: the mixing of the gel and the solvent ΔG_m, and the elastic response of the network ΔG_{el}. [81, 82]

$$\Delta G = \Delta G_m + \Delta G_{el}$$

From Flory-Huggins solution theory and Flory's elasticity gel theory: [83]

$$Q_m^{5/3} = [(i/2v_2S^{1/2})^2 + (1/2 - \chi_1)/v_1]/(v_c/V_0)$$

Where V2 is the volume of the system. V_1 is the molar volume of water. φ_2 is the volume fraction of the polymer inside the swollen gel, ρ_2 is the density of polymer. Mc is the molecular weight between crosslinks. X is the Flory-Huggins parameter, representing the affinity of the solvent for the polymer. Where $(1/2-\chi_1)/v_1$ is the affinity between polymer and solution, and v_c/V_0 is the crosslink density, V_0 is the total volume of the system. i/v_2 is the concentration of fixed charge, S is the ionic strength.

In the equation above, the swelling capacity of superabsorbent increases with molecular weight between crosslinks Mc, and has a negative relation with the affinity

between the liquid and the polymer molecule χ. [78, 79, 84]

1.5.6 Environmental Concern

The pollution caused by plastics or rubber products is more and more serious in the United States.[85-87] The "one-time use" diaper or feminine napkins contain non-degradable polymeric parts, with a negative impact on the environment. Composting the acrylate superabsorbents requires hundreds of years to degrade, and produces a series of toxics during this period. [88] The itaconate superabsorbent provides the potential to solve these problems above. Over 90% of superabsorbent products are disposable. According to reports from Sanders, 2001, 18 billion disposable diapers are used per year in the US alone, 3.4 billion gallons of oil is needed annually to manufacture them [78, 89]. In one infant's lifetime, approximately 8,000-10,000 disposable diapers is used. Each one of those diapers takes approximately 500 years to degrade in a landfill. [90] In the late 1980s bans or taxes on disposable diapers were being considered in at least 20 states.[91, 92]

However, we have biodegradable superabsorbents made from grafted starch,[72, 86, 93-99] which was actually the first superabsorbent. However, the process of preparing grafted starch is too complex and time-consuming, limiting its large scale commercial applications.

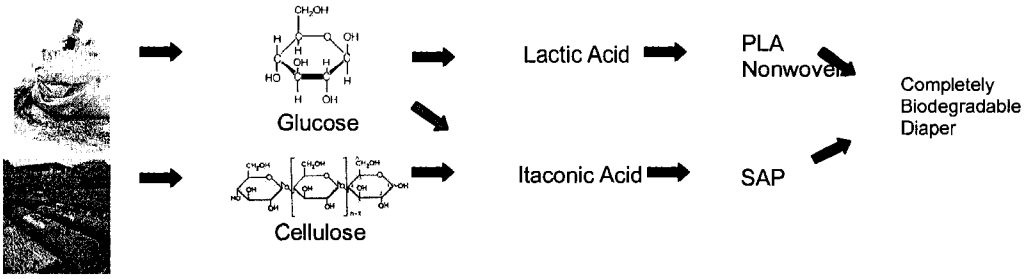

Figure 2 Future process for completely biodegradable diapers.

From the literature review above, there are several major problems which have held back the industrial applications of homopolymerization of IA and copolymers with a high percentage of IA. Namely: limited conversion in the final products, very long polymerization times, and low molecular weights. The purification of polyitaconic acid from itaconic acid is difficult. It is particularly interesting for the process we report here, that it can reach 100% conversion. Additionally, polymerization times in excess of one day are not acceptable for cost efficient considerations. The applications are not limited to oligomers due to the efficient process with low molecular weight available currently. The oligomers can be widely used as dispersant agent in industrial applications of paint, printing inks. The novel simple synthesis process we developed resolves these issues. Itaconic acid was proved to be capable of reacting as efficiently as acrylic acid, and the kinetics related to the synthesis process have been studied.

With the efficient process for the homopolymerization of itaconic acid reported in the thesis, we expected the application of homopolymer of itaconic acid will expend. Since the price of itaconic acid is similar to that of acrylic acid, the price of polyitaconic acid should be affordable. Also, with the fast increase in the demand for itaconic acid monomer, a decrease of its price is expected, which is important for the future development of homopolymers of itaconic acid.

CHAPTER II

POLYMERIZATION PROCESS OF ITACONIC ACID

2.1 Experimental

2.1.1 Materials

Itaconic Acid (IA) (99%+, Aldrich); Sodium hydroxide (Acros Organics), Tertiary Butyl hydroperoxide (tBHP) (Aldrich) were used without further purification.

2.1.2 Synthesis method

A typical batch polymerization process was applied. Itaconic acid was half neutralized with NaOH in DI-water with cooling by ice water, forming a concentrated solution, which was deoxygenized by purging with N_2, and then heated to the reaction temperature. It takes 30±15 minutes to reach the reaction temperature. 70wt% tBHP water solution was injected to start the polymerization. we used tBHP as a high temperature thermal initiator (228 hours half life at 100°C, 10 hours half life in benzene at 170°C according to Aldrich catalogue) to try to achieve a high yield of PIA. The half life is much less in the Itaconic acid water solution than that in pure water, since the acid itself is catalyst for thermodissociation of tBHP. Itaconic acid combined with tBHP is a redox initiator system here. With a similar process, we used initiators such as AIBN and persulfate and obtained unsatisfactory results. Figure 3 shows the image of a final sample in aluminum pan. Figure 4 shows the polymerization process of itaconic acid. All the samples we prepared in this chapter were shown in table 1.

One typical temperature control of the reactions is shown in Figure 5. At the beginning half an hour, a heat kick was observed due to the heat generated by the polymerization reaction. The temperature of the oil bath was always 3 to 5 degree above the temperature in the reactor. The reactant solution becomes viscous with the polymerization time. At the end of the reaction, samples are packaged and cooled down.

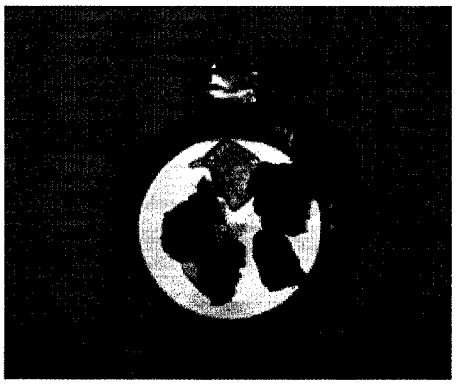

Figure 3 PIA by solution polymerization

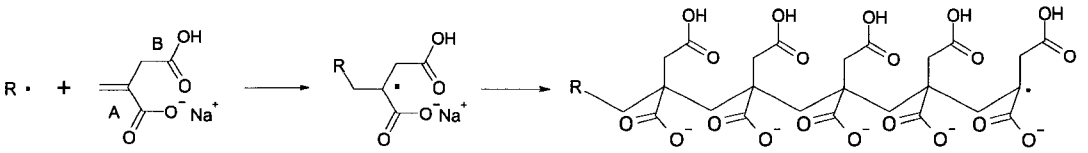

Figure 4, Reaction equation of polymerization of half neutralized itaconic acid

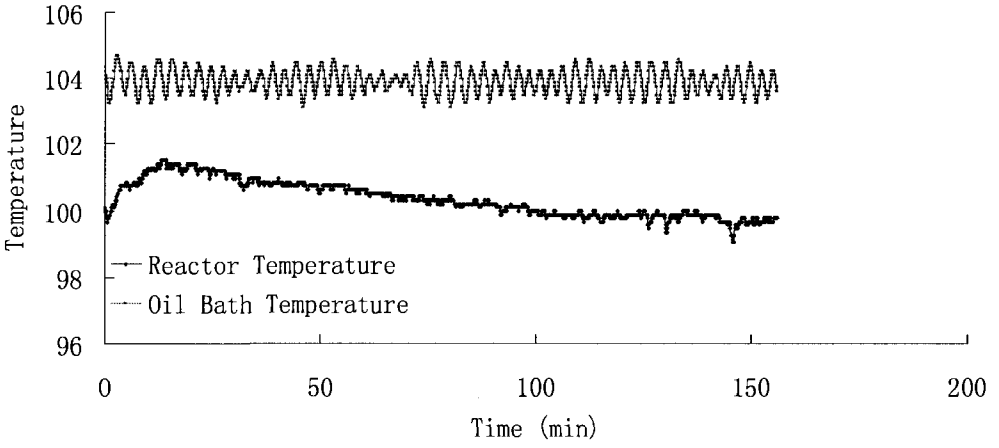

Figure 5 Temperature Control of PIA-9

Sample No.	IA (g)	NaOH (g)	DI-H2O (ml)	tBHP(70%) (ml)	Temp.(°C)	Reaction time (hrs)
PIA-1	100.19	31.42	50	0.625	100±2	2.5
PIA-2	100.21	30.77	50	0.5	100±2	4
PIA-3	100.24	30.79	50	0.1	100±2	2
PIA-4	100.02	30.86	50	2	100±2	2
PIA-5	100.21	30.82	100	0.5	100±2	2
PIA-6	100.09	30.79	30	0.5	100±2	2
PIA-7	100.73	0	50	0.5	100±2	2.5
PIA-8	100.33	18.55	50	0.5	100±2	2.5
PIA-9	100.15	43.07	50	0.5	100±2	2.5
PIA-10	100.15	61.54	50	0.5	100±2	2.5
PIA-11	100.31	30.8	50	0.5	70±2	1.5
PIA-12	100.44	30.87	50	0.5	80±2	1
PIA-13	100.24	30.89	50	0.5	90±2	0.5

Table 1 Recipe of polymerization of poly(itaconic acid)

2.1.3 Conversion ratio calculation- ^{1}H-NMR analysis

^{1}H-NMR and ^{13}C-NMR spectra were obtained with a 400MHz Varian NMR spectrometer at 25 °C in D_2O.

Figure 6 shows the ^{1}H-NMR spectra for the neutralized itaconic acid samples. Itaconic acid monomer spectra can be found in figure 7. The two sharp peaks around 5.4 and 5.7ppm represent the protons in group CH_2= and the sharp peak around 3.0 ppm represents CH_2- in the side groups of the unreacted itaconic acid. The biggest peak around 4.7 ppm is for H_2O remaining in the sample and also present in the D_2O solvent.

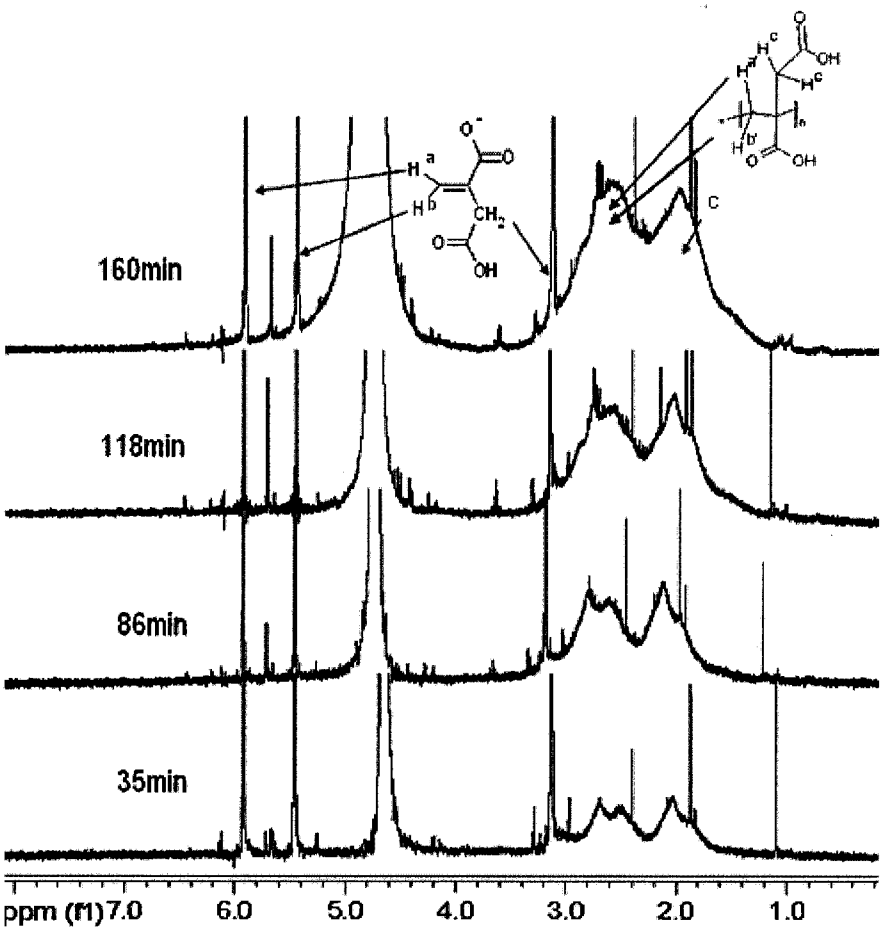

Figure 6 The ^{1}H-NMR spectra of the polymerization of itaconic acid at four separate times with [M]=6.20 mol/l (PIA-2)

^{1}H-NMR was used to calculate the conversion ratio of the polymerization of itaconic acid. Figure 6 shows the ^{1}H-NMR spectra for samples at certain polymerization time. In addition to the peaks for itaconic acid monomer, another two distinct broad peaks with similar integrals around 2.7 and 2.0ppm describe the CH_2- in side group and backbone of PIA separately. The conversion is equal to half of the areas of CH_2- in side group and backbone divided by areas of two vinyl groups. With the increase in polymerization time, the conversion of the monomer increases as seen in figure 6 by the reduction in the peaks at 5.4 and 5.7ppm, with the increase of the broad peak at 2-3ppm..

$$Conversion = \frac{\frac{1}{2}\int H_{a'} + H_{b'} + H_c}{\int H_a + H_b + \frac{1}{2}\int H_{a'} + H_{b'} + H_c}$$

2.1.4 Reaction kinetics Study with Reaction Calorimeter

A reaction Calorimeter is an instrument which can detect the heat flow vs reaction time during a chemical reaction. A 250ml flat bottom reaction calorimeter reactor equipped with thermometer, pressure guage and mechanical stirring was immersed into 15 L of water or ethylene glycol for providing a constant temperature surrounding.

For our experiments, we used a Reaction Calorimeter CPA2000. Ethylene Glycol was used as thermostatting liquid (Temperature range from 70 to 200°C), in order to provide fast heat transfer because of its low viscosity. For each experiment, final conversion was measured by NMR as previously described on the final product. The stirring speed was set at 500 rpm. Pressure during the reaction was always one

atmosphere.

The final report from reaction calorimeter was a curve of heat flow (KJ) during reaction VS polymerization time. The heat, Q, is generated from polymerization, which has a linear relation with the conversion of monomer. Combining the information, a plot for conversion ratio VS reaction time can be obtained. In addition, polymerization enthalpy can be obtained from the reaction heat and the relative conversion. The value of enthalpy of the reaction ΔHp can be deduced:

$$\Delta Hp = \frac{\int Qdt}{0.77P}$$

Here P is the conversion of monomer. 0.77 is the number of moles of monomer we used in all our samples.

Unfortunately, reaction calorimeter only gives us reliably the polymerization rate during the first half an hour. After more and more polyitaconic acid forms during reaction, the system becomes more viscous. At that point, the heat was not only generated by polymerization of the monomer, but also from the mechanical stirring of the viscous polymer solution. The second part of heat was not negligeable once the conversion reached more than 50%. The data by reaction calorimeter from the beginning is continuous and accurate. But it needs to be combined with NMR to detect the entire process of high conversion polymerization of itaconic acid.

2.1.5 Molecular Weight Analysis

HP 1100 Series High performance liquid chromatography (HPLC) Systems and three TSK gel GPW_{XL} columns packed with G4000 PW_{XL}, G5000 PW_{XL}, G6000 PW_{XL} resins were used to analyze the molecular weights. 20 mM PBS (Phosphate

Buffered Saline) solution was used as eluent and filtered through 0.22 μm PES bottle top filter from Corning Incorporated, Corning, NY. The columns and detector were kept at 35°C. The flow rate was set to be 1 ml/min. The calibration was made with five polyacrylic acid standard samples with molecular weight ranging from 830 to 153,250 Daltons. The analysis was performed on the crude reaction mixture without precipitation. Sample injection volume was 100μL. All the samples were filtered through 0.1μm inorganic membrane filter from Whatman before injection.

2.2 Results and discussion

2.2.1 The effect of neutralization

We recorded the NMR spectra of IA monomer at various level of neutralization. Overall, with the increasing neutralization degree of itaconic acid, the two peaks of CH_2= in the itaconic acid monomer shift to lower resonance. Figure 7 shows all these three peaks for itaconic acid shifted. The peak for H_2O at 4.6 ppm is reference here.

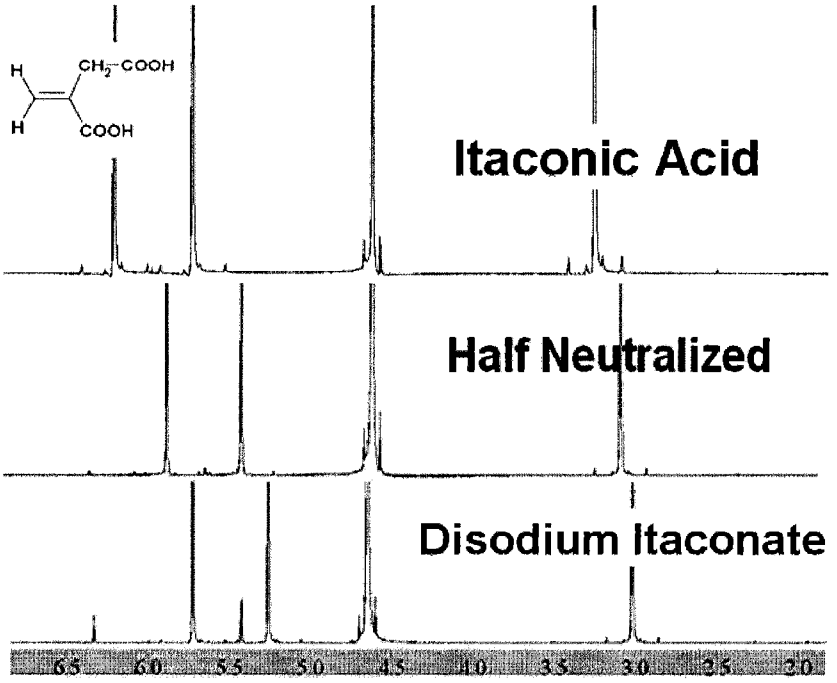

Figure 7 Peak shift for different neutralization degree of monomer.

It is important to understand the neutralization process of IA, in order to study the polymerization mechanism. Two different pKas for the two carboxyl groups were previously reported [20, 100, 101], 3.85 and 5.45 for the carboxyl groups, labeled A and B in the molecular formula below. In the neutralization process of itaconic acid monomer, since carboxyl group A is next to a double bond, a conjugative effect is generated with A, while CH_2 as a electron donating group connects to carboxyl group B, we assigned the PKa of carboxyl group A at 3.85 and dissociation of A occurs first. This helps us understand the effect of neutralization degree on polymerization process.

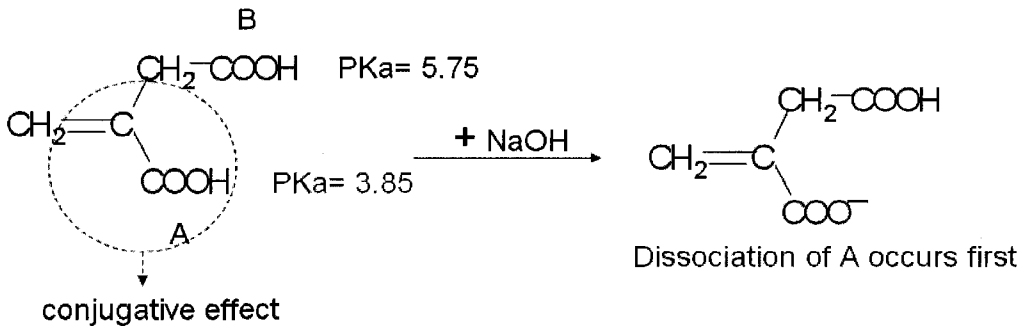

Figure 8 partial neutralization of itaconic acid monomer

2.2.2 Polymerization

In Figure 9, initiation shows the mechanism for the initiator radical to react with the itaconic acid monomer. It attacks CH_2= side of the double bond because of high steric hindrance on the other side of the double bond. And then, the double bond is open and forms monomer radical.

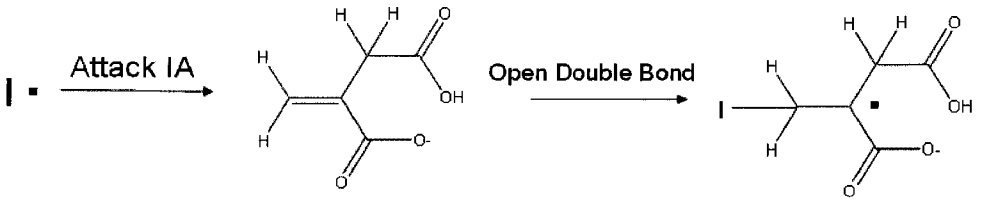

Figure 9 Initiation step

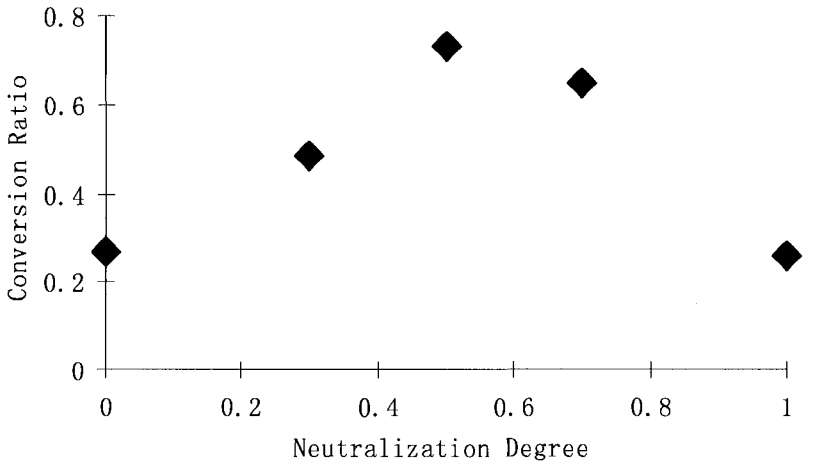

Figure 10 The effect of neutralization degree of IA on conversion at 100° C. Polymerization time is two and half hours. Neutralization Degree: 0% (PIA -7); 30% (PIA-8); 50% (PIA-2); 70% (PIA-9); 100% (PIA-10)

To study the neutralization effect on the polymerization rate, IA with different neutralization degree at 6.2mol/l monomer concentration was polymerized in two and half hours at 100°C. Figure 10 shows the relation between conversion for the final sample and neutralization degree of the monomer. During the neutralization process of IA and NaOH, water is generated and change the monomer and initiator concentration. The conversions also depend on monomer and initiator concentration. We evaluated the monomer and initiator concentration for these experiments. The evaluated conversions without considering the neutralization effect and less than 8% variation was predicted. Consequently, the data of figure 10 is showing a significant effect of the neutralization degree on the polymerization rate. We obtained significant polymerization yields only at 50 to 70% neutralizion. where carboxylic acid A is dissociated. One explanation is that the conjugative effect between carbonate and the free radical makes the latter more stable (Figure 8).

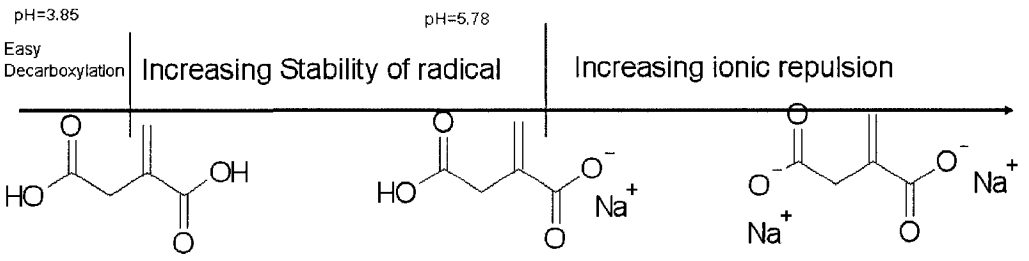

Figure 11 Neutralization effect of itaconic acid on free radical polymerization

Possibly, from 0% to 50% neutralization degree of itaconic acid, the stability of the radical of IA monomer increases with the neutralization degree once the itaconic acid is attacked by initiator radical. All carboxyl groups A are dissociated at 50% neutralization degree. With the further increase of neutralization degree, carboxyl group B starts to be dissociated. The dissociated carboxyl group B does not increase the stability of radical of monomer any more; instead, it increases ionic repulsion between monomer, which decreases the polymerization rate. Moreover, the stability of the radical highly reduces the possibility of decarboxylation [35, 37, 38, 102, 103] during the polymerization process. The radical on IA monomer can be transferred to the $-CH_2-$ group and generate another radical •COOH, which results in decarboxylation.

2.2.3 Cooling in the neutralization process

Two ^{1}H-NMR spectra were compared. One is neutralized itaconic acid kept cold during the neutralization, within ice water, and the other sample without cooling during the neutralization. The neutralization of itaconic acid always generated large amount of heat, which can heat the sample up to 100°C without cooling, resulting in small amount of itaconic acid (up to 1%) changing its structure. The structure change

of neutralized itaconic acid was indicated by extra peaks pointed by red arrow in Figure 12, which will affect the polymerization process of itaconic acid. The detail of the structure change will be discussed in the next chapter.

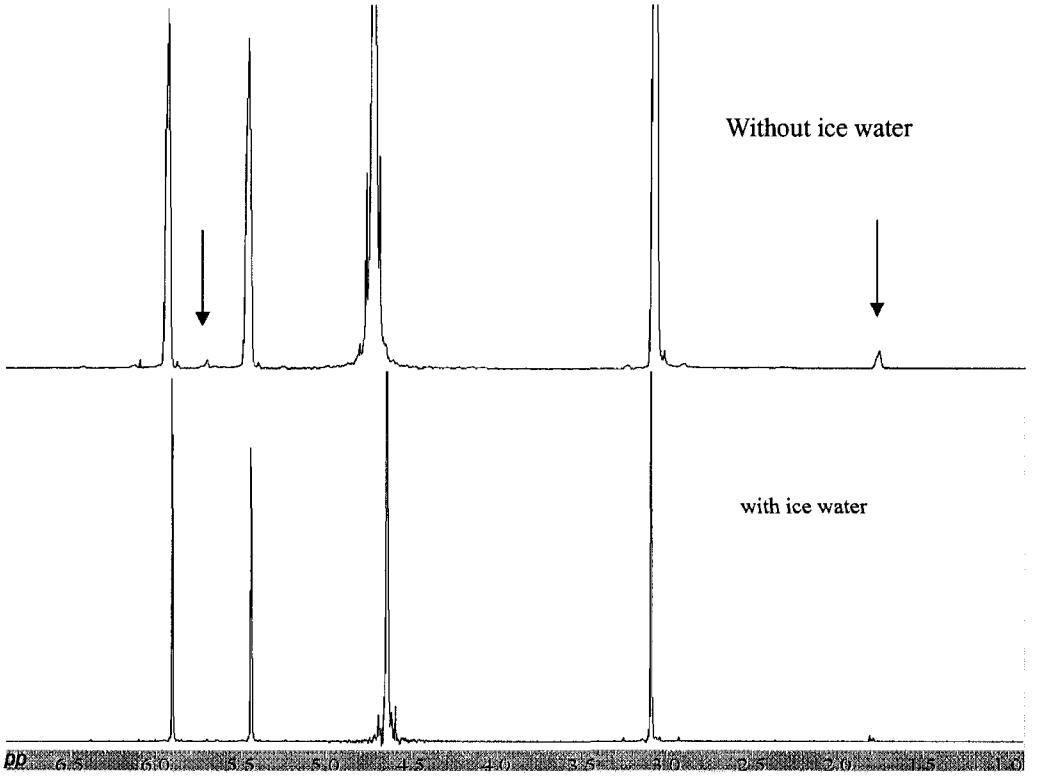

Figure 12 ^{1}H-NMR spectra for neutralized itaconic acid with its neutralization process cooling by ice water and another sample without cooling.

2.2.4 Structure analysis of polyitaconic acid

Process can be referred to synthesis method above. 100 gram of itaconic acid was half neutralized. 0.625ml 70wt% tBHP was fed with syringe pump in 2.5 hrs at 100°C. (PIA-1) After reacted 2 and half hours, ^{1}H-NMR and ^{13}C-NMR analysis were performed on the sample. ^{1}H-NMR shows no peaks around 5.4 and 5.7ppm indicating total consumption of monomer. 100% polyitaconic acid calculated according to **Error! Reference source not found.**, combined with ^{13}C-NMR spectra, in which all the

peaks related to carbon for PIA are shown in **Error! Reference source not found.**. The ^{13}C-NMR peaks for polyitaconic acid are enlarged to give a clear view in **Error! Reference source not found.**, compared with the ^{13}C-NMR peaks for itaconic acid. From monomer to polymer, chemical shift for carbon 1 and carbon 2 changed from 128 and 130.5 to 47.8 and 49.2ppm. Carbons on the double bonds of the monomer were shifted to carbons on the backbone of the polymer. Slight changes of chemical shifts for the rest of the carbons were observed. Chemical shifts of all peaks for monomer and polymer are shown in table 2. Polymerization kinetics for PIA-1 is shown in **Error! Reference source not found.**13. About 90% conversion can be reached in one hour. And 100% conversion can be reached in 2 and half hours. The reaction is slower than expected at the beginning. Oxygen dissolved in the sample might be the reason for this inhibition.

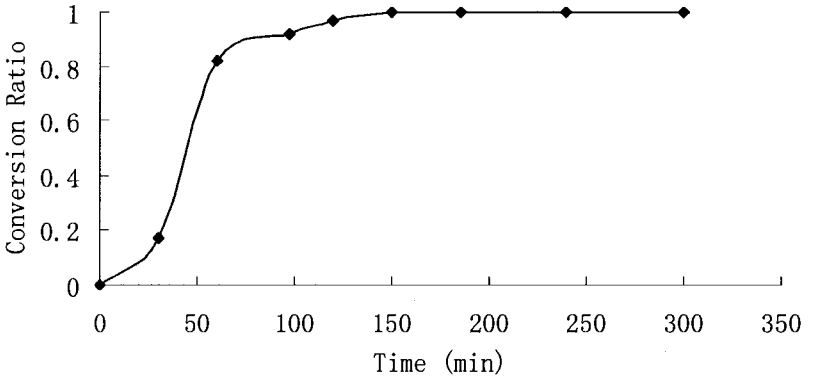

Figure 13 Conversion curve for PIA-1 sample with 100% conversion

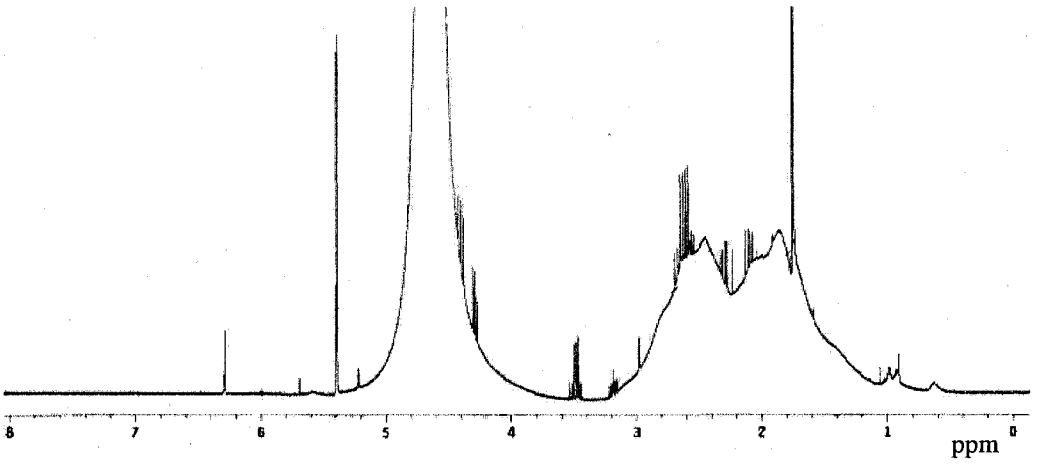

Figure 14 Polyitaconic acid PIA-1 sample with 100% conversion.

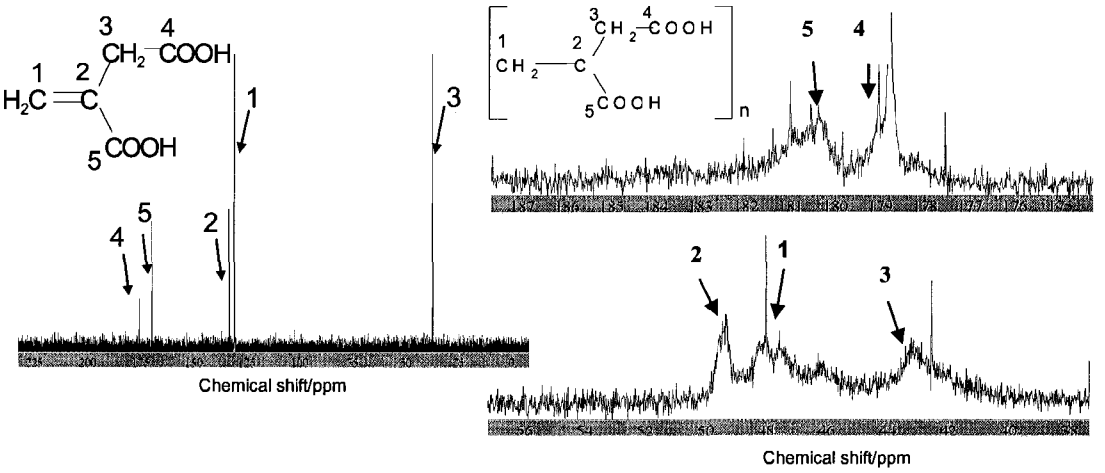

Figure 15 ^{13}C-NMR for itaconic acid monomer and PIA-1

Carbon	C1	C2	C3	C4	C5
Chemical shifts for IA	128.0	130.5	36.8	176.2	171.1
Chemical shifts for PIA	47.8	49.2	42.8	178.9	180.6

Table 2 ^{13}C NMR chemical shifts in ppm for PIA-1 and itaconic acid monomer

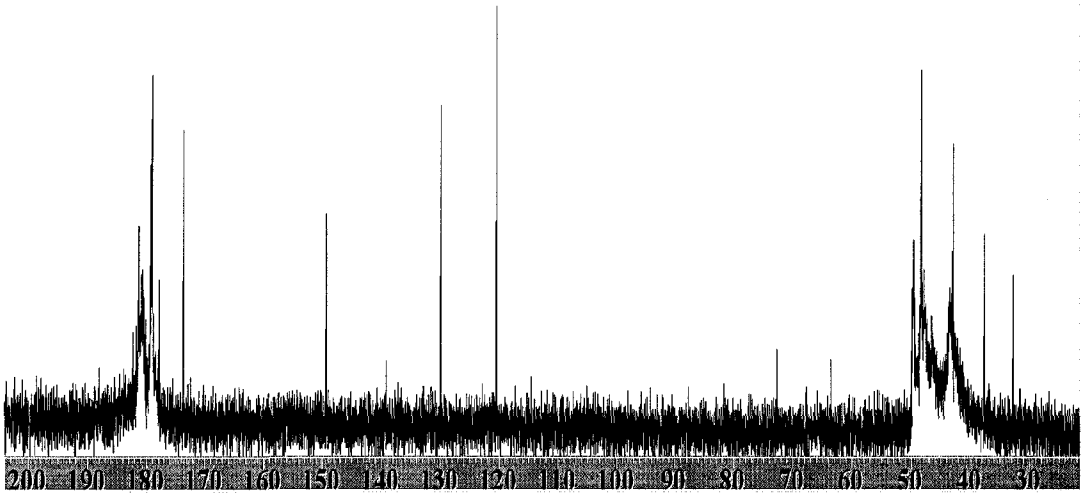

Figure 16 Full ^{13}C-NMR spectra for PIA-1

2.2.5 The selection of the initiator

In this work, tBHP was used as the initiator in all effective polymerizations due to three reason. First, high temperatures are required to overcome the strong intermolecular repulsion of the double carboxylic acid and to give a higher rate of molecular collisions, we used tBHP as a high temperature thermal initiator (228 hours half life at 100°C, 10 hours half life in benzene at 170°C according to Aldrich catalogue) to try to achieve a high yield of PIA. The half life is less in the presence of itaconic acid than in pure water, since the acid itself is a catalyst for the thermodissociation of tBHP. Itaconic acid combined with tBHP is effectively a redox initiator system here. The real half llife of the system is unknown. With the similar process, we used common initiator, such as AIBN and persulfate and obtained unsatisfactory results shown in apendix. Last, the higher polarity and electroneutrality of the tBHP radicals make it easy to overcome the ionic and steric hindrance of the neutralized itaconic acid.

2.2.6 Effect of initiator concentration

In order to determine the initiator concentration effect on polymerization rate, 6.20 mol/l half neutralized itaconic acid water solution was polymerized at three different initiator concentrations ranging from 0.00626mol/l to 0.125mol/l. The polymerization kinetics measured by NMR are reported in figure 17.

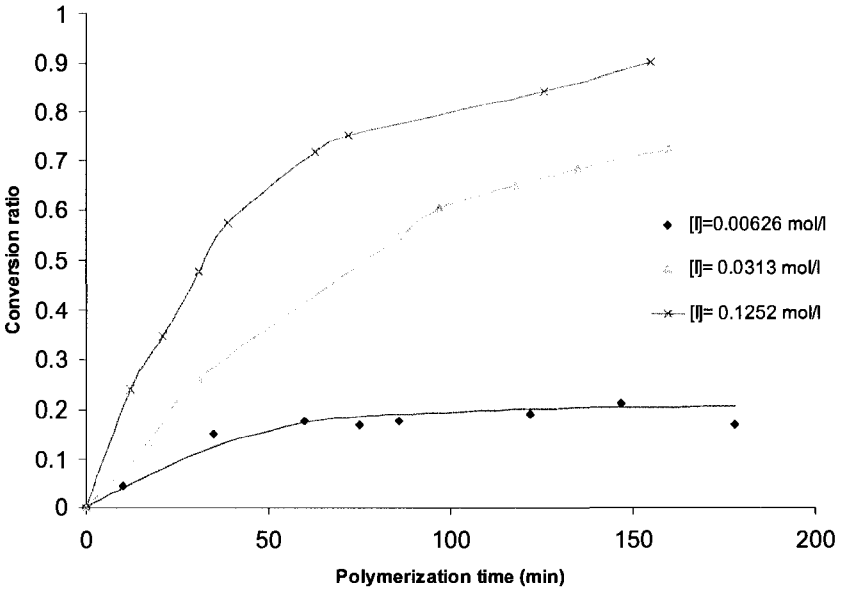

Figure 17 polymerization conversion vs time at different initiator concentration for half neutralized itaconic acid at 100 °C. [M] is 6.2 mol/l.

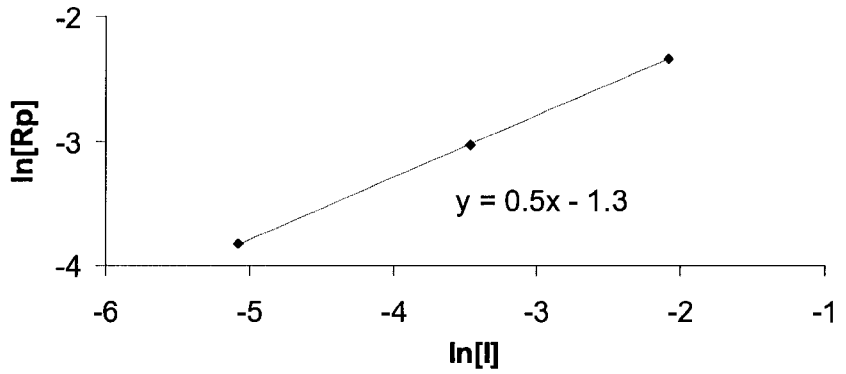

Figure 18 I logR_p vs log [I] for half neutralized itaconic acid at 100 °C. [M] is 6.2 mol/l.

As expected, the initial polymerization rate and final conversion increases with the increase of initiator concentration. Initial polymerization rates can be calculated as the slopes at time=0. Figure 18 of the polymerization rate vs initiator concentration shows that the reaction rate is proportional to $[I]^{1/2}$, indicating a classic free radical mechanism. With initiator concentration at 0.00626mol/l, the conversion at 3 hours is 20%. With initiator concentration at 0.125mol/l, above 90% conversion can be obtained.

2.2.7 Effect of monomer concentration

To determine the monomer concentration dependence on the the polymerization rate, three conversion vs time curves with different monomer concentration were obtained at 100 °C by batch process with itaconic acid concentration at 7.69 mol/l, 6.20 mol/l and 4.42 mol/l. These reactions were repeated in reaction calorimeter to give accurate initial polymerization curves.

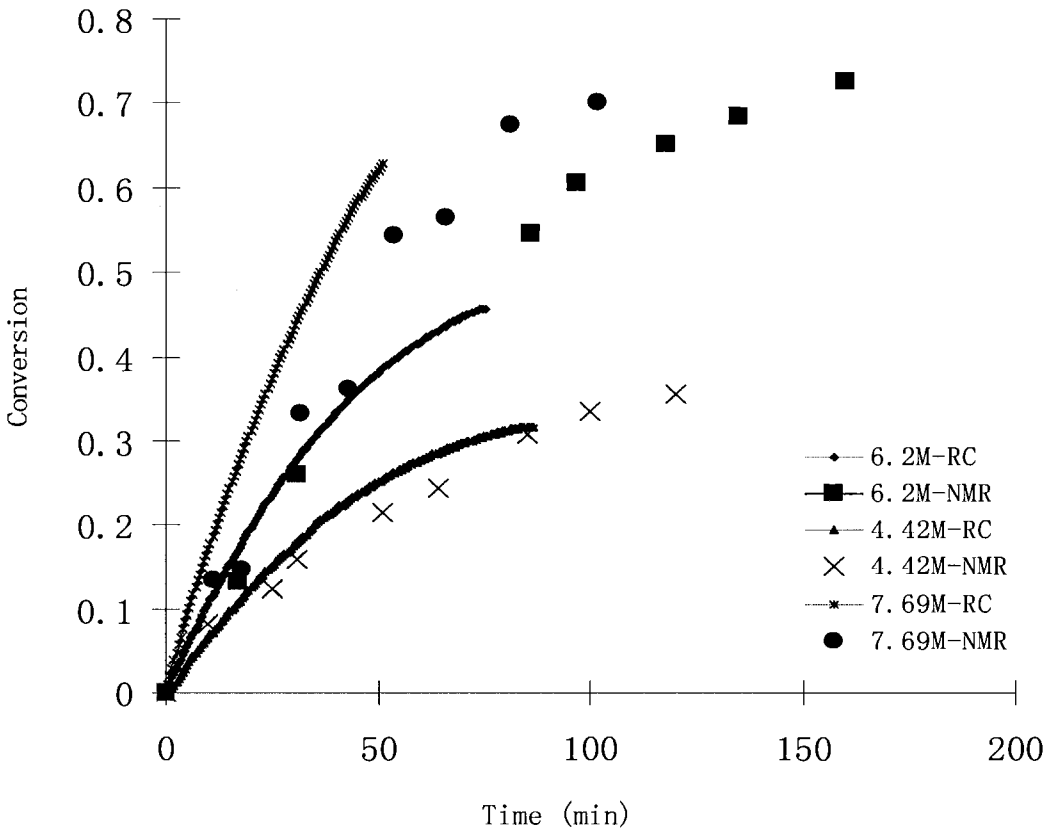

Figure 19 polymerization yield vs time at different monomer concentration of half neutralized itaconic acid at 100 °C. The continuous lines are the result of the reaction calorimeter (RC). The dots are the result obtained by NMR.

The initial slope as well as the conversion ratio increases steadily with the monomer concentration. The Reaction Calorimeter data and NMR data fit well, but a small deviation is observed for the reactions at 7.69M monomer concentration.

7.69mol/l sodium itaconate monomer solution was found to be highly viscous, much more viscous after polymerization which results in challenges when recovering the sample. Therefore, 6.2mol/l [M] or lower concentration of monomer is recommended for practical applications. During the polymerization at 7.69 mol/l [M] bubbles were observed in the samples. Decarboxylation during polymerization may be favored at high concentration.

	PIA-2	PIA-6	PIA-5
Reaction time (min)	75.5	51	86.5
Conversion	0.4572	0.6281	0.3164
Total Heat (J)	15301.5	16772.4	9228
ΔHp (KJ/mol)	43.51	34.71	37.91

Table 3 calorimetric results for determination of polymerization enthalpy of IA in different monomer concentration reaction.

The final conversions, total reaction heat and polymerization enthalpy values are presented in table 3. The value of ΔHp is 38.7 $\pm$ 4.8 at 100°C.

2.2.8 Kinetics model

We studied the kinetics of polymerization of itaconic acid for isothermal batch process at high temperature. To measure the conversion, about 0.2g of samples were taken *in situ* at certain polymerization time and cooled immediately in iced water to avoid further formation of polymer. The samples were directly dissolved in D_2O without drying and ^{1}H-NMR analysis was performed. With the method to calculate the conversion ratio we discussed previously, a set of data with different polymerization time can be used to plot polymerization kinetics curves.

Also, GPC can be used to plot the polymerization kinetics curve. Figure 20 shows the molecular weight of PIA sample at different polymerization time. Separated peaks represented monomer in low molecular range and polymer in high molecular range. From the ratio of the integral of the peaks for the polymer to the monomer, the conversion can be obtained. We compared data from NMR and from GPC. Figure 21 is two polymerization curves from NMR and GPC. The data set by GPC fits well with the NMR data we obtained. However, the curve plotted by NMR is "smoother". We found out the method using NMR is more reliable.

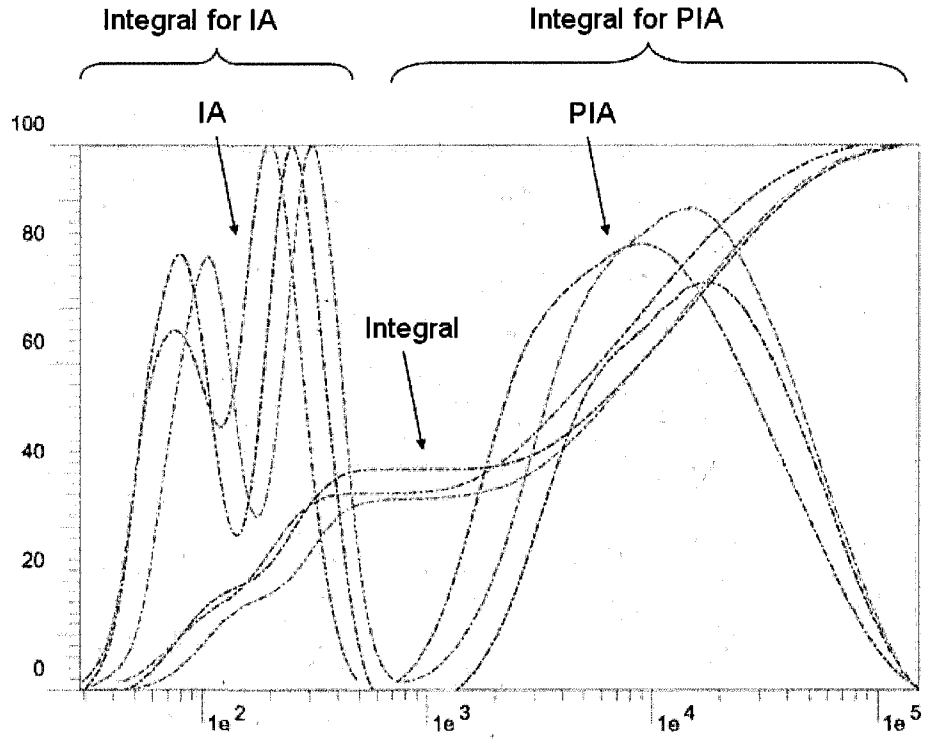

Figure 20 GPC data for polymerization sample with [M]=6.2mol/l and [I]=0.0388mol/l in three different reaction time: 118minutes (green); 135minutes (red); 160minutes (blue).

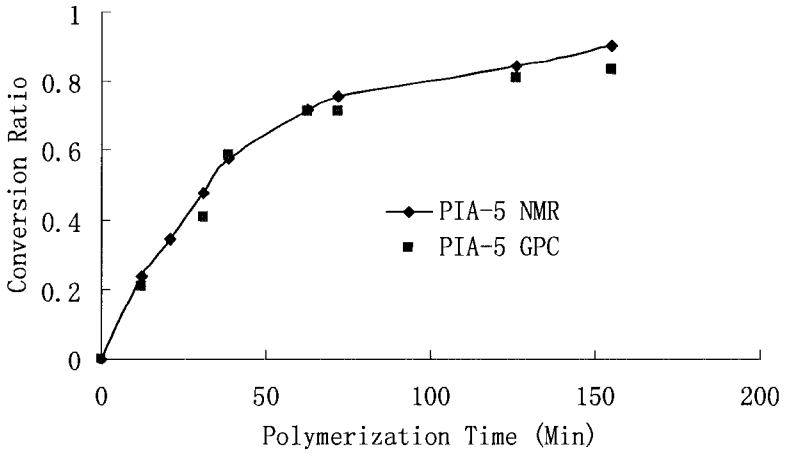

Figure 21, The comparation of polymerization curve ploted based on NMR spectrum and GPC data. [M]=6.2 mol/l and [I]=0.155 mol/l.

A classic polymerization model was applied here to study our polymerization kinetics. The isothermal polymerization rate is a function of time, monomer, initiator concentration and degree of neutralization.

At polymerization time = 0, initiator was added at reaction temperature. tBHP is dissociated into radicals: $\bullet O(CH_3)_3$ and •OH. Because radical •OH is significantly less active enough to open a double bond, only one radical is accounted after dissociation of each tBHP.

$$I \xrightarrow{kd} I\bullet$$

The initiator radical attacks IA monomer and form itaconic acid radical.

$$I\bullet + M \xrightarrow{ki} R_1\bullet$$

Initiator dissociation rate: $\frac{d[I\bullet]}{dt} = fk_d[I]$

where f is the initiator efficiency resulting from cage effect.

Polymer chain growth:

$$RM\bullet \xrightarrow{+M} RMM\bullet \xrightarrow{+M} RMMM\bullet \ldots\ldots \xrightarrow{+M} R_n\bullet$$

Termination of the radicals: $R_n\bullet + R_m\bullet \xrightarrow{k_t} R_{m+n}$

The coupling termination mechanism of the radicals is discussed later in this document.

We apply the pseudo steady state assumption. The radical concentration is assumed constant in the system:

$\frac{dR\bullet}{dt} = 0 = R_t + R_i$ so we can write: $k_t[R\bullet]^2 = fk_d[I]$

We rearrange the equation above to obtain: $[R\bullet] = (\frac{fk_d[I]}{k_t})^{\frac{1}{2}}$

The monomer consumed in the propagation steps:

$$R_p = -\frac{d[M]}{dt} = k_p[M][R\bullet] = k_p[M](\frac{fk_d[I]}{k_t})^{\frac{1}{2}} = k_p(\frac{fk_d}{k_t})^{\frac{1}{2}}[M][I]^{\frac{1}{2}}$$

Where k_p is the propagation rate constant, k_d is the initiation rate constant, k_t is termination rate constant.

½ power of [I] indicates termination of the radical process

The polymerization constant is a function of reaction temperature and we assumed a classic Arrhenius model

$k = Ae^{-Ea/RT}$ where $k = k_p(\frac{fk_d}{k_t})^{\frac{1}{2}}$

A is the Arrhenius coefficient, R is the molar gas constant, T is the reaction temperature.

When we derive the equation above we obtain:

lnk = lnA - Ea/RT

From equation, the polymerization rate can be expressed as:

lnRp = C – Ea/RT

Where C is constant, equal to lnA + ln[M] + 0.5ln[I]

2.2.9 Model Fitting

In order to calculate the reaction constants, we built a model to fit the experimental data including the NMR data set and the Reaction Calorimeter data set for sample 2 to sample 6. Microsoft Office Excel 2007 was used to to find the best constant fk_d and $k_p(k_t)^{-\frac{1}{2}}$ to fit the model and data, by minimizing the sum of square of the difference between the model and experiment.

From the Initiator dissociation rate: $\frac{d[I\bullet]}{dt} = fk_d[I]$

We can obtain the instant initiator concentration:

$[I] = [I]_0 \exp(-fk_d t)$

From the polymerization rate

$R_p = -\frac{d[M]}{dt}$

We can obtain the instant monomer concentration by applying a discrete step model:

$[M](t_j) = [M](t_i) \div R_p(t_i) \times (t_j - t_i)$

$[M](t_j)$ is the monomer concentration at time tj, $[M](t_i)$ is the monomer concentration at time t_i. In our model, we take t_j-t_i = 6minutes.

The polymerization rate $R_p(t_i)$ at time ti can be obtained from the equation:

$$R_p(t_i) = k_p(\frac{fk_d}{k_t})^{\frac{1}{2}} \times [M](t_i) \times [I](t_i)^{\frac{1}{2}}$$

With the information above and an interactive evaluation of the polymerization

constants fK_d and $K_p/(k_t)^{1/2}$, theoretical conversion VS reaction time with different initiator concentration and monomer concentration can be plotted as in Figure 22 and Figure 23. By adjusting the constants, the most fitting model and the comparison between theoretical and experimental data was found. The constant $fK_d = 2x10^{-4}$ and $K_p/(k_t)^{1/2}$ in the range of 0.07 to 0.1 is found to fit best the experimental data. $K_p/(k_t)^{1/2}$ is 0.07 for model fitting in Figure 22 and 0.1 for model fitting in Figure 23 and Figure 24.

Figure 23 and Figure 24 are for monomer concentration effect. The model curves we plotted fit well sample 2 and 5. For sample 6 with the highest monomer concentration, the data from the reaction calorimeter (RC) and NMR has a 10% variation. A small amount of kinetics sample not cooled down immediately could yield a higher conversion at the end of the reaction. It is possibly the effect that leads to different values of the final conversion. The model curve for sample 6 is between the polymerization curves obtained by RC and NMR.

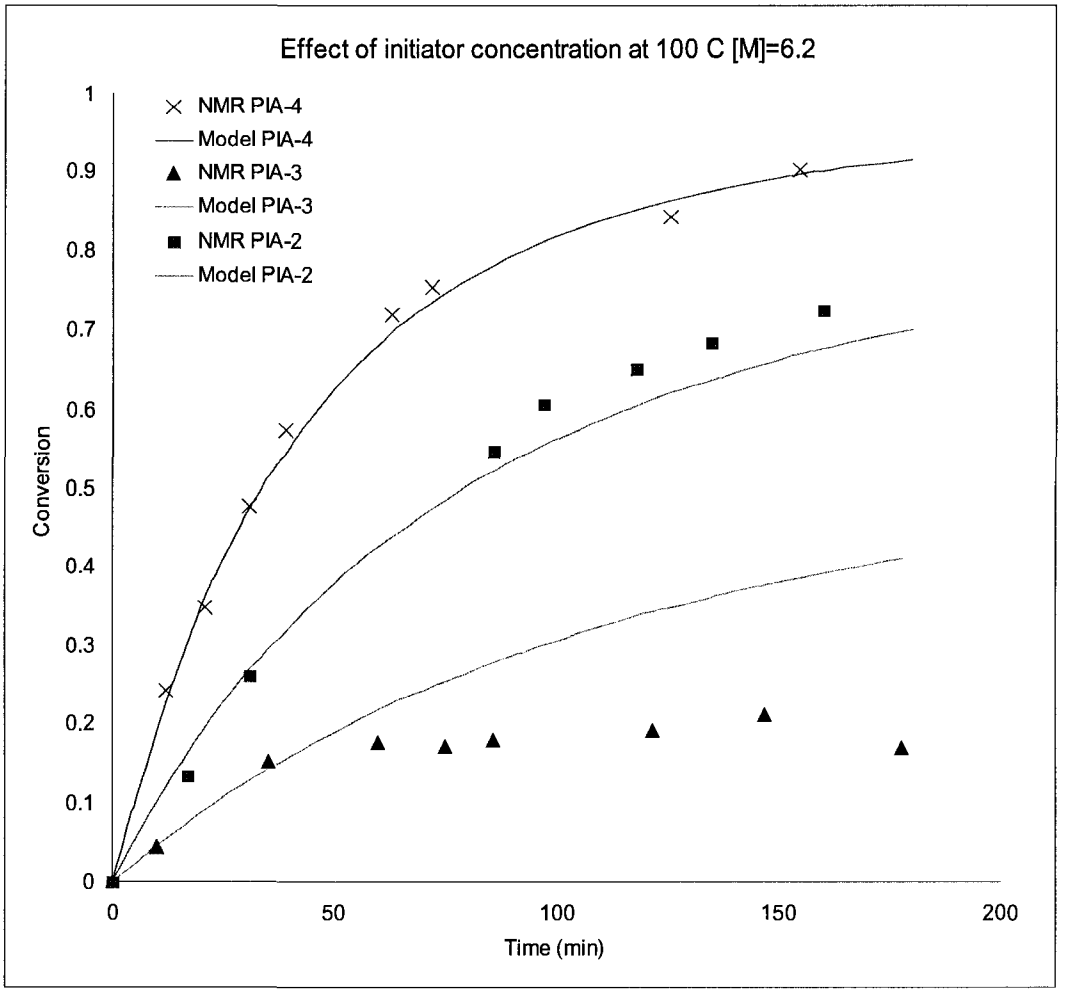

Figure 22 Model fitting of initiator concentration effect by NMR from sample 2 to 4. [M] for these experiment is 6.2M. Initiator concentration is: 0.0313M (PIA-2); 0.00626M (PIA-3); 0.125M (PIA-4)

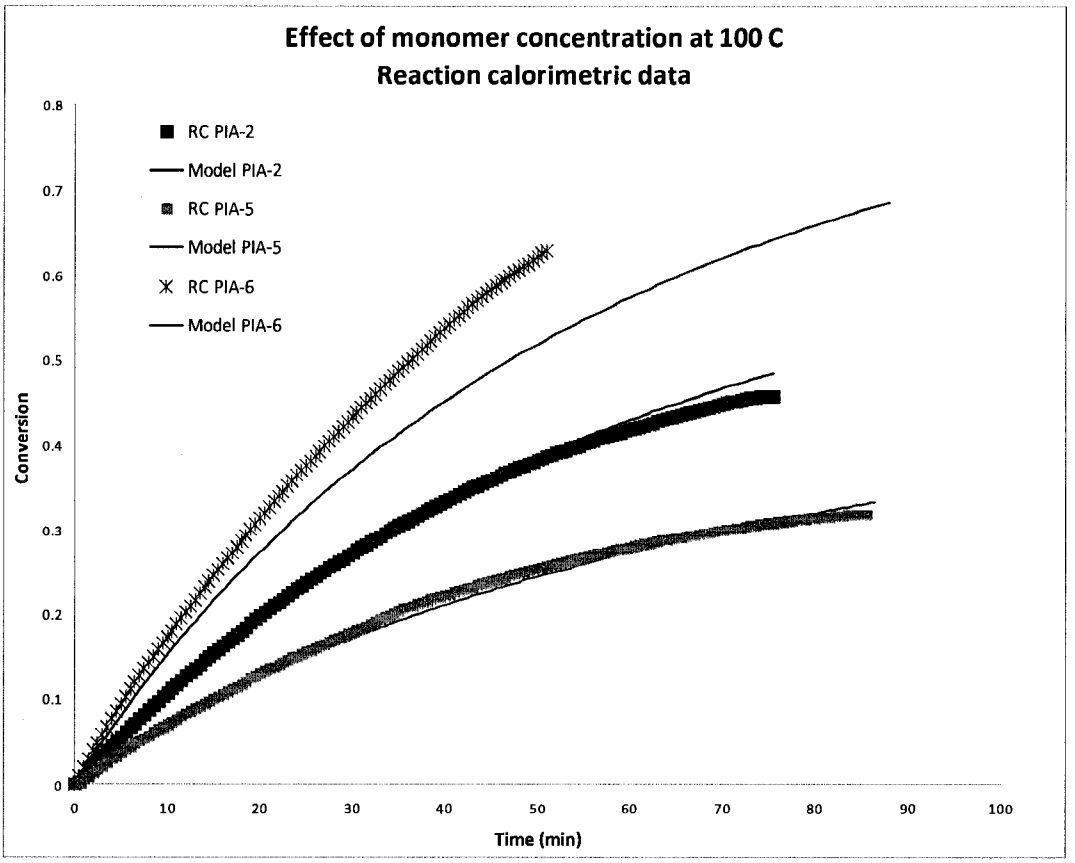

Figure 23 polymerization kinetics at different monomer concentration of half neutralized itaconic acid at 100 °C. Continuous thin lines are the best model fittings of the data by reaction calorimeter (RC) for PIA-2, PIA-5, PIA-6.

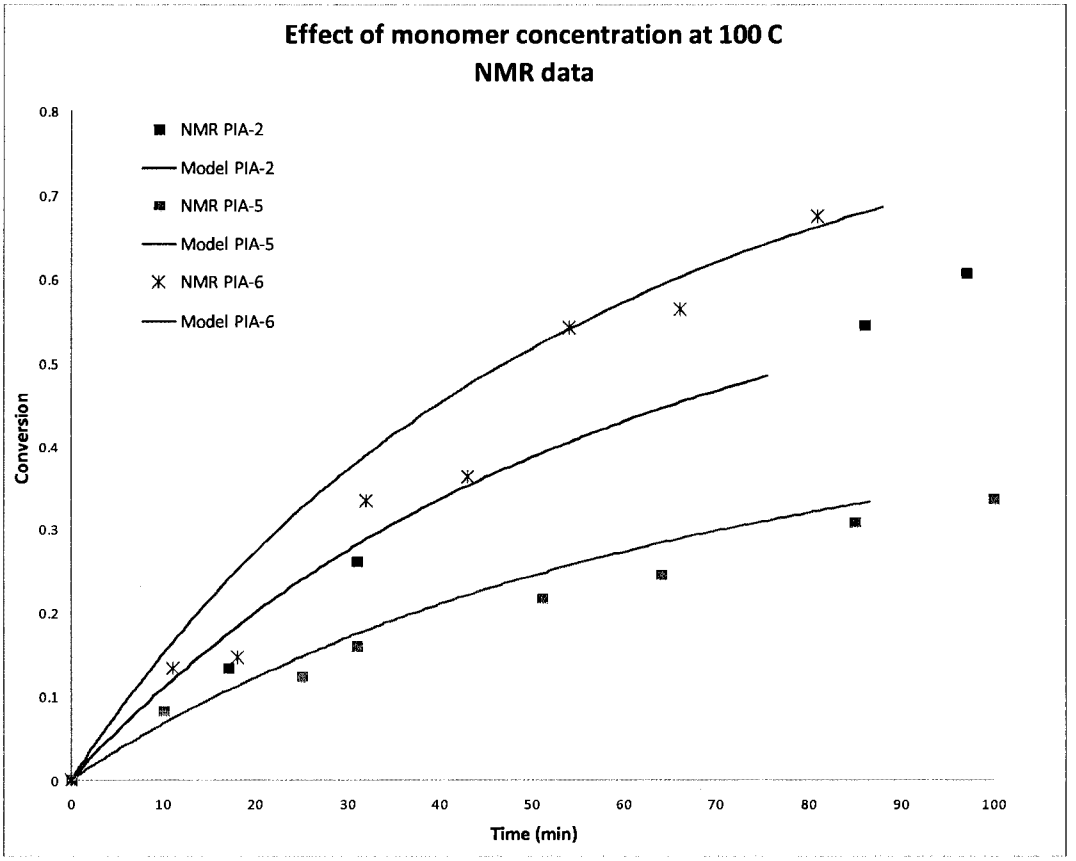

Figure 24 polymerization kinetics at different monomer concentration of half neutralized itaconic acid at 100 °C. continuous lines are the best model fitting of the data by NMR for PIA-2, PIA-5, PIA-6.

2.2.10 Effect of temperature and its model fitting

The effect of temperature was also studied. Figure 25 illustrates the polymerization kinetics at different temperatures.

For the temperature effect, the constant k can be evaluated by changing the activation energy Ea to fit the model with polymerization kinetics at different reaction temperatures.

$$k = Ae^{-Ea/RT} \qquad \text{where} \quad k = k_p\left(\frac{fk_d}{k_t}\right)^{\frac{1}{2}}$$

The best model fitting at different reaction temperature is shown in Figure 25.

The constant $fK_d = 2x10^{-4}$ and $K_p/(k_t)^{1/2} = 0.082$ is found to fit best our experimental data.

Temperature control was set at 70 °C, 80 °C, 90 °C and 100 °C, and polymerization kinetics were monitored by reaction calorimetry. The monomer concentration for all these reactions is 4.42mol/l. The reaction rates at the beginning of the four low conversion reactions are used to calculate the temperature effect. Initiator concentration was 0.0223 mol/l at time = 0. Initiator was injected into the reactor once sample reached reaction temperature. It took 30±15minutes to reach the desired reaction temperature starting from room temperature.

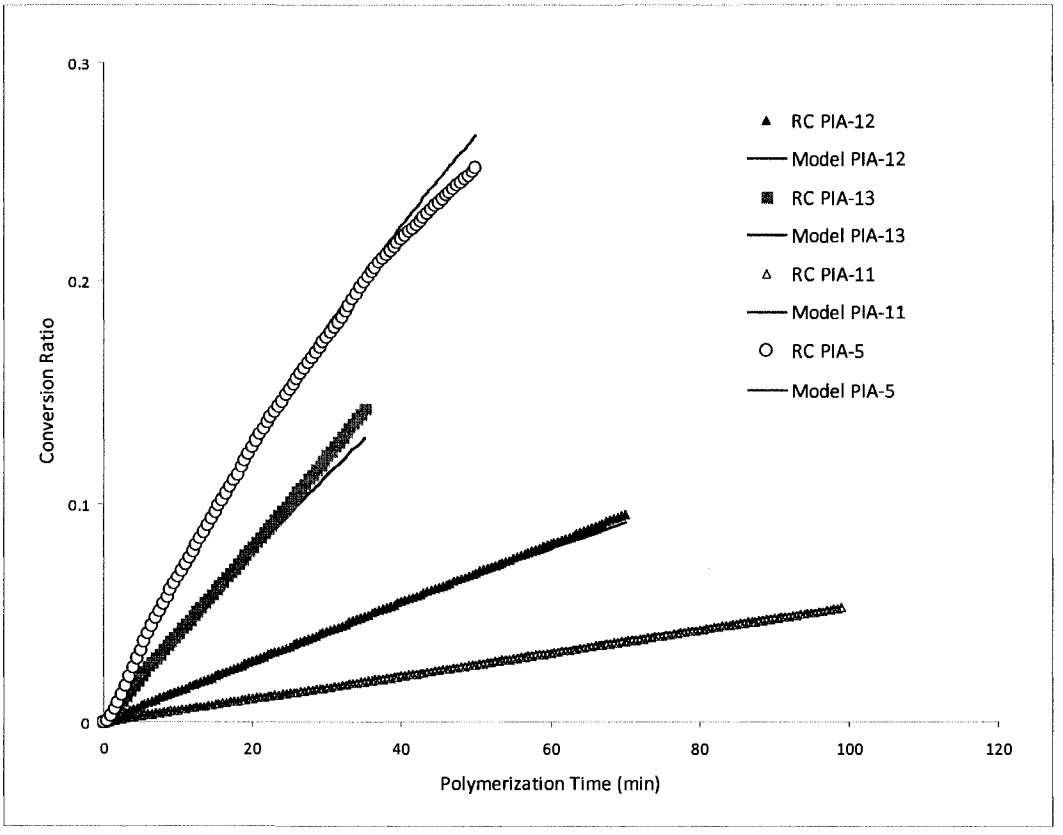

Figure 25 Model fitting of polymerization curve by Reaction Calorimeter at 70 °C (Red, PIA-11), 80 °C (Purple, PIA-12), 90 °C (Green, PIA-13), 100 °C (Blue, PIA-5).

The polymerization rate can be calculated from the initial slopes of these

curves in Figure 25. The relation between polymerization rate and 1/T (K^{-1}) is plotted in Figure 26. The initial polymerization rate is nine times higher at 100 °C compared to 70 °C. The apparent activation energy is the slope of the linear ln(Rp) versus 1/T plot.

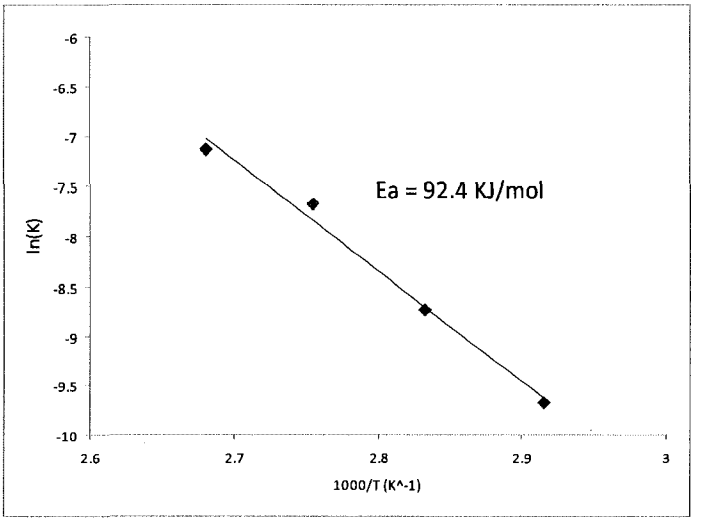

Figure 26 Arrhenius plot for the polymerization of itaconic acid

From the slope in Figure 26, we can calculate the value of Arrhenius energy Ea = 92.4 kJ/mol for polymerization of itaconic acid. The activation energy of half neutralized acrylic acid polymerization are 10.6 Kcal = 44.35 KJ/mol. The activation energy of acidified acrylic acid polymerization is 9.6 Kcal/mol = 40.17Kj/mol. The higher activation energy means that the polymerization rate of IA is more sensitive to temperature than that of acrylic acid.

2.2.11 Molecular weight of polyitaconic acid

Low molecular weight of polyitaconic acid in previous patents and papers is a limit to the application of PIA. Compare with US patent 5,336,744 and US patent 5,233,592, the molecular weight of PIA with our process is more than 4 times higher

than theirs. Figure 27 shows the number average molecular weight of polyitaconic acid at different conversion ratio during the reactions. Molecular weights were compared at different initial monomer concentration and initiator concentration. It reveals that the molecular weight decreases with the conversion and follows roughly a linear relationship. This is generally observed in free radical solution polymerization. The sample with the highest monomer concentration and lower initiator concentration has the highest molecular weight.

The equation bellow relates the kinetic chain length and the monomer and initiator concentration:

$$\upsilon = \frac{k_p[M]}{(k_d k_t[I])^{1/2}}$$

Where υ is kinetic chain length.

In the equation, monomer concentration has a large effect on kinetic chain length. Also, kinetics chain length increases with the decease of initiator concentration. With the decrease of monomer remaining, kinetic chain length decreases with polymerization time.

The number average molecular weight can be expressed as:

$$\overline{X_n} = \frac{R_p}{R_t + \sum R_{tr}}$$

R_t is the rate of termination. R_{tr} is the rate of chain transfer. For polymerization of itaconic acid, the chain transfer to monomer is overwhelming.

$$\overline{X_n} = \frac{k_p[M\bullet][M]}{2k_t[M\bullet]^2 + k_{trm}[M\bullet][M]}$$

Re-organizing the equation, instant number average molecular weight can be obtained:

$$\frac{1}{\overline{X_n}}(t) = \frac{2k_t R_p}{k_p^2[M]^2} + C_M$$

Where $\frac{k_{trm}}{k_p} = C_M$

The number average molecular weight $M_n(t_i)$ at time ti can be obtained from the equation:

$$M_n(t_i) = \frac{\int_0^{t_i} \overline{X_n}(t_i)([M](t_{i-1}) - [M](t_i))dt}{\int_0^{t_i} ([M](t_{i-1}) - [M](t_i))}$$

By adjusting the value of C_M, we obtained the best fitting model for the number average molecular weight by GPC. The best fitting model of the number average molecular weight data is shown in Figure 27. The constant $fK_d = 2x10^{-4}$, $K_p/(k_t)^{1/2}$ =0.07 and $C_M = 0.012$ were used in that fit.

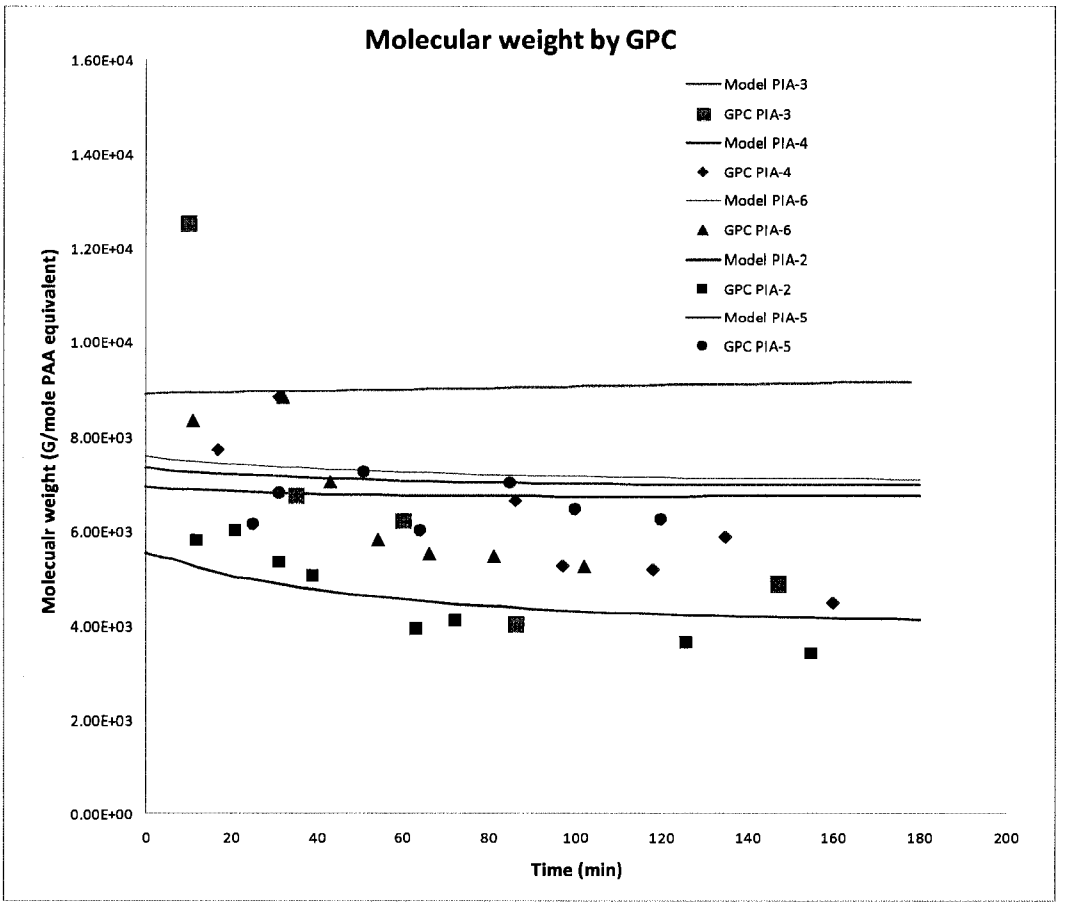

Figure 27 Comparison of number average molecular weight of polyitaconic acid vs. conversion ratio. Polyitaconic acid was prepared with tBHP at 100 ℃. Five continuous lines represent evaluated Mn vs. conversion model.

In conclusion, the conversion of our polymerization process for polyitaconic acid can reach 100% in two and half hours under certain condition. Polymerizatioin rate is affected by neutralization degree, reaction temperature, monomer and initiator concentration.

CHAPTER III

STRUCTURE ANALYSIS

In 1966, Braun and Sayel, Kenji, Yokota [40] found out that a large amount of carbon dioxide caused by decarboxylation was collected during the free radical polymerization of itaconic acid. After that, it was believed that decarboxylation was the major structural change observed during IA polymerization. Furthermore, PIA can change to polyitaconic anhydride during drying process above 60°C with vacuum. The final structure after decarboxylation is still unknown. Even though numerous papers mentioned decarboxylation, based on the data in literatures, most of their evidences came from IR spectrum and elementary analysis data. [100, 101] I believe that these two methods were not suitable for analyzing the structural changes. Because of the difficulty of drying water from polyitaconic acid samples, it is not sufficient to use IR and elementary analysis to determine the appropriate chemical structure.

For our polymerization system, the structure change of itaconic acid has been investigated. In chapter II, I already mentioned that half neutralization of the monomer has the potential effect of preventing the decarboxylation of itaconic acid. Carbon dioxide was not clearly observed for our reaction systems. Structure changes of itaconic acid do exist. However, decarboxylation is not the major one we encountered.

We found that most of our reactions, as presented in the previous chapters were slow down after about 80 minutes polymerization. Large amount of monomer remained and can not continue to react. We contemplated that we may run out of

initiator radicals. However, based on the long half life of tBHP/COOH redox system ($fk_d=10^{-4}$) we found out in previous chapter, it must be some other reasons causing the end of the reaction.

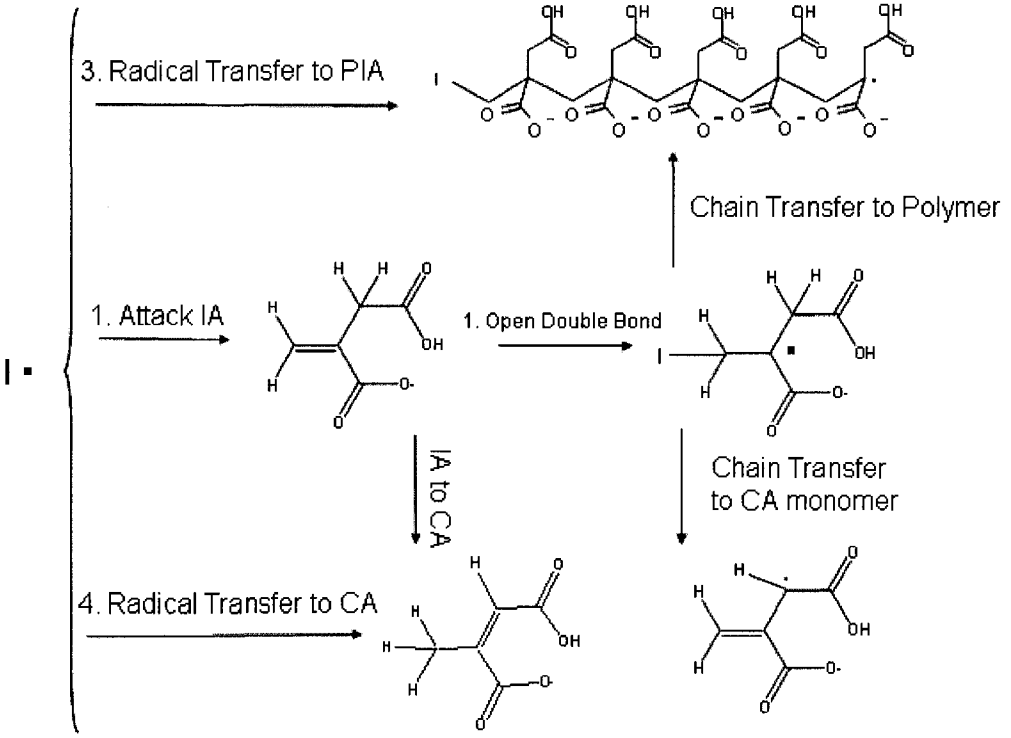

Figure 28 map of several possible paths for attack of active radical. I• represents the initiator radical

The map above indicates all possible paths for the reaction of the active radical. Path 1 is the polymerization of the monomer. Path 2 is the radical transfer to IA monomer. Path 3 is the radical transfer to polymer. The radicals are transferred to PIA instead of IA. Path 4 is the radical transfer to citraconic acid (CA). In this chapter, I provide evidence for path 4 which strongly affect the polymerization rate and conversion for PIA.

Figure 29 shows the structure change of half neutralized itaconic acid at high temperature in aqueous solution. The double bond of itaconic acid shifts its position

and citraconic acid is formed. A better understanding of the structure change can be obtained from Figure 29. The majority of isomers of half neutralized IA are half neutralized citraconic acid, which has a hydrogen bond between two carboxyl groups inside the molecule. Less than 1% of the isomers is mesaconic acid, which is the trans structure of citraconic acid. There is no intramolecular hydrogen bond in half neutralized mesaconic acid, so the fraction of citraconic acid among the isomers is favored.

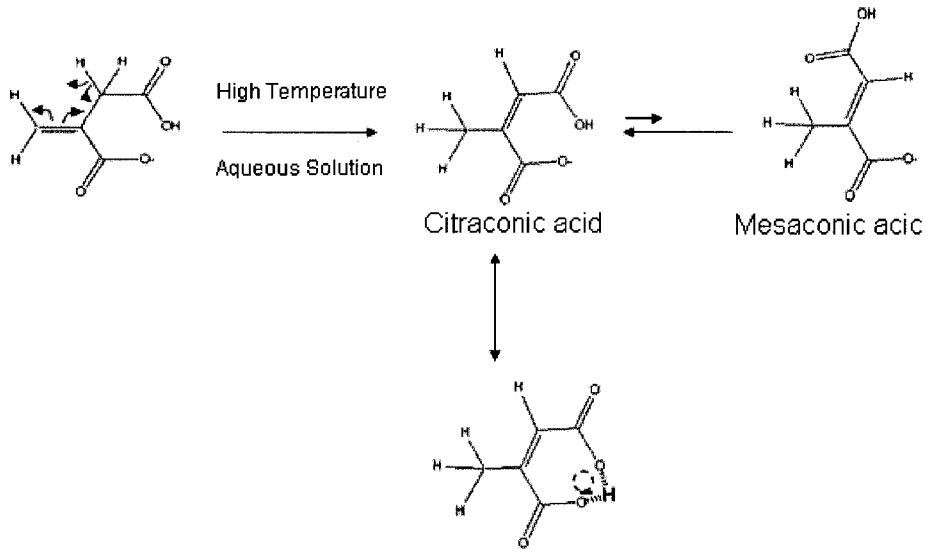

Figure 29, Structural change of Itaconic acid to citraconic acid and mesacnic acid during heating

3.1 Experimental

First, several granules of hydroquinone were added to a 6.2mol/l half neutralized itaconic acid aqueous solution. The solution was replaced in a 3-neck flask equipped with condenser and nitrogen feed. Several samples were prepared at different temperature with different heating times. The solution were blanketed with nitrogen.

^{1}H-NMR was used to analyze the structure change of the itaconic acid. The samples were dissolved in D_2O without separation, due to the difficulty to separate IA and CA. Furthermore, Heteronuclear Multiple Quantum Coherence (HMQC) and Heteronuclear Multiple Bond Coherence (HMBC) were run on a 400MHz NMR to analyze the structure change of itaconic acid monomer after heating. HMQC and HMBC are 2-dimensional inverse H,C correlation techniques, which can be used to determine the connectivity of carbon to hydrogen. HMQC is specific to for direct C-H coupling, while HMBC gives longer range couplings (2-4 bond coupling). One IA samples prepared at 110°C for 5 hrs was used for long range proton NMR testing. Temperature for these NMR experiments was set to be 25°C. Width for HMQC is 6410 Hz, 2D width is 17094 Hz. Total acquisition time for HMQC is one and a half hours. Width for HMBC is 6410 Hz, 2D width is 24096 Hz. Total acquisition time for HMBC is 35 minutes.

3.2 Result and discussion

Figure 30 shows us the NMR spectrum which has several additional peaks compared with that of itaconic acid in Chapter II. More extensive NMR techniques were used to give us a clearer idea of what they represent.

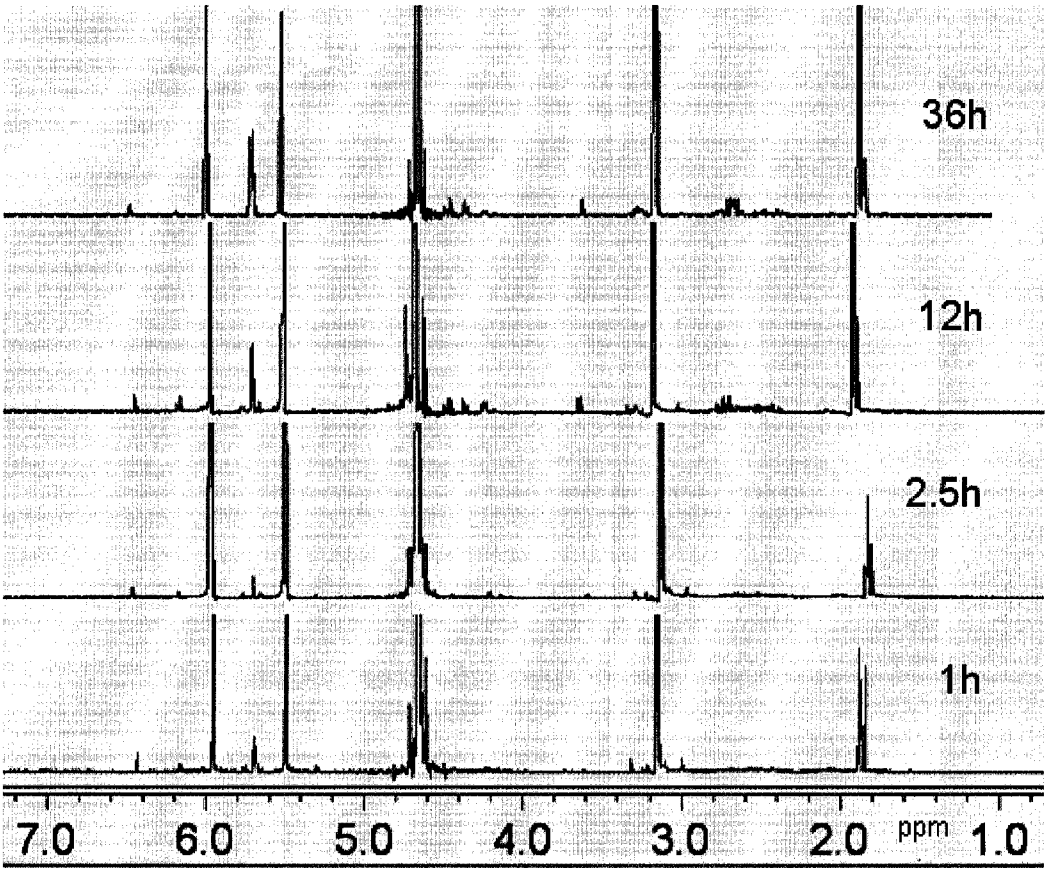

Figure 30, ^{1}H-NMR for half neutralized itaconic acid monomer in water solution after heating at 110°C with different heatinig time: 1h, 2.5h, 12h, 36h.

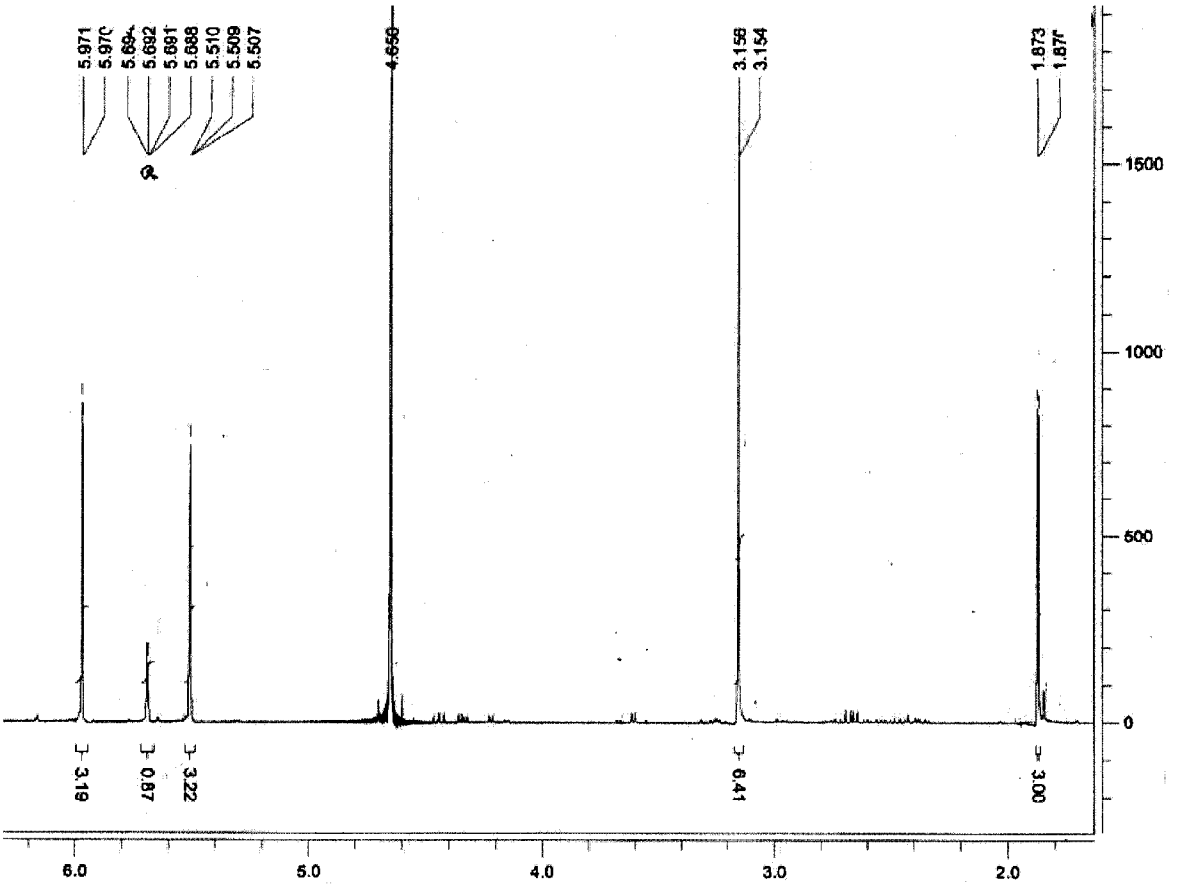

Figure 31 ^{1}H-NMR for half neutralized itaconic acid after heating in 110°C for 20 hours. The split of peaks is clearly seen at 5.7ppm.

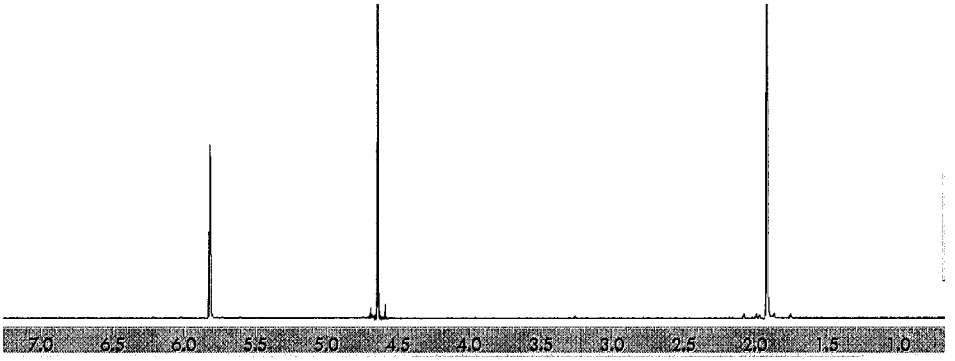

Figure 32 ^{1}H-NMR for citraconic acid

3.2.1 Chemical structure of itaconic acid during polymerization

Figure 31 is the ^{1}H-NMR spectrum of the IA sample after heating at 110° C for 20 hours. Except for the peaks of itaconic acid, two major extra peaks around 1.95

and 5.75 were shown in Figure 31. The integral of these peaks increases with the heating time. We interpret this results as some of the itaconic acid changes to citraconic acid during heating, and the ratio between citraconic acid and itaconic acid increase with time at high temperature. The peaks around 1.95 and 5.75ppm respectively represent the proton on the =CH group and protons on methyl groups of citraconic acid. HMBC and HMQC show the structure of a mixture of IA and CA. HMQC spectrum in Figure 33 shows the hydrogen bearing carbons of citraconic acid, positioning the =CH and $-CH_3$ groups. In ^{13}C-NMR of Figure 34, the sharp peaks around 22 and 118ppm is the typical peaks for carbon of group –CH= and $-CH_3$. HMBC spectrum in Figure 34 shows the long range correlation between hydrogen on $-CH_3$ and carbons on =CH and $-CH_3$ groups.

In addition, the sharp peaks at 6.4ppm and 1.84ppm in NMR spectrum in 1H-NMR for neutralized IA after heating, the signature of mesaconic acid. It always has a very low percentage out of the two isomers based on integral of peaks – less than 1%.

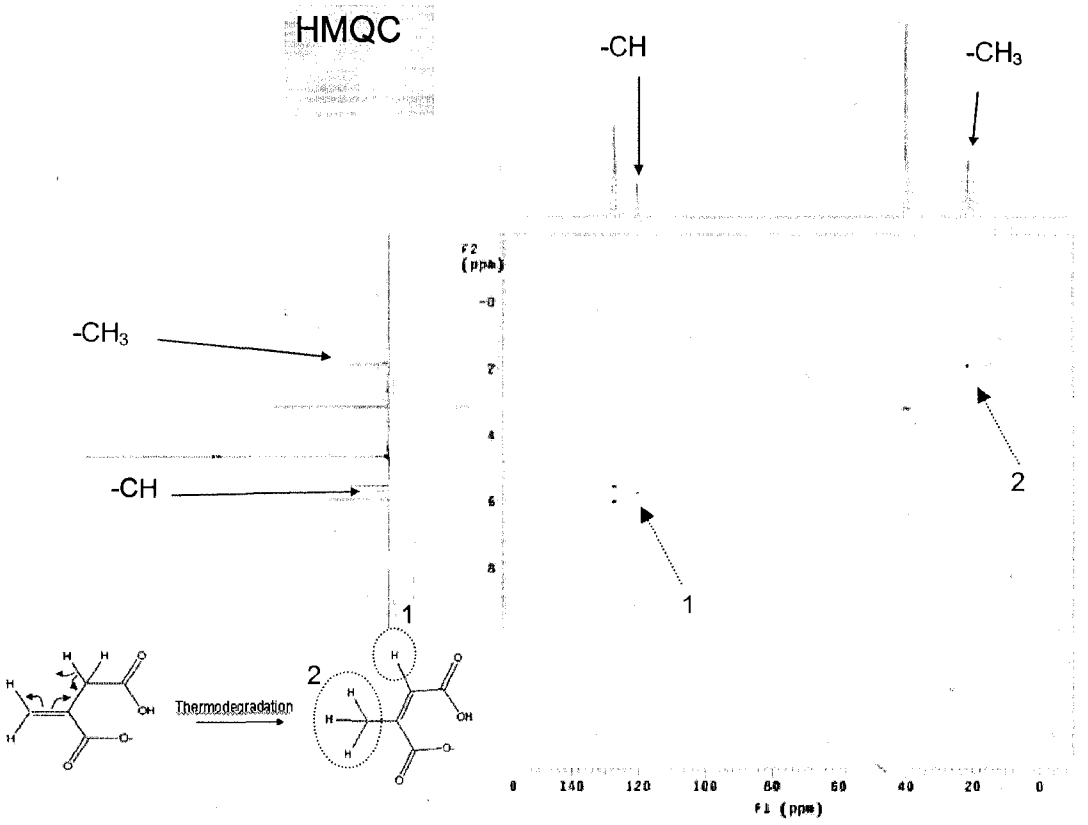

Figure 33, HMQC of itaconic acid after heating at 110 °C for five hours

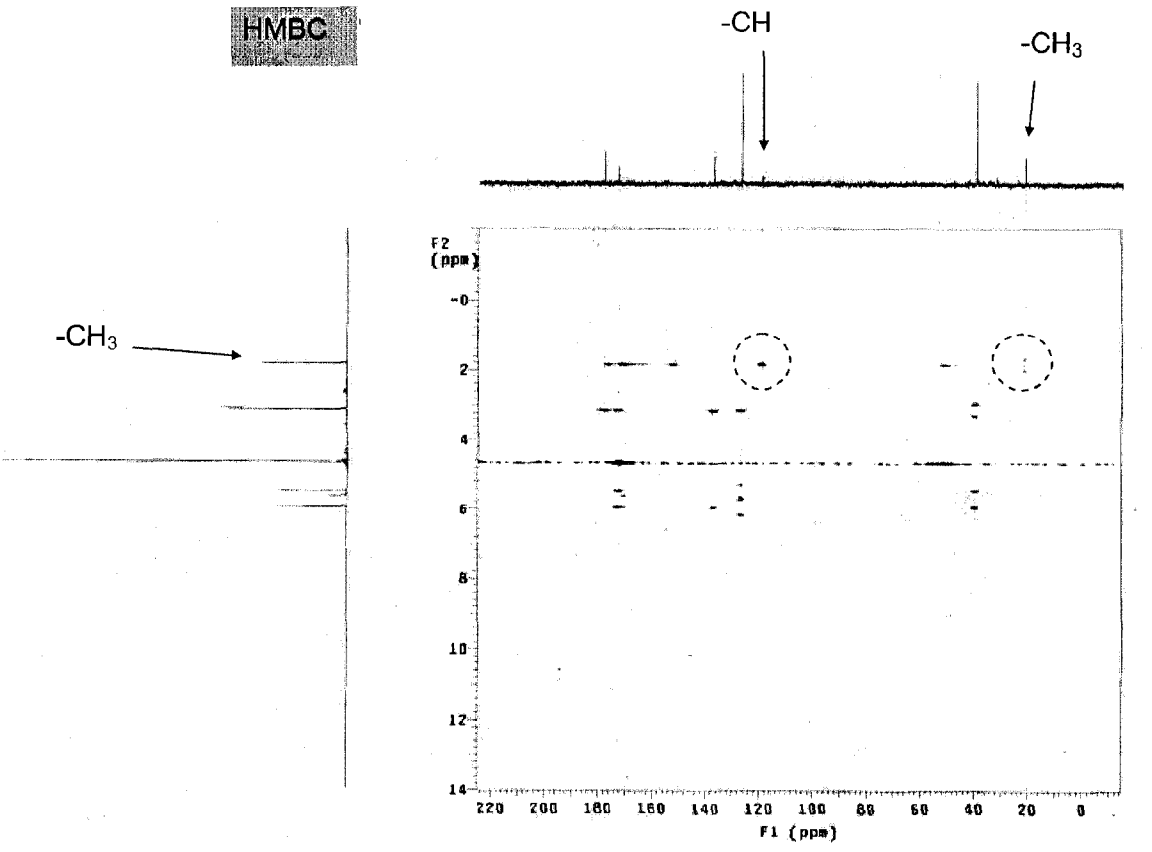

Figure 34, HMBC of itaconic acid after heating at 110 °C for five hours

The ratio of CA and IA can be calculated by ratio of integral of peaks at 5.75 and 6.00 ppm. Figure 35 indicates the ratio of IA and the mixture of IA and its isomer in different heating time, we show the percentage changed with the heating time from 100 at the beginning to 33 after three days.

3.2.2 The effect of citraconic acid on polymerization process of itaconic acid

Citraconic acid generated from itaconic acid during reaction is the reason for the fast consumption of the radicals. Citraconic acid is acting as an inhibitor for

polymerization of itaconic acid. To study and confirm this opinion, 6.2 mol/l half neutralized itaconic acid in water solution was heated at 110°C in reaction calorimeter.

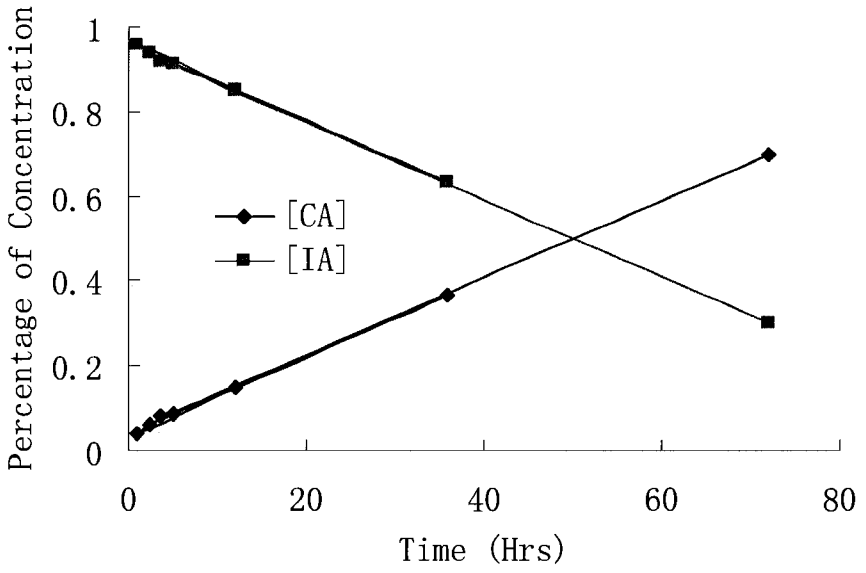

Figure 35, Percentage of concentration itaconic acid remained and citraconic acid generated during the heating time at 110 °C

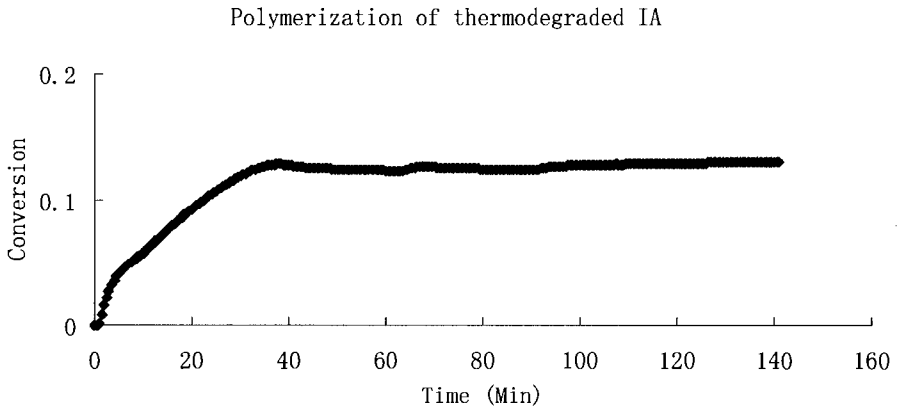

Figure 36, Polymerization curve of itaconic acid by reaction calorimeter after heating at 110 °C. 0.5 ml 70wt% tBHP water solution was injected into reactor at 100 °C.

Figure 36, Polymerization curve of itaconic acid by reaction calorimeter after heating at 110 °C. 0.5 ml 70wt% tBHP water solution was injected into reactor at 100 °C. In 40 minutes, no further heat flow is observed, indicating the end of reaction. The radicals are exhausted at that point. After 145 minutes, the final sample was taken out and analyzed by NMR. ^{1}H-NMR shows that only 13% conversion of itaconic acid was obtained. The isomer-citraconic acid generated during the heating before starting the reaction has the effect of an inhibitor for the polymerization of IA. The active radical was transferred to isomer citraconic acid and formed non-reactive radical. This explains why we need a higher concentration of initiator for polymerization of itaconic acid than the initiator concentration in classic free radical polymerization. In order to avoid generating citraconic acid, it is better for the reaction to be done in a short time.

Even though we will generate citraconic acid during heating, we still can get more than 100% conversion of itaconic acid in a short time. Within 2 hrs, itaconic acid can finish polymerizing. In the NMR spectrum for the reaction with 100% conversion in chapter II, the peaks of itaconic acid no longer present but sharp peaks remained around 5.85ppm and 1.95ppm. All the itaconic acid was polymerized, and only less than 0.5% monomer of the reactant remained in the form of citraconic acid.

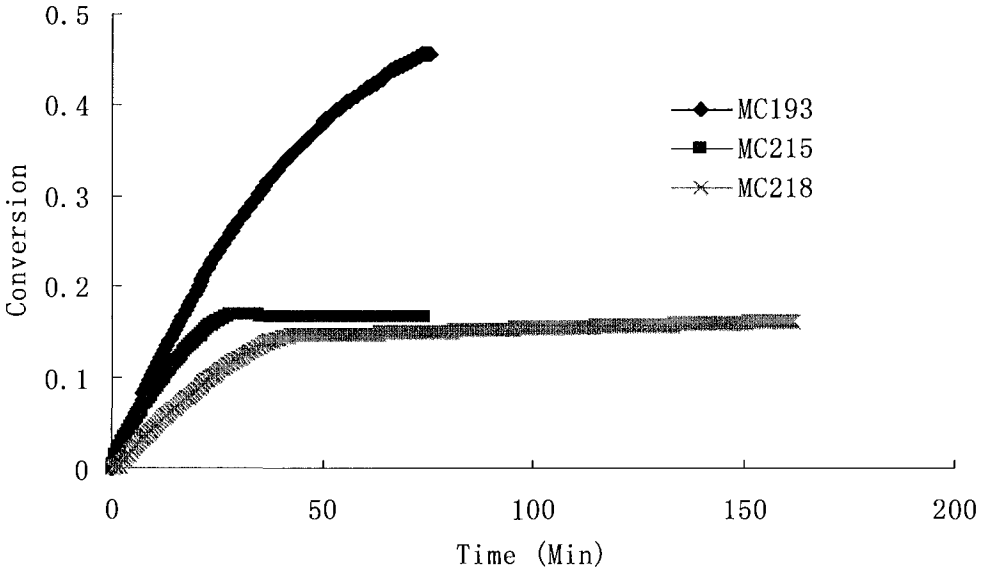

Figure 37, IA/CA copolymerization kinetics was compared with IA polymerization kinetics with the reaction calorimetry CPA 300. MC193 was the polymerization of IA. MC215 was the polymerization of IA/CA with ratio of 9:1. Ratio of IA/CA of MC218 was 19:1. Reactions were conducted at 100 °C. 0.5 ml 70wt% tBHP solution was added for all these reactions.

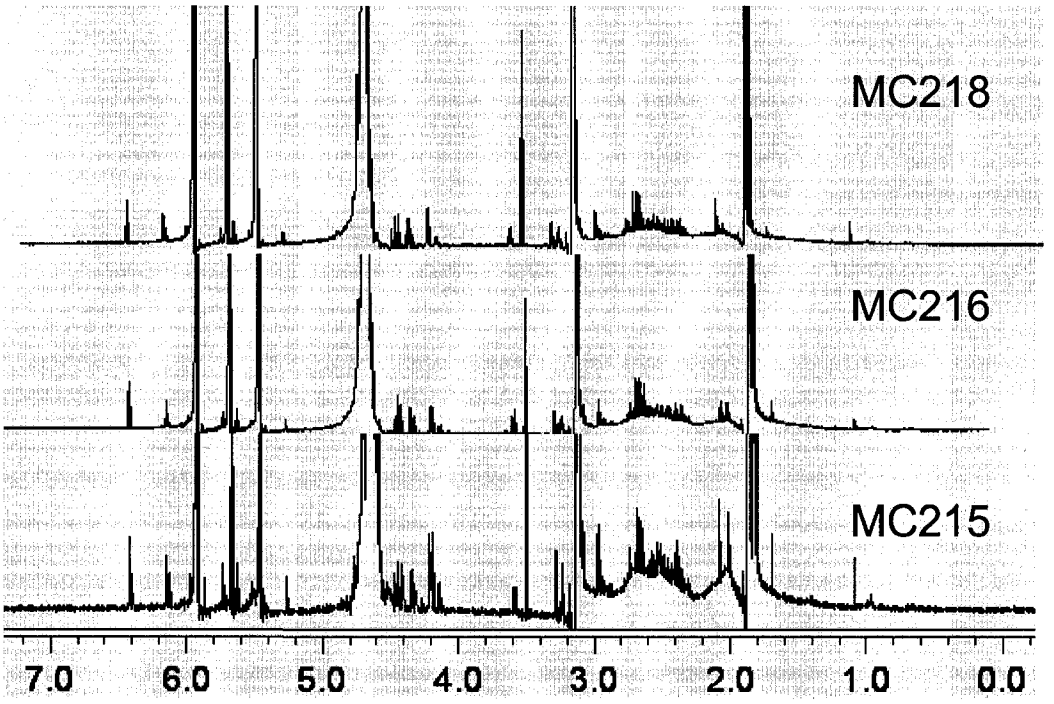

Figure 38, Polymerization of IA and CA mixture. MC215: IA/CA=9:1. MC216: IA/CA=4:1. MC218: IA/CA=19:1.

In order to further prove the existence of citraconic acid and its effect. We studied the polymerization of mixture of CA and IA. Citraconic acid and itaconic acid was mixed in aqueous solution. Sodium hydroxide was added to the mixture gradually with the cooling of an ice water bath to give half neutralization degree. The polymerization was done with a 6.2mol/l monomer concentration in the reaction calorimeter. 0.5 ml 70% tBHP solution was added at 100°C. The final sample was run in NMR with D_2O as solvent to give the final conversion. Polymerization kinetics with 10% CA and 5% CA in the mixture are plotted in figure 37. The polymerization kinetics are compared with that of itaconic acid in the same condition.

The effect of citraconic acid on polymerization rate is shown in Figure 37, heat flow for polymerization of CA/IA mixture ended in 40 minutes, indicating the end of the reaction. The polymerization of the mixtures reached lower conversions than the homo-polymerization of the itaconic acid alone. The conversion for the mixture with 10% CA reached 16% at the end of the reaction. The conversion is very close to that of Figure 36. The conversion for the mixture with 5% CA reached 14% at the end.

Figure 38 shows the NMR for the polymerization of IA and CA mixture. The spectrum for the mixture in Figure 38 indicates the same peaks as that in Figure 31 There is no bump around 1.0ppm in Figure 38 for all the spectrum in different ratio of the mixture, indicating there is no methyl group in the polymers. There is no copolymer structure of citraconic acid and itaconic acid. The polymer we obtained from the reaction of the mixture was pure homopolyitaconic acid.

During the polymerization, part of itaconic acid is changed to citraconic acid, the active radicals during polymerization process of IA were easily transferred to citraconic acid monomer. Radicals formed are very stable and non-reactive. The detail

of the product in this process needs further exploration. As a result, the CA generated during heating of IA is an inhibitor of polymerization of itaconic acid.

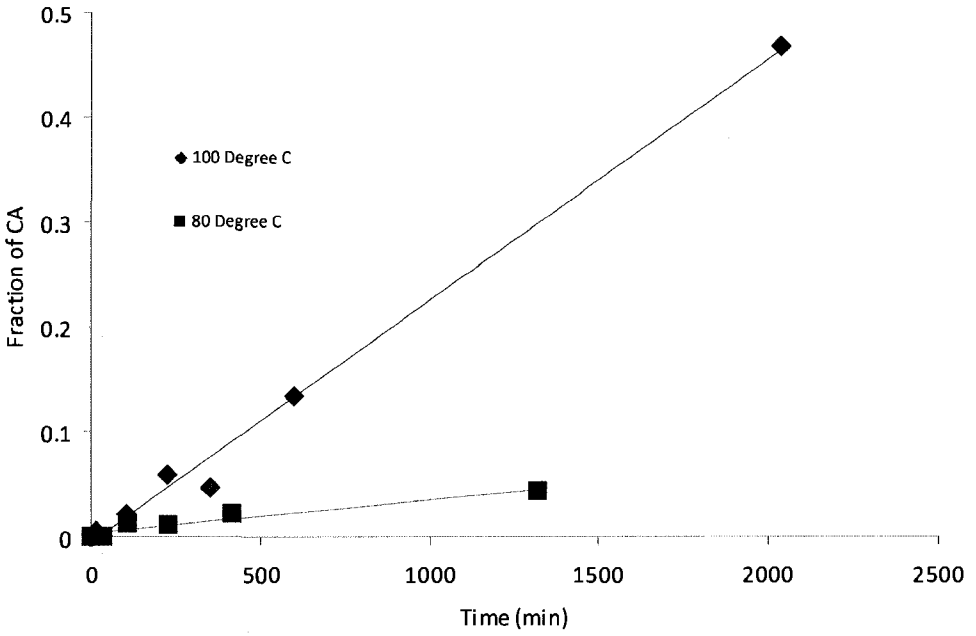

Figure 39 Fraction of Citraconic acid out of IA generated from heating at 80°C and 100°C.

Figure 39 shows the comparison of fraction of citraconic acid generated from heating at 80°C and 100°C. The reaction process is the same as the one we discussed at 110°C in this chapter. Obviously, the fraction of CA at 80°C is much less than that at 100°C. In four hours heating, only 1% of citraconic acid was generated at 80°C and 5% of CA at 100°C, and 10% at 110 °C. The Arrhenius constant Ea for this reaction is 88.1KJ/mol.

It is reasonable that we could obtain a certain conversion with less initiator at lower temperature. In order to prove the assumption, 0.77mol half neutralized IA was dissolved in 50 ml water and heated to 80°C. 0.1ml 70% tBHP solution was added.

The polymerization curve is shown in Figure 40. 50% conversion can be reached in 2 hours and 79.5% conversion can be reached in 18 hours polymerization.

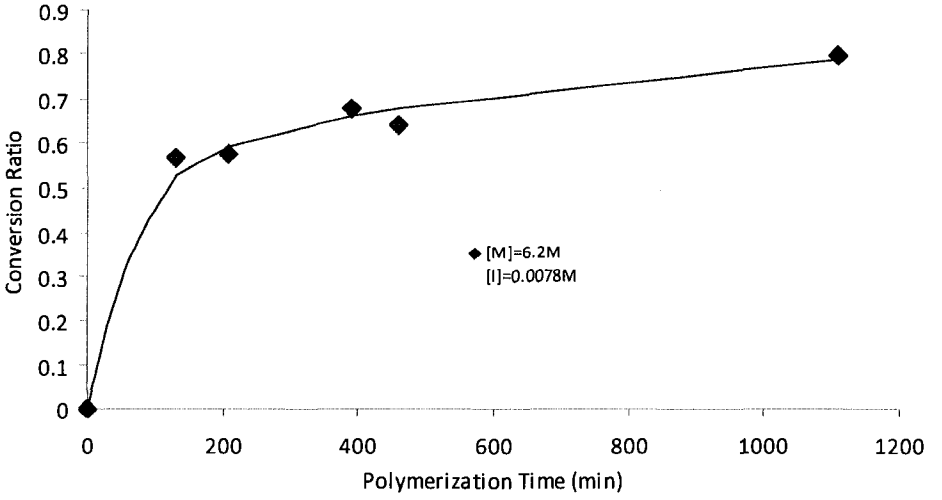

Figure 40 polymerization curve of IA at 80°C with 0.1ml 70wt% tBHP.

CHAPTER IV

SYNTHESIS AND CHARACTERIZATION OF ITACONIC SUPERABSORBENTS

We disclose a novel superabsorbent made from renewable resources. This SAP is a low crosslink density polyitaconic acid. The advantage is that itaconic acid was obtained from renewable resources. The biosynthesis of itaconic acid by fungi from carbohydrates was first reported by Kinoshita (1932). [2]. Compared with other SAPs made from renewable resource such as starch SAP and cellulose SAP, the process for the itaconate SAP is much simplier.

4.1 Commercial superabsorbent

Nowadays, most commercial superabsorbents are made by crosslinked partially neutralized acrylic acid. The pollution caused by plastics or rubber products increasingly serious in the United States. The disposable use of diapers containing non-degradable polymeric parts, create a serious threat to the environment. Composting the acrylate superabsorbents [102] requires hundreds of years to degrade. A superabsorbent based on itaconate can provides a potential solution to solve these problems above. Itaconic acid can be regarded as an α-substituted acrylic acid, which has two carboxyl groups in one monomer. Itaconic acid may be considered as a potential monomer to make a novel superabsorbent.

Nowadays, the price of itaconic acid is similar to the one of acrylic acid. And there is a large commercial supply of itaconic acid. These raw materials are used to make products based on the unreacted IA or an copolymers of itaconic acid with other

monomer. With the development of homopolymers of itaconic acid as we described in the previous chapter, it is expected that a large potential exist to further reduce the price of itaconic acid if the output of itaconic acid grows even larger.

The polymerization and characterization of acrylate superabsorbents is well described in the literature. There are three ways to prepare superabsorbent: 1. polymer chains are crosslinked by multivalent cations [12, 103-106]. 2. Polyol [107-110] such as glycerol are used to esterify carboxyl groups before or after polymerization. 3. The most common way to prepare superabsorbent, to copolymerize the monomer with a multifunctional crosslinker. The swelling capacity and elasticity are two key properties for SAP to be considered, which depend in part on the degree of neutralization, crosslinking density and distribution.

4.2 Crosslinked Gel by cation

We successfully obtained crosslinked PIA with cation at room temperature. 15g linear PIA (PIA-1) was dissolved in 260 DI-water and calcium cation was added dropwise over two hours. Faster addition of cation resulted in non-reversible precipitation. The PIA solution was continuously stirred with magnetic stir bar for one day to obtain a homogenous hydrogel. The recipe is shown in table 4.

Component	Amount
PIA sample(wet)	15g
H_2O	260ml
$CaCl_2$	2g
	25°C
	24 hr stir

Table 4 The recipe of cation crosslinked polyitaconic acid

The positive charge on cation and negative charge on the carboxyl groups of polyitaconic acid form a salt linkage. Beside Ca^{2+} used here, other multivalent cation can also crosslink the polyitaconic acid linear chains.

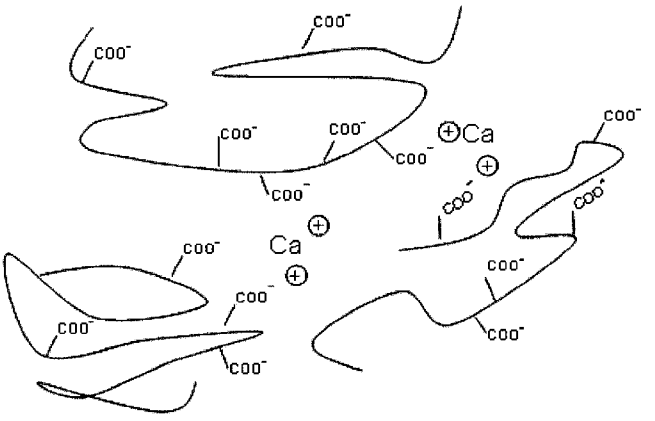

Figure 41 mechanism of PIA crosslinking with multivalent cation

The hydrogels were dried in vacuum for 24 hrs. The dried samples were tested for their swelling capacity in DI-water. The swelling process is reversible. The swelling capacity can reach 20 times. However, this method is not suitable for industrial application because of the time and energy consumption involved in this process.

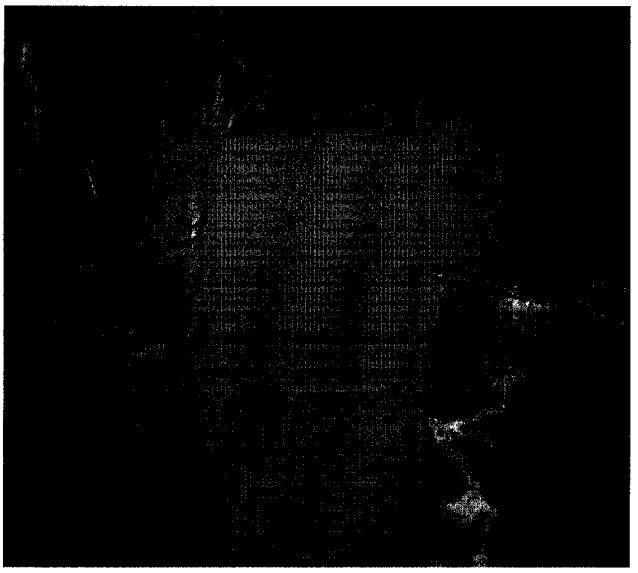

Figure 42 Ca2+ crosslinked poly(itaconic acid) gel swelled 20 times with water

4.3 Itaconic superabsorbent prepared by copolymerization

The most efficient way to prepare itaconate SAP is to copolymerize monomer with a crosslinker during polymerization.

4.3.1 Experimental

Materials

All solvents and monomers were purchased from Aldrich. Itaconic acid (99+%), 70% tert-Butyl hydroperoxide solution (tBHP), Tetra(ethylene glycol) diacrylate (tEGDA) were used without further purification, divinyl benzene (DVB), ethyleneglycol dimethacrylate (EGDMA) and ethyleneglycol diacrylate (EGDA) were purified by activated alumina to remove MEHQ.

4.3.2 Free-radical polymerization of itaconic superabsorbent in aqueous solution

Different ratios of tEGDA and 0.77mol half neutralized itaconic acid were dissolved in 50 ml DI-H_2O. Polymerization was initiated by 0.5ml 70% tBHP at 100 °C under a N_2 environment. Crosslinked samples were obtained. Swelling capacity of crosslinked polymers was measured without further drying the sample. Since water and PIA form strong hydrogen bonds, it is very difficult to dry samples.

The experiments have been repeated with 4 ml of tEGDA and with different neutralization degree of IA monomer at 70% and 90 %. Final samples are soluble in water.

4.3.3 Swelling Properties measurements

1 square inches heat-sealable tea bags [111, 112] were used to measure swelling capacity. 0.5 gram of the crosslinked polyitaconic acid powder was sealed into the bag, and then the bag was immersed into DI-water or sodium salt aqueous solution at different concentration to absorb water for a given length of time. The swelling capacity and the absorption rate were measured at room temperature without additional stirring. The weight of swollen sample in tea bag was measured after removing the unabsorbed fluid with paper towels. The water absorption was calculated as a mass ratio of absorbed liquid over dry crosslinked polymer. [113-116]

$Q = (W_s - W_d)/W_d$

Where Q (g/g) is the liquid absorption, W_s is the weight of swollen sample and W_d is the weight of dry sample. The weight of dried sample was evaluated from the recipe of the reactants. The maximum swelling is considered to be at 10 hours

swelling.

Sample No.	Crosslinker Concentration (mol/l)	Initiator Concentration (mol/l)	Max. Swellling (g/g)
cPIA-1	0.148	0.0313	32.16
cPIA-2	0.118	0.0313	40.81
cPIA-3	0.0889	0.0313	56.64
cPIA-4	0.0593	0.0313	Soluble in water
cPIA-5	0.118	0.0626	98.34
cPIA-6	0.118	0.0939	80.20
cPIA-7	0.118	0.1252	50.17

Table 5 Swelling ratio and fraction of soluble polymer as function of the concentration of crosslinker. The monomer concentration for the polymerizations was 6.2 mol/l. All reactions were done in 100°C for 2 hours

4.4 Result and discussion

There are three important properties for superabsorbent: swelling capacities, absorbency rate and absorbency under pressure. Swelling capacities were primarily affected by crosslink density and neutralization degree. Crosslink density and particle size and morphology influence the absorbency rate. The absorbency under load has an exponential relation with crosslinking density.

4.4.1 Free absorbency

The water superabsorbent swells in water according to the following steps[117-119]: the charged groups of polymer form hydrogen bond with water from external surroundings. The electrostatic repulsion between charged groups gives more

room for water to come in. The driving forces for the liquid mobility are the Gibbs-Donnan effect and free energy of mixing of the solvent and polymer. The equilibrium is achieved when the ionic and mixing effect are balanced by the elastic response of the network.

The chemical potential[120-122] is the combination of the three contribution $\Pi=\pi_{mix}+\pi_{net}+\pi_{ion}$

The lower the crosslink density of superabsorbent is, the lower the absolute value of π_{net} is. π_{net} is the negative item in the equation. The chemical potential increases with the decrease of crosslink density, which allows the sample to absorb more liquid.

4.4.2 Selection of Crosslinker

The crosslinker is the most sensitive factor in the successful preparation of PIA superabsorbents. There are three major aspects of crosslinker: 1. The solubility of the crosslinker decides the effective concentration of crosslinker in the reaction. 2. the reactivity ratios of crosslinker and itaconic acid. The higher the reactivity ratio of the crosslinker is, the more tendency of the crosslinker to be depleted at the early stage of the reaction, which results in a larger soluble fraction in the product. For example, in preparation of acrylate superabsorbent, methylene bisacrylamide (MBA)[123-127] and trimethylol propane triacrylate (TMPTA) [128-131] are depleted in earlier stage of polymerization to produces more soluble polymer in the end.[58, 74, 132, 133] The relatively low reactivity of the first vinyl group of crosslinker ensures it can incorporate into the polymer networks at the end of the polymerization. However, reactivity ratio is difficult to be measured directly for crosslinked superabsorbent

polymers without dissolving it in any solvent. 3. The reactivity ratio of pendent vinyl group of crosslinker. In general, the crosslinker molecule contains two or more double bonds. After the first vinyl group is incorporated into polymer chain, the steric hindrance increases and mobility of the vinyl group is reduced. The reactivity ratio of the pendent vinyl group is much less than the first one. In order to be incorporated into polymer network, the reactivity of the second vinyl group must be high enough.

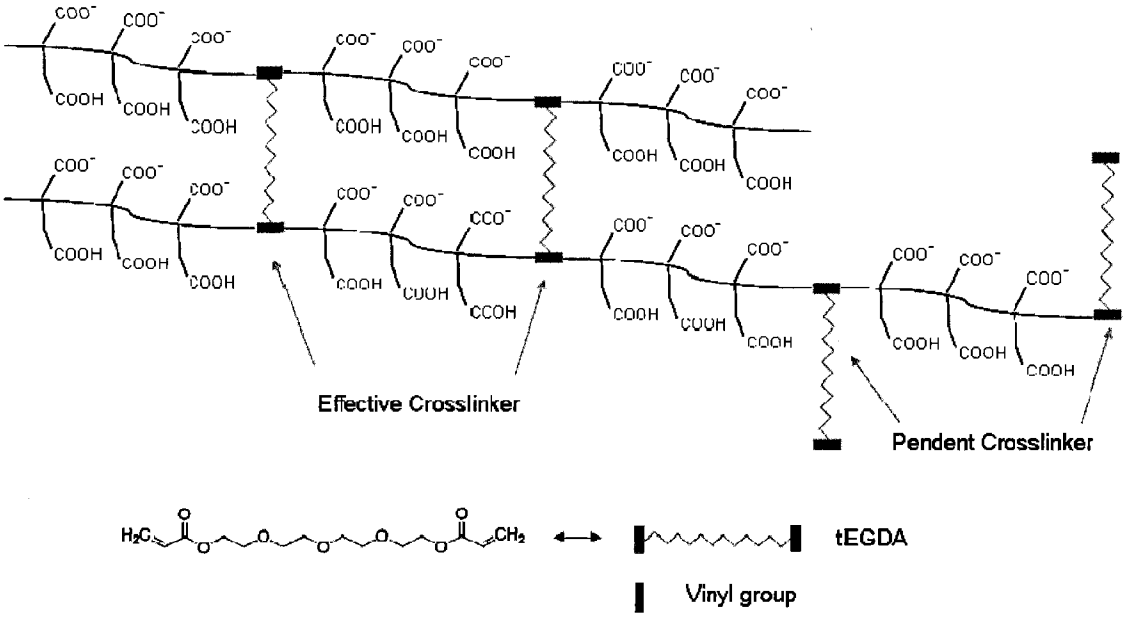

Figure 43 Structure of copolymer of tEGDA and IA.

tEGDA is the crosslinker we selected for our polymerization process to yield itaconic superabsorbent. The swollen itaconic superabsorbent with tEGDA as a crosslinker is shown in figure 45. Two reasons gives this success: 1. tEGDA is miscible with water. 2. The reactivity ratio of pendent vinyl group of tEGDA is relatively high. tEGDA has the same acrylate residue in the molecule as TMPTA and EGDA, so the reactivity ratio of first vinyl group of crosslinker do not have large differences. But the reactivity ratio of pendent vinyl group is high compared to other

crosslinker (see below). The flexibility of tEGDA molecule provides relatively high mobility. It is a required feature of crosslinker in this system to copolymerize two vinyl groups with itaconic acid, giving an effective structure for networks as seen in Figure 43 shows. Figure 43 also indicated that the unreacted pendent vinyl groups do not contribute for the network formation.

We failed at effectively crosslinking PIA with TMPTA, divinyl benzene (DVB), ethyleneglycol dimethacrylate (EGDMA), ethyleneglycol diacrylate (EGDA) as crosslinker using the same free-radical polymerization process as described above. These crosslinkers are slightly soluble in water. The solubility of these crosslinkers in water can satisfy the requirement for crosslinking polyacrylic acid, which requires less than 0.1% crosslinker out of all reactants. Since the Mn of itaconic acid is much less than that of polyacrylic acid, it requires higher crosslinker concentration to form a polymer chain network at the end of the reaction. The solubility of these crosslinkers is not satisfying for itaconic system. The low reactivity of remaining vinyl group might be the other reason for the failure.

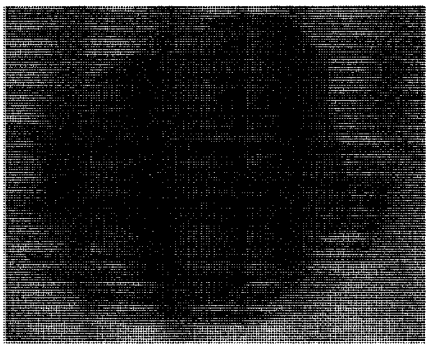

Figure 44 Swollen crosslinked polyitaconic acid

4.4.3 Polymer-solvent interaction

When water is added to SAP, there is a polymer-solvent interaction including

hydration and formation of hydrogen bonds. The polymer-water interaction parameter χ takes account of the energy of dispersing the polymer molecules and the water. In order to evaluate the value of solvent-polymer interaction parameter, we assume that the crosslinker in the PIA network is the same as crosslinker fraction in the reactants, and Mn can be evaluated from the data for linear PIA with the same process except no crosslinker (Mn=7,930 g/mole). We can calculate the value of Mc and Mc/Mn. We calculated that χ - the polymer-solvent interaction parameter for sodium itaconate SAP is 0.451. Compared with Flory-Huggins interaction parameter for sodium acrylate SAP: χ = 0.469, [134] the values are similar. The interaction of itaconate SAP and water is as strong as that of acrylate SAP and water.

4.4.4 Polymerization time

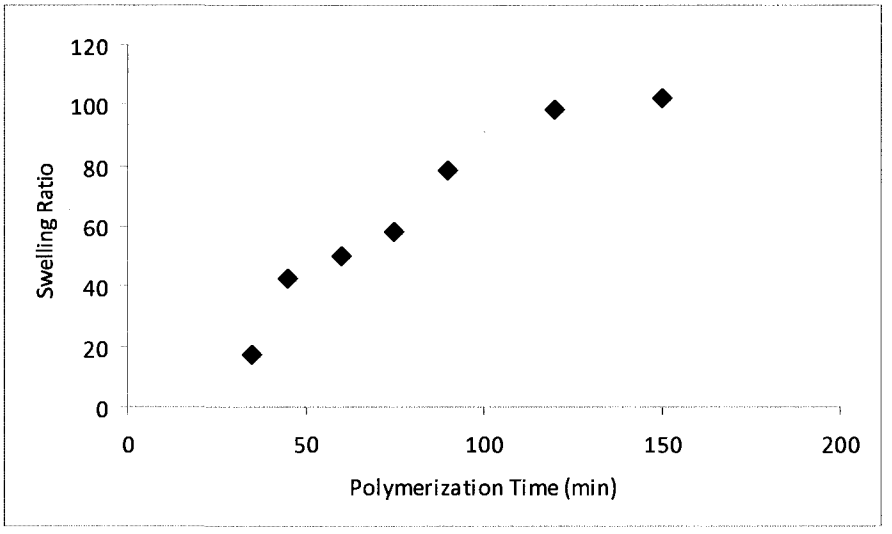

Figure 45 swelling capacities at various polymerization times. Crosslinker concentration of this sample is 0.118 mol/l. (Sample 5)

Various samples were prepared at different polymerization time with 0.118

mol/l crosslinker concentration. With the polymerization time, the swelling capacity increases until 2 and half hours of reaction time. More pendent vinyl groups from the crosslinker are incorporated into polymer chains. More and more polymer network forms with polymerization time.

4.4.5 Ionic effect on swelling capacity

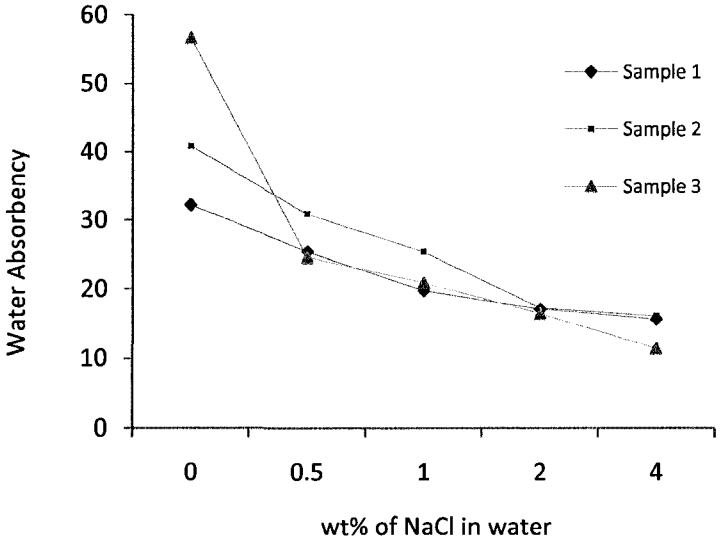

Figure 46 Water absorbency versus concentration of NaCl as a function of the different ratios of crosslinker to itaconic acid.

It is necessary to measure the absorbency of superabsorbent in an ionic environment because most products application of superabsorbent are used for body liquid with 0.9 % ion concentration. The equilibrium swelling behavior of itaconic superabsorbent is shown in Figure 46. With the increase of concentration of ions in the environment, the chemical potential difference between the polymer gel and the

solvent decreases rapidly, resulting in dramatically reducing the absorbency rate and swelling ratio in equilibrium. The swelling ratio at equilibrium can be expressed by a function of ionic strength[78, 135-137].

$$Q_m^{5/3} = [(i/2v_u S^{1/2})^2 + (1/2 - \chi_1)/v_1]/(v_e/V_0)$$

Where $(1/2-\chi_1)/v_1$ is the affinity between polymer and solution, and v_e/V_0 is the crosslink density, i/v_u is the concentration of fixed charge, S is the ionic strength.

In Figure 47, shows a linear relationship of $Qm^{5/3}$ and 1/S. With this relation, the value of absorbency at any ionic concentration can be calculated.

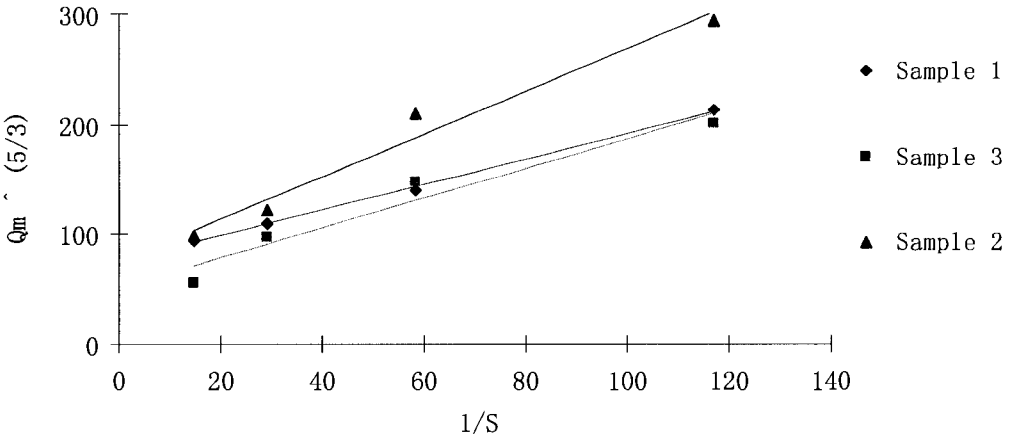

Figure 47 linear relationship of $Qm^{5/3}$ and 1/S

4.4.6 The Effect of Degree of Neutralization on Swelling Capacity

To study the effect of neutralization degree on the swelling rate of itaconate superabsorbent (Sample 2), certain amounts of sodium hydroxide were added into half neutralized PIA in 67wt% aqueous solution at 100°C with 400rpm mechanical stirring. The mixture was stirred for half an hour to give a clear solution and a specific neutralization degree. The final samples were taken out, cooled down and sealed into

tea bag and the swelling ratio was measured in DI-water. We did not obtain homogeneous sodium itaconate hydrogel just by mixing sodium hydroxide and the initial hydrogel to reach certain neutralization degree at room temperature. Part of the sodium hydroxide stays outside of the hydrogel.

The neutralization degree of itaconic acid definitely affects the water absorption. 75% neutralization degree [48] for the acrylic superabsorbent was found to have the best swelling capacity. For itaconate superabsorbent, the maximum swelling capacity happens when 70 % neutralization is reacted. Lower neutralization degree decreases the ionic concentration in the polymer gel phase, so that the osmotic pressure decreases because of the lower chemical potentials between the network and the solution. When the neutralization degree goes higher than 70%, there are no available carboxylic groups on the polymer chain to be dissociated. The other 30% of carboxylic groups are buried in the polymer network and can not be reached by sodium cation. The extra salt we added is free in the solution, reducing the chemical potential of the sample in water environment instead of neutralizing carboxyl groups. The swelling capacity decreases.

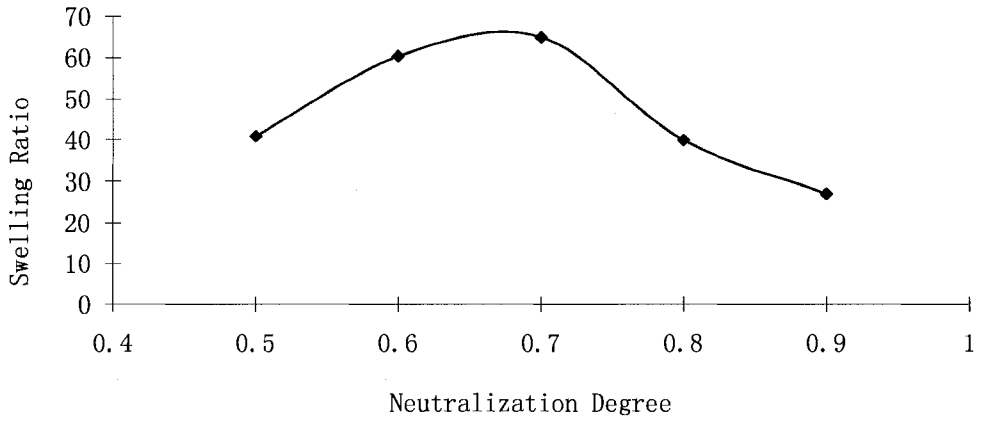

Figure 48 Effect of the neutralization on swelling capacity of itaconate superabsorbent. (Sample 2) Neutralization degree of the sample was adjusted during mechanical stirring at 100°C.

4.4.7 Initiator Concentration

The polymerization rate increases with the increase of initiator concentration, meanwhile, molecular weight in linear polyitaconic acid reaction decreases, which is commonly observed in free radical polymerization. For crosslinking polymerization of IA, the initiator concentration affects the crosslink density and fraction of soluble part. In table 5, the highest swelling capacity was obtained in sample 5 with initiator concentration at 0.0626mol/l. With the increase of initiator concentration, the molecular weight between crosslink decreases, so that the increase the crosslink density of the sample, results in the decrease of the swelling capacity. However, a smaller initiator concentration causes an increase of the fraction of soluble polymer.

4.4.8 Absorbency under load (AUL)

In practice, the external pressure must be considered when making superabsorbent as a product.

In order to characterize the SAP to simulate applications to diapers, the swelling behavior of the SAP was measured under load. Three samples with different crosslinker concentration were ground, and the powder was screened with standard sieve (Fisher Science) to desired size. The sample with mesh size 25 to 32 was used for AUL testing. 0.3 gram of sample was sealed into tea bag. And then was replaced to a 250 ml beaker. Sample powder was spread as even as possible. Bottles with 1.2 square inch bottom area and different weight were placed on the top of the tea bags to apply different pressures. Small amounts of DI-water were added to the beakers. After 10 hrs, the samples were taken out and the surfaces were blotted up with napkin and weighed. As Figure 49 shows, the absorbency under load decreases with the pressure as expected. The higher the crosslink density is, the more capability to keep liquid

under load is expected to be.

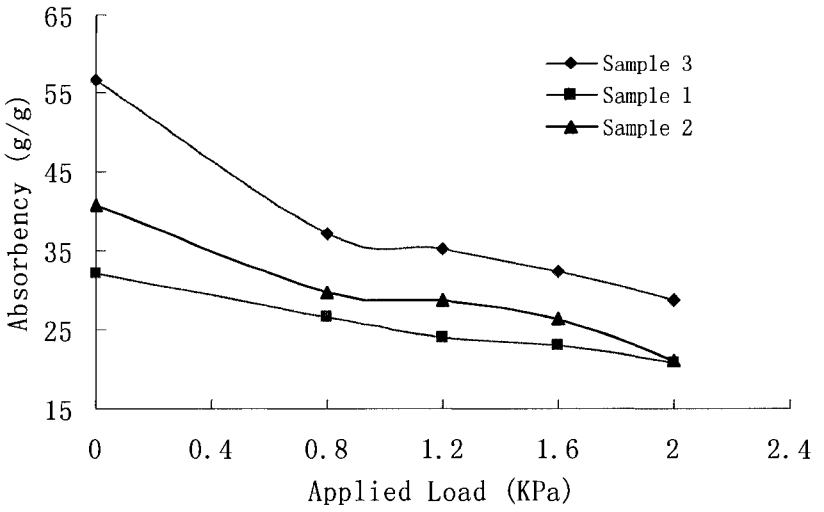

Figure 49 Absorbency versus applied pressure for three different samples. Sample 1, sample 2 and sample 3. All samples were swollen in DI-water

Also, the crosslink density can be evaluated with the storage modulus of the network chain. The storage modulus can be calculated by the equation below, High storage modulus of network means high crosslink density. With the increase of crosslinker concentration added into the reaction, higher storage modulus were obtained. The storage modulus is 1.47±0.19 for sample1, 0.88±0.23 for sample 2, 0.603±0.07 for sample 3. Highest crosslink density was observed for sample 1 with initial crosslinker concentration at 0.148mol/l.

$$Q = \frac{Q_e}{1.02(1+P/G_e)^{0.44}}$$

Where P is the applied load, Ge is the elastic modulus of the network, Q is the swelling capacity without load, Qe is the swelling capacity under load. [138, 139]

Applied Load (KPa)	Storage Modulus (KPa)		
	Sample 1	Sample 2	Sample 3
0.8	1.675297	0.819935	0.540438
1.2	1.430235	1.081222	0.670143
1.6	1.530651	1.03529	0.658598
2	1.223976	0.582845	0.545216

Table 6. Storage modulus and fraction of swelling ratio under load were calculated for different samples. 0.8, 1.2, 1.6, 2KPa external pressure was applied on each sample.

4.4.9 Swelling kinetics

The absorbency rate is shown in Figure 50. The swelling process can be considered as a diffusion process [118, 140-142]. The swelling kinetics of superabsorbent without load can be expressed by Fick's second law of diffusion [143-145]:

$$Q(t) = Q_{max}\left(1 - e^{-kt}\right)$$

where Q_{max} and Q(t) are the maximum swelling capacity at equilibrium and swelling capacity at certain swelling time. k is the constant for swelling rate. The constant k is affected by the structural feature of the network such as crosslink density and distribution and particle size.

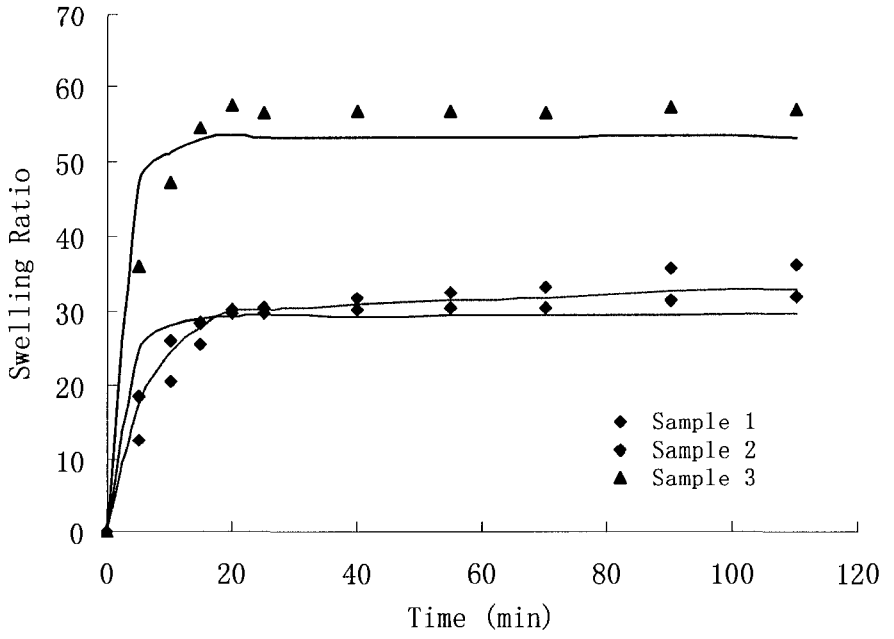

Figure 50 The swelling kinetics for PIA sample 1, 2 and 3. The line is the theoretical curve of the swelling rate for the DI-water environment. Particle size is 25-32 mesh.

Sample No.	Max. Swelling (g/g)	K (min^{-1})
1	32.16	0.08
2	40.81	0.05
3	56.64	0.045

Table 7 constant for swelling rate for sample 1, 2 and 3.

In order to plot a theoretical curve for best fitting of experimental data, the value of the constant k was adjusted. The maximum swelling ratios and values of K for different samples are shown in table 7.

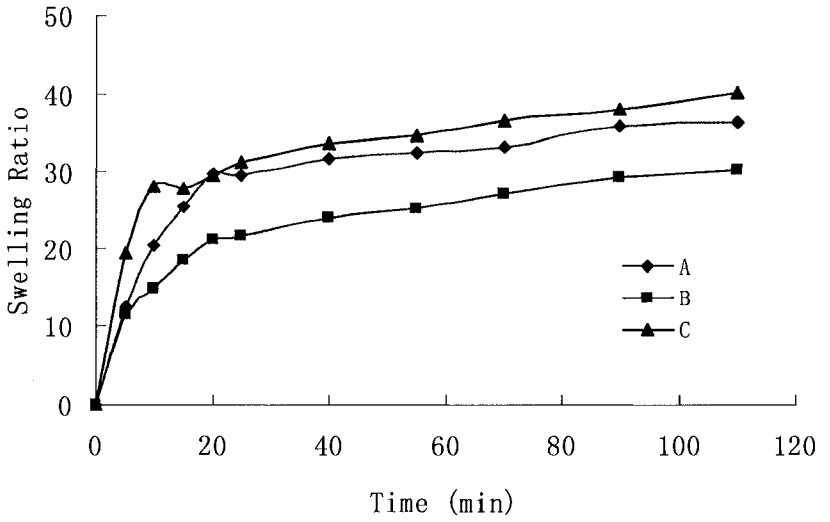

Figure 51 swelling kinetics for sample 2 with different particle size. A: 25-32 mesh, B: 35-60 mesh, C: 150-200 mesh.

Figure 51 shows the swelling kinetics with different particle size. The sample with size at 150 – 200 mesh has the fastest initial absorbency rate and highest swelling ratio at 120minutes.

4.4.10 Swollen gel under compression

0.5 gram of sample was sealed into 1 square inch tea bag and immersed into DI-water or salt solution until it reaches maximum swelling. Swollen samples in the tea bag were replaced in a 250 ml plastic beaker. The tea bags can cover the bottom of the beaker perfectly. 250 ml plastic bottles filled with water were replaced on the top of the sample to apply 1.6 KPa pressure. After 10 hrs, the samples were taken out and their surface was blotted dry with paper napkins and weighed. Figure 52 shows the swelling capacities after compression. The liquid comes out of the gel under the external pressure until a new equilibrium forms. The higher crosslinker concentration during polymerization, the more capability to keep liquid under load was observed. It

is also observed that the percentage of absorbency under compression do not change with the NaCl concentration for each sample.

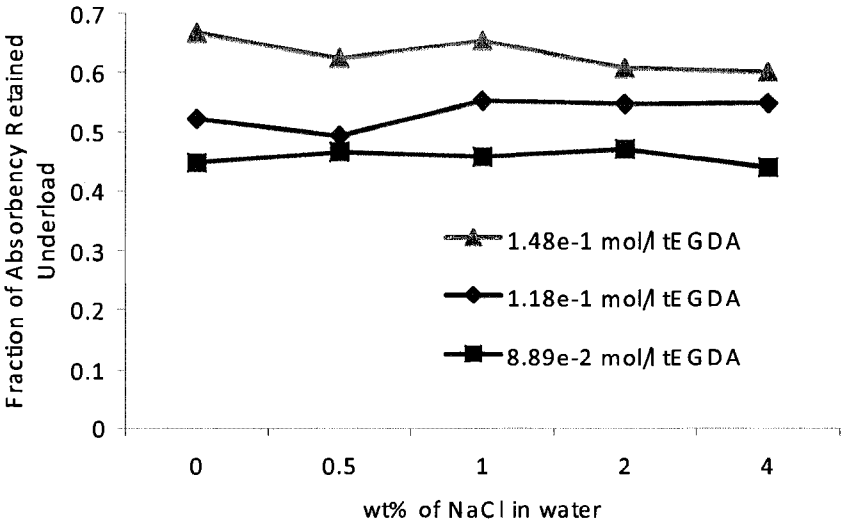

Figure 52. Retained absorbency under load as a function of concentration of NaCl.

4.5 HEA/IA and HEMA/IA Superabsorbent.

We obtained superabsorbent by copolymerizing HEA with IA and HEMA and IA at different molar ratios. The advantage of these novel superabsorbents – crosslinked poly(sodium itaconate-co-hydroxyethylmethacrylate) and crosslinked poly(sodium itaconate-co-hydroxyethylacrylate) is not required a crosslinker during the polymerization process. Some work for AA/HEA or AA/HEMA superabsorbent crosslinked with multivinyl crosslinker is reported, such as crosslinked poly(sodium acrylate-co-hydroxyethylmethacrylate) with N,N-methylene-bis-acrylamide (NMBA) as crosslinker. [146]

4.5.1 Experimental

Materials

Itaconic Acid (IA); Tertiary Butyl Hydroperoxide; DI-water were used without

further purification. 2-hydroxyethyl methacrylate (HEMA); 2-hydroxyethyl acrylate (HEA) was purified by activated alumina to remove MEHQ. All samples were purchased from Aldrich.

4.5.2 Synthesis for Poly(itaconic acid/2-hydroxyethyl acrylate) in aqueous solution

100g (0.77 mol) of itaconic acid was half neutralized with 30.8g (0.77 mol) sodium hydroxide, and was dissolved in 50ml of deionized water into a flask, different amount of 2-hydroxyethyl acrylate or 2-hydroxyethyl methacrylate were added. The mixtures were heated to 100°C. Nitrogen was purged in the solution for 10minutes before heating, and 1ml tBHP (70wt% water solution) was added. Reactions were conducted for 2 hours. The swelling capacity of the products was measured without drying.

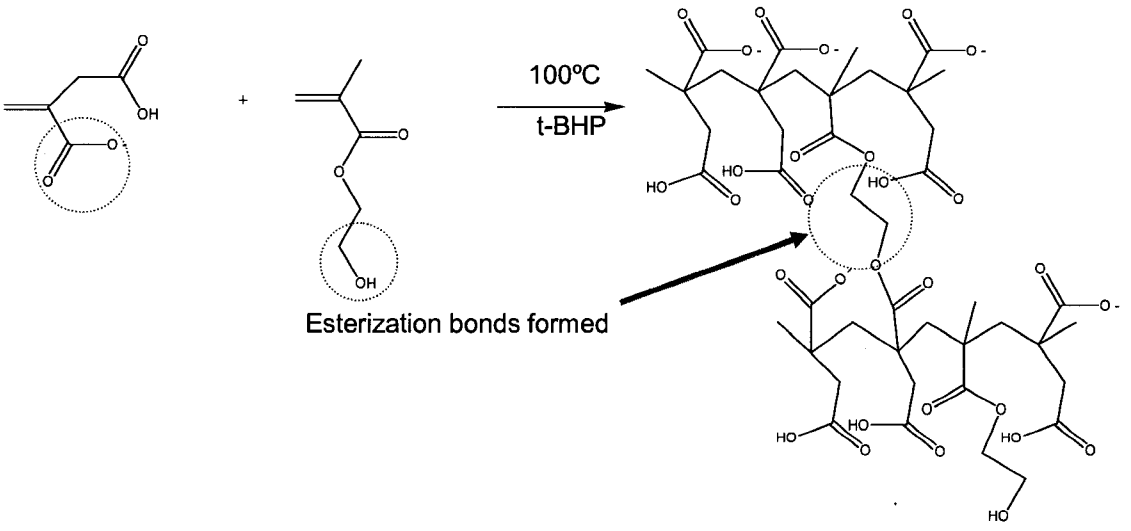

Figure 53 Synthesis for Poly(itaconic acid/2-hydroxyethyl acrylate) in aqueous solution

4.5.3 Results and discussion

Table 8 shows the composition and properties of the crosslinked hydrogels prepared. The swelling capacities are all above 100. Low crosslinking network densities were obtained. Ester bonds formed between the hydroxyl and carboxyl groups to provide the network structure. The key factor of the formation of ester bonds is the high concentration of reactant. The reaction was driven to the ester side by using as little water as possible.

Sample No.	Co-1	Co-2	Co-3	Co-4	Co-5	Co-6
Component	IA/HEMA	IA/HEA	IA/HEA	IA/HEA	IA/HEA	IA/HEA
Mole Ratio	4/1	3/2	4/1	4/1	9/1	19/1
Reaction Time (hrs)	1.5	1.5	0.75	1.5	1.5	1.5
Swelling Capacity (g/g)	144.8	165.7	138.9	115.8	-	-
Absorbency in 0.9% NaCl (g/g)	34.9	43.3	37.8	35.3	-	-
Fraction of Soluble Part	35.7	-	5.3	30.3	100	100

Table 8 Copolymers of IA/HEMA or IA/HEA were prepared according to the ratios shown in the table. Swelling capacity was measured in heat-sealable tea bag without extraction of soluble part. Ultimate swelling capacity was assumed to be reached at 10 hours. The fraction of soluble polymer was obtained by drying the water phase in vacuum oven for 3 days under 120 °C. Monomer concentration is 6.2M.

In table 8, Co-2 and Co-3 with ratio of IA/HEA at 3/2 and 4/1 have the highest swelling capacities above 130. We can not obtain crosslinked polymer when ratio of IA/HEA is above 9/1. It means there is not enough ester bonds between carboxyl groups and hydroxyl groups formed to provide a network structure at that low fraction of HEA. Swelling capacity of IA/HEA SAP at 0.75 hrs reaction time (Co-3) was observed as similar as that of SAP at 1.5 hrs (Co-4). More soluble polymer were observed for Co-4 than Co-3. The ester bonds are reversible in the presence of water at high temperature.

The hydroxyl group of HEA does not dissociate in water. With the increase ratio of HEA used, the total amount of dissociated ions in the hydrogel decreases. The lower absorbency is expected if other parameters are the same. However, absorbency of Co-2 is higher than Co-4. The reason might be that lower crosslink density or less soluble part are present in Co-2. This needs further exploration.

Moreover, the swelling capacity of these SAPs was measured in 0.9% NaCl water solution. More than 70 % loss in absorbency in 0.9% salt water was observed.

4.6 Morphologic feature of SAP particle

Scanning electron microscopy were used to measure the surface details with a depth of field and high resolution. Morphologic features of SAP particles such as size distribution and porosity can be determined. A sample of the depth of field is shown in Figure 54. Particle size was determined by Microtrac. The particles were first suspended in air through a nozzle. The air velocity remains constant in the measurement region. As the particles pass through laser for measurement, the light is scattered and particle size is calculated.

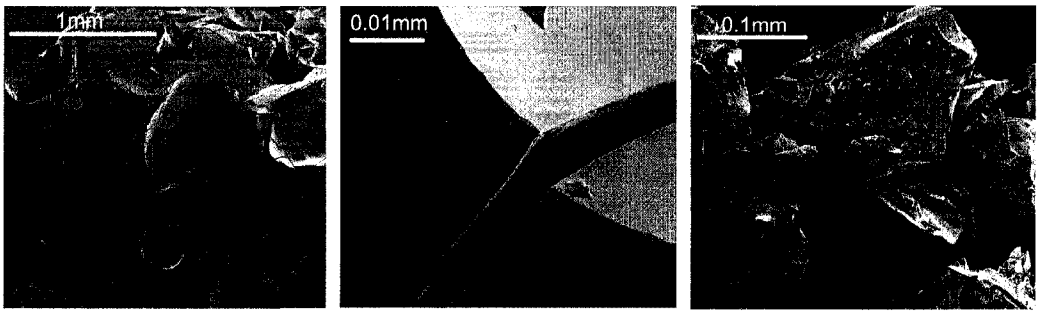

Figure 54 Foam particle with porosity structure Surface detail with depth of field Ground fine powder with area average size MA = 21.18 micrometer

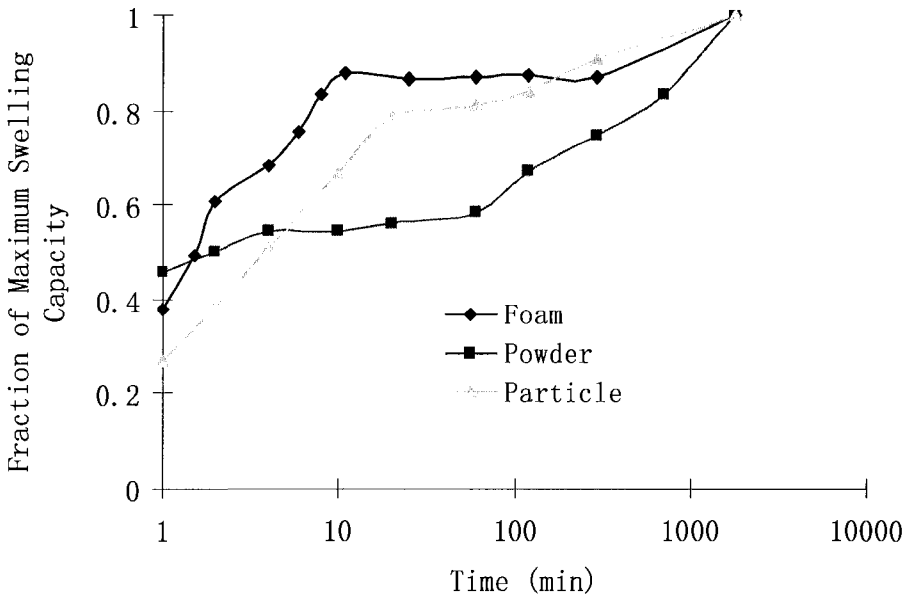

Figure 55 Fraction of Maximum swelling capacity as a function of swelling time with different morphologic feature of samples. Size of foam: 1-3mm, particle: 1-3mm, power: MA=0.021mm

A foam sample was prepared with compression molding of 38% water content HEA/IA copolymer. Porosity structure and crack can be seen from the surface detail in the SEM image. The porosity structure of this SAP helps increase its swelling rate. SAP particle used in industrial products cover the range of particle diameters from 100 to 850 micrometer.

4.7 Thermo-analysis of itaconic superabsorbent

Table 9 shows itaconic acid and polyitaconic acid samples used for thermo-analysis. Thermogravimetry analysis were run in a TA 4000. Heating speed were 10 °C. The weight of each sample was about 20 mg. Samples were heated under protection of nitrogen flow. The nature of each Samples were is in the table below. Differential scanning calorimetry was run in a TA Q2000. Heating speed was 10 °C.

Sample No.	Component
1	Itaconic acid
2	Half Neutralized Itaconic acid (36% water content)
3	Acidified polyitaconic acid with 100% conversion
4	Acidified crosslinked polyitaconic acid (mole ratio of IA/tEGDA: 42:1)
5	Neutralized crosslinked polyitaconic acid (mole ratio of IA/tEGDA: 42:1)

Table 9 The samples of itaconic acid and polyitaconic acid used in thermoanalysis

In Figure 56, over 90% weight loss was observed at 210 °C for itaconic acid. For neutralized polyitaconic acid (Sample 3), we observed two major changes in the curve; the first one is 12% weight loss was observed at 125 °C. It is the evaporation of water existing in the sample. Therotically, more than 30% water was remained in the sample, water form strong hydrogen bond with neutralized carboxyl groups so that prevent the loss of the rest of water. The other one around 270 °C is the formation of polyitaconic anhydride. 80% weight out of total weight remained in 400 °C.

4.7.1 Drying

Moisture percentage in PIA sample is an important feature. PIA or crosslinked PIA with too much moisture may become sticky and difficult to grind, package and transport.

Traditionally, the percentage of moisture in SAP was obtained after heating at 105 °C for 3 hours, which was recommended by the Technical Association of the Pulp and Paper Industrial. [147] Significant moisture remains in neutralized PIA after heating 105 °C for 24 hours. Previsouly, PIAn was observed to form at acidified PIA after drying at 60 °C for 10 hours with vacuum. [148]

Neutralized PIA solution was added extra amount of HCl and precipitated in 5 times acetone for three times. The precipitated acidified PIA was drying in the oven with vacuum at room temperature. Drying in room temperature instead of higher temperature is for avoiding formation of anhydride. Figure 56 shows only 0.74% weight loss for the dried acidified PIA at 140 °C.

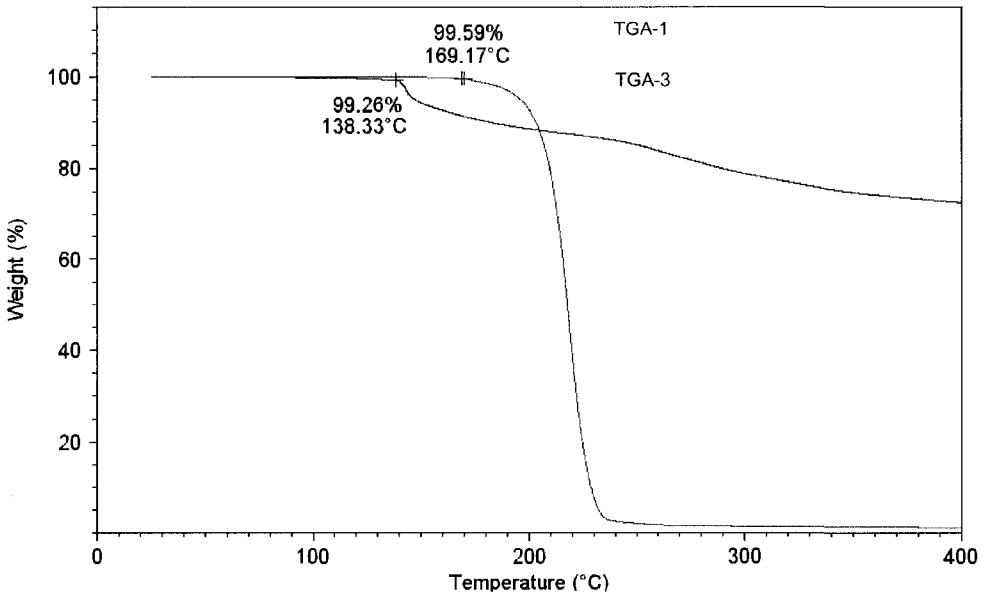

Figure 56 TGA data for dried itaconic acid and polyitaconic acid with vacuum oven in room temperature

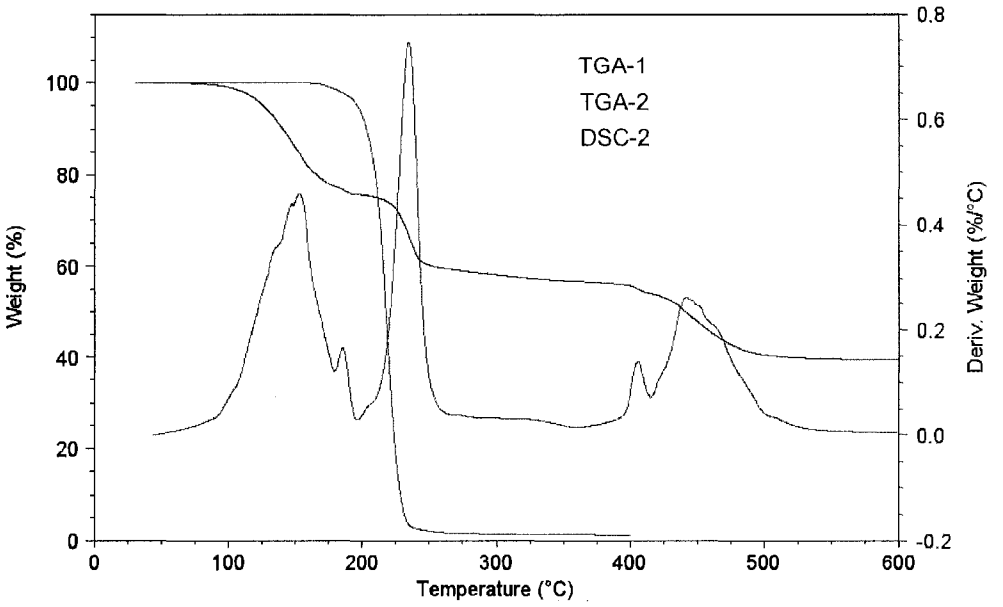

Figure 57, Thermodegradation analysis and DSC of itaconic acid (sample-1) and half neutralized IA samples (sample 2). TGA and DSC was run from room temperature to 600 °C.

Figure 57 shows the thermodegradation of half neutralized IA. There are two carboxyl groups in IA, one is neutralized and the other is in acid form. The neutralized carboxyl group forms much stronger hydrogen bond with each other. In the TGA data, the first 22% weight loss before 180 °C is for water evaporation. The second 18% weight loss at 230 °C is for anhydride formation of acid form carboxyl group. The third 18% weight loss around 400 °C is for dehydrate of the other neutralized carboxyl group. This temperature is the dehydrate point for sodium carbonate. Compared with acidified IA, there is no boiling point for neutralized IA.

4.7.2 Glass transition temperature

The glass transition occurs at micro-Brownian motion of the chain segments in the polymer chain backbone. [149] Figure 58 is the DSC data for dried acidified PIA (Sample DSC-3). Thermo-transition of the sample was clearly shown in the DSC

curve. Tg for dried acidified polyitaconic acid is 61 °C.

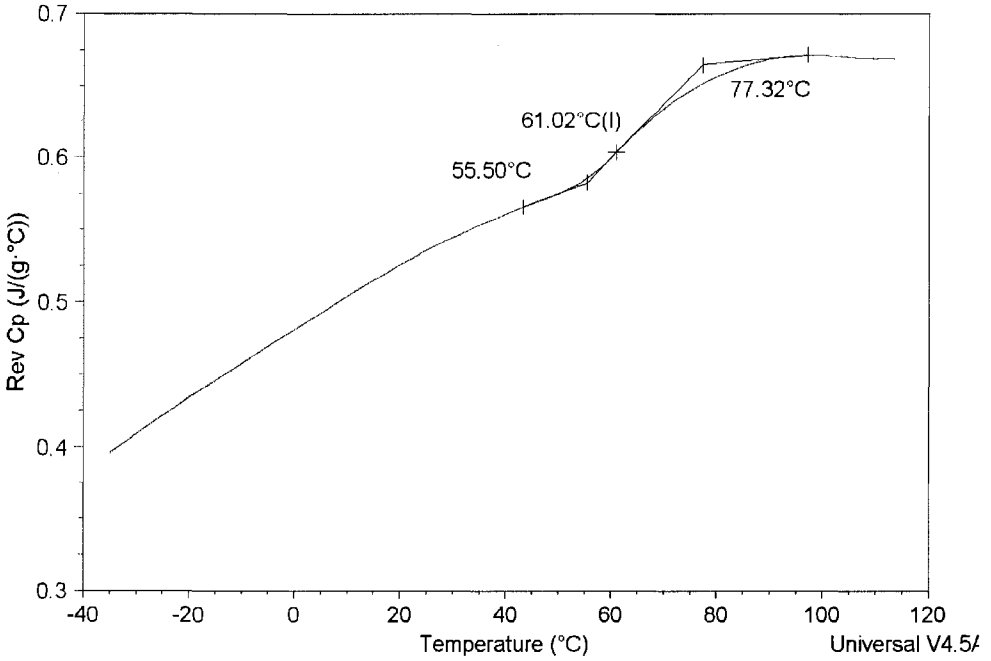

Figure 58 Tg of sample (DSC-3)

Tg was found to be a function of water concentration for polyacrylate. [67]For a crosslinked homopolymer, Tg always increases with increasing moisture and crosslink density. [150] We expect the same situation for polyitaconic acid.

CHAPTER V

BIODEGRADATION TESTING OF POLYITACONIC ACID AND ITACONATE SUPERABSORBENT

In this chapter, we study the biodegradability of polyitaconic acid.

5.1 Materials

Compost (Kingman's Farm, Durham, NH), Sludge (Waste Water Treatment Center, Durham, NH), Potassium Hydroxide (Pellets, EM Science), Cellulose Powder (20 micrometer, Aldrich), Polyacrylate Superabsorbent (100-500 micrometer, Emerging Technologies Inc.), Polyitaconic acid (Sample with 100% conversion, Mw=10,180 g/mole, Mn= 3,920 g/mole), Crosslinked Polyitaconic acid (Sample 1 in Chapter IV)

5.2 Biodegradation Testing in Compost

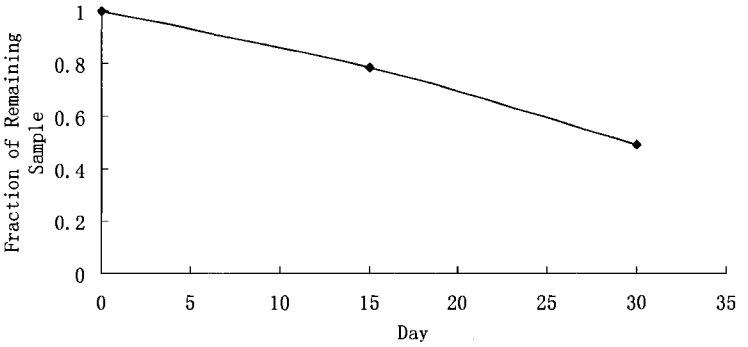

Figure 59 biodegradation of polyitaconic acid superabsorbent in compost.

Compost was taken from the Kingman's farm at the University of New Hampshire in Durham, NH. Before we bury the samples into compost, crosslinked PIA sample (MC172) was sealed into a tea bag and rinsed with DI-water five times, in

order to make sure we remove all the soluble parts. Samples were then buried into the compost for a certain period of time. Tea bags were cleaned, and the samples were dried in a vacuum oven. The dried samples were weighted and a percentage of sample left was calculated. Unfortunately, most of the tea bags were broken during composting and only two data point were obtained. The other disadvantage of the method is the uncertainty of the degradation product. Most likely, crosslinked polyitaconic acid is degraded into small molecule or linear polymer which can be extracted from the tea bag. We decided to pursue another more efficient and reliable method.

5.3 Biodegradtion testing by sludge

During the past 10 years, some unsuitable biodegradation standardizations [88] were used for biodegradation testing. As a result, starch blended with polyethylene was accepted to be biodegradable, in which the polyethylene part still remains non-degraded for 500 years. These methods are no longer accepted. For example, polyethylene and starch blend was proved to be biodegradable because of same proof of structural change during the degradation time. However, only the starch part of the sample was degraded and the polyethylene part was simply dispersed. We believe that the loss of mechanical properties or the oxidation of plastic samples can not prove biodegradability.

Biodegradation Testing of polyitaconic acid was done by following ASTM D 5271: Standard Test Method for Determining the Aerobic Biodegradation of Plastic Materials in an Activated Sludge-Wastewater-Treatment System.[87, 88, 151-154] Activated sludge was used as the bacteria source. PIA samples and sludge were mixed in sealed erlen myers. These sealed bottles were connected with a rubber tubing to

another erlen myer containing a solution of potassium hydroxide inside. The PIA solutions were stirred by magnetic stirrer. Bacteria and other microorganisms digest the polymers. Oxygen is consumed during the process of biodegradation; meanwhile, carbon dioxide is generated as a product which is absorbed by potassium hydroxide. The pressure decreases since the total amount of gas in the bottle is reduced. The change of the pressure can be measured by gas pressure sensors (Vernier Software & Technology) to evaluate the O_2 consumption.

BOD testing is measured with industrial waste. Sludge samples were taken from municipal Waste Water Treatment Center, Durham, NH. Samples were bubbled with air pump in a 3L container for hours at room temperature before use. Concentration of upper layer of sludge is 6g/l.

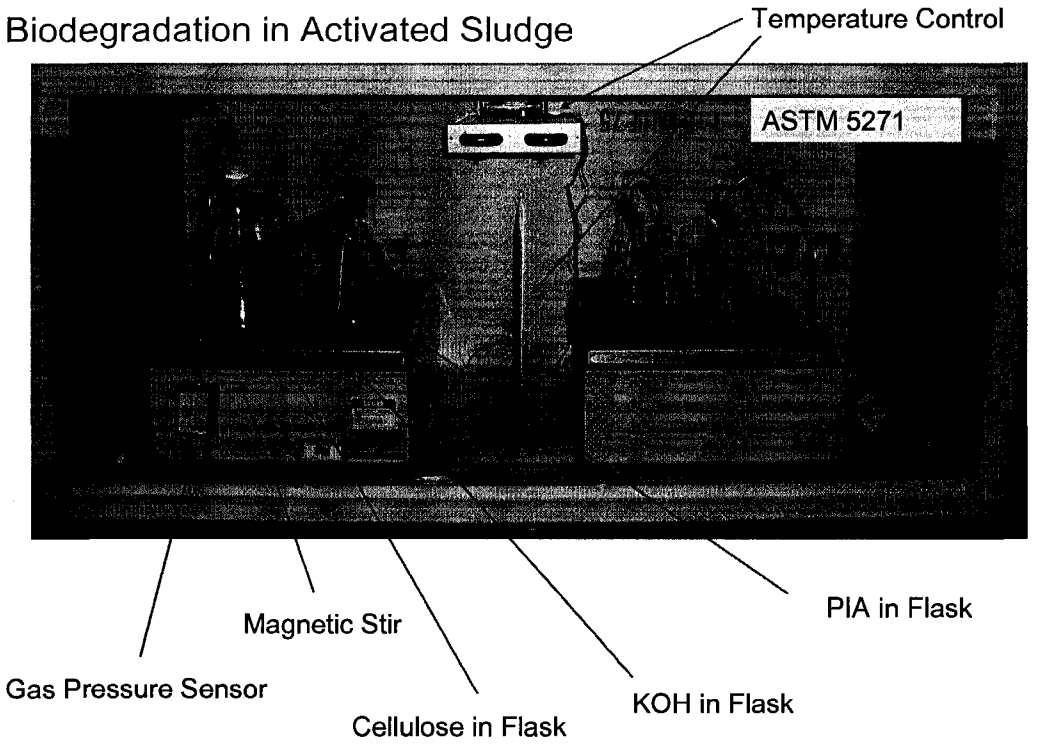

Figure 60 Biodegradation set up with temperature control, gas pressure sensor, and magnetic stirring.

The testing is called Biological Oxygen Demanding Testing (BODT).[155, 156]

The equipment is shown in Figure 60 above. About 400ml of 200mg/l solid sludge was mixed with polyitaconic acid samples. Cellulose and sludge alone were used as reference. 1ml 36.4g/l calcium chloride aqueous solution, 1ml 22.5g/l $MgSO_4 \cdot 7H_2O$ aqueous solution, 1ml 0.25g/l $FeCl_3 \cdot 6H_2O$ aqueous solution were added to the solution of samples.The concentration of polyitaconic acid in the test samples was kept to be around 200mg/l. The PH value of the mixtures was adjusted to 7 with a PBS buffer. The temperature in the experiments was set at 23± 1 °C. With the set-up in Figure 60, All the vessels were kept in dark. Sludge itself was prepared in one set-up for reference control.

5.3.1 The calculation of degradability

BODT is the biological oxygen demand calculated by the gas pressure reduction. TBOD is the theoretical biological oxygen demand of the test sample. Control is the oxygen demand of the sludge itself.

$$D = \frac{BODT - Control}{TBOD}$$

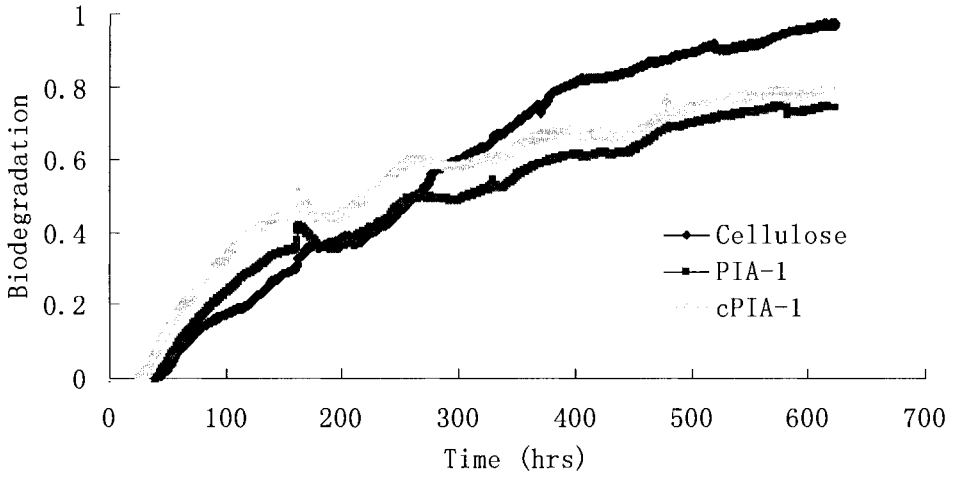

Figure 61 Biodegradation curve for polyitaconic acid (Sample PIA-1 and cPIA-2) with cellulose as reference

In Figure 61, the biodegradation curve of polyitaconic acid was compared with the curve of cellulose as reference. We found that polyitaconic acid samples were degraded faster than cellulose at the beginning. The reason is because polyitaconic acid is soluble in water and can be transported directly though the membrane of the bacteria cells. 97% biodegradation can be reached for cellulose, 78% biodegradation can be reached for linear polyitaconic acid (PIA-1), and 74% biodegradability of crosslinked polyitaconic acid (cPIA-1) can be reached in 26 days, which proved that polyitaconic acid is biodegradable. The degradation rate in nature would be much slower than that in laboratory condition, but this ASTM test is the accepted method to quantify biodegradability.

CONCLUSION

Currently, the application of itaconic acid is limited to its monomer and copolymers because of the difficulty to homopolymerize it. Three major problems for the existing processes limited the application of polyitaconic acid: low conversion ratio, low molecular weight and long polymerization times. In this work, we successfully synthesized poly(itaconic acid) in aqueous solution, and the structure of PIA was confirmed by ^{1}H-NMR, ^{13}C-NMR. 100% conversion can be reached at 100°C in two and half hours. A high temperature dissociation initiator such a tBHP is the key factor for the success polymerization of itaconic acid. The degree of neutralization of the two acid functions is critical, and only one of the two acids should be neutralized to give fastest polymerization rate. Molecular weights of polyitaconic acid with different conversion were measured. Molecular weight of polyitaconic acid can reach Mn=10,000g/mol. The constant $fKd = 3x10^{-4}$ and $Kp/(kt)^{1/2}$ in the range of 0.07 to 0.1 were determined. The molecular structure change of the itaconic acid during polymerization and the effect on polymerization rate was investigated. Itaconic acid was proved to partially change to citraconic acid which is an inhibitor of polymerization of itaconic acid.

Superabsorbent were successfully synthesized based on the polyitaconic acid process, tEGDA was used as the crosslinker. The swelling capacity of the sample was measured in sealed tea bags and the absorption capability in water can reach 160 times. The effect of neutralization degree and crosslinker concentration on swelling capacity of itaconate SAPs were studied. The maximum swelling rate was found at 70% neutralization. Swelling capacity in ionic solution and under external pressure was investigated. Absorbency capability and rate were both found to drop

dramatically with the salt concentration of environment. Models for evaluation absorbency rate and salt concentration effect on absorbency were compared with the experimental data. Highest elastic modulus of the network was found at highest crosslinker concentration incorporated during reaction. The biodegradation rate of polyitaconic acid was found to be as fast as that of cellulose.

RECOMMENDATION ON FUTURE WORK

With this novel simple polymerization process, high conversion can be reached in short times. Molecular weights are higher than the previous processes in patents and papers. However, the molecular weights are still not high enough for the preparation of superabsorbent with swelling capacity up to 1000 times. To reduce the crosslink density of itaconic superabsorbent, the polymerization process needs to be improved to increase the molecular weight of linear PIA by adjusting the parameters: temperature, concentration, time, etc.

The discovery of the superabsorbent made from the copolymerization of IA/HEA is worth further exploration. Their absorbency has high potential. In future work, a lower crosslinker density can be obtained by adjusting the concentration of reactant, ratio of HEA and IA, and reaction temperature.

tEGDA is most likely non-biodegradable. We may need to replace this crosslinker with a biodegradable alternative. It should be noticed that the solubility in water and molecular flexibility of the crosslinker are key factors for choosing the right crosslinker.

LIST OF ABREVIATIONS

AIBN: 2,2'-azo-bis(isobutyronitrile)

D_2O: Deuterium Oxide

CA: citraconic acid

EGDA: ethylene glycol diacrylate

EGDMA: ethyleneglycol dimethacrylate

MA: mesaconic acid

Mw: weight average molecular weight

Mn: number average molecular weight

IA: itaconic acid

PBS: Phosphate Buffered Saline

PKa: acid dissociation constant

PAA: poly(acrylic acid)

PIA: polyitaconic acid

PIAn: polyitaconic anhydride

SAP: superabsorbent

tBHP: tert-Butyl Hydroperoxide

tEGDA: tetra(ethylene glycol) diacrylate

TMPTA: Trimethylolpropane triacrylate

BIBLIOGRAPHY

1. Bressler, E. and S. Braun, *Conversion of citric acid to itaconic acid in a novel liquid membrane bioreactor.* Journal of Chemical Technology and Biotechnology, 2000. **75**(1): p. 66-72.

2. Bonnarme, P., et al., *Itaconate Biosynthesis in Aspergillus-Terreus.* Journal of Bacteriology, 1995. **177**(12): p. 3573-3578.

3. Mattey, M., *The Production of Organic-Acids.* Critical Reviews in Biotechnology, 1992. **12**(1-2): p. 87-132.

4. Fischer, J.W., L.H. Merwin, and R.A. Nissan, *Nmr Investigation of the Thermolysis of Citric-Acid.* Applied Spectroscopy, 1995. **49**(1): p. 120-126.

5. Kojima, E., *Perspective of the relationship between hydrodynamics and reactor performance in bubble column and airlift bioreactors.* Kagaku Kogaku Ronbunshu, 2001. **27**(4): p. 419-429.

6. Boudevsk.H and Platchko.S, *Polymerization of Itaconic Acid-Esters in Presence of Zinc Chloride.* Makromolekulare Chemie-Macromolecular Chemistry and Physics, 1973. **174**(Dec31): p. 231-233.

7. Boudevsk.Hn and Plachkov.Sp, *Copolymers of Itaconic Acid Monoesters with Some Acrylic Monomers.* Dokladi Na Bolgarskata Akademiya Na Naukite, 1972. **25**(1): p. 63-&.

8. Pascale, M., et al., *Use of itaconic acid-based polymers for solid-phase extraction of deoxynivalenol and application to pasta analysis.* Analytica Chimica Acta, 2008. **609**(2): p. 131-138.

9. Rivas, B.L., et al., *Synthesis and properties of styrene copolymers. Preparation of film-modified electrodes to detect Pb2+ ions.* Journal of Applied Polymer Science, 2006. **100**(3): p. 2380-2385.

10. Chmielewski, A.G., M. Haji-Saeid, and S. Ahmed, *Progress in radiation processing of polymers.* Nuclear Instruments & Methods in Physics Research Section B-Beam Interactions with Materials and Atoms, 2005. **236**: p. 44-54.

11. Linden, L.A., J.F. Rabek, and H. Kaczmarek, *Poly(Carboxylic Acids) Metal-Salts Complexes - Formation, Structure, and Application in Dentistry.* Molecular Crystals and Liquid Crystals Science and Technology Section a-Molecular Crystals and Liquid Crystals, 1994. **240**: p. 143-154.

12. Lee, Y.A., et al., *Synthesis and structural properties of (diamine)platinum (II) complexes of itaconic acid.* Inorganica Chimica Acta, 1998. **279**(1): p. 116-120.

13. Bajaj, P., D.K. Paliwal, and A.K. Gupta, *Acrylonitrile Acrylic Acids Copolymers .1. Synthesis and Characterization.* Journal of Applied Polymer Science, 1993. **49**(5): p. 823-833.

14. Bajaj, P., K. Sen, and S.H. Bahrami, *Solution polymerization of acrylonitrile with vinyl acids in dimethylformamide.* Journal of Applied Polymer Science, 1996. **59**(10): p. 1539-1550.

15. Buchenska, J., *H-1-NMR spectroscopic investigation of polyamide fibers crafted with vinyl monomers.* Journal of Applied Polymer Science, 1996. **60**(4): p. 519-529.

16. Coskun, R., *Graft copolymerization of itaconic acid-methacrylamide comonomers onto poly(ethylene terephthalate) fibers.* European Polymer Journal, 2007. **43**(4): p. 1428-1435.

17. Coskun, R., M. Sacak, and M. Karakisla, *Graft copolymerization of an itaconic acid/acrylamide monomer mixture onto poly(ethylene terephthalate) fibers with benzoyl peroxide.* Journal of Applied Polymer Science, 2005. **97**(5): p. 1795-1803.

18. Bajaj, P., T.V. Sreekumar, and K. Sen, *Effect of reaction medium on radical copolymerization of acrylonitrile with vinyl acids.* Journal of Applied Polymer Science, 2001. **79**(9): p. 1640-1652.

19. Bajpai, S.K. and S.S. Saggu, *Water uptake behavior of poly(methacrylamide-co-N-vinyl-2-pyrrolidone-co-itaconic acid) as pH-sensitive hydrogels: Part I.* Journal of Macromolecular Science Part a-Pure and Applied Chemistry, 2006. **43**(8): p. 1135-1150.

20. El-Hamshary, H., *Synthesis and water sorption studies of pH sensitive poly(acrylamide-co-itaconic acid) hydrogels.* European Polymer Journal, 2007. **43**(11): p. 4830-4838.

21. Abdollahi, M., A.R. Mahdavian, and A. Nouri, *Kinetic study of radical polymerization VIII. A comprehensive study of solution copolymerization of vinyl acetate and methyl acrylate by H-1-NMR spectroscopy.* Journal of Macromolecular Science Part a-Pure and Applied Chemistry, 2007. **44**(7-9): p. 839-848.

22. Bajaj, P., et al., *Structural investigations of acrylonitrile-vinyl acid copolymers by NMR Spectroscopy.* Journal of Applied Polymer Science, 2003. **88**(5): p. 1211-1217.

23. Devasia, R., C.P.R. Nair, and K.N. Ninan, *Solvent and kinetic penultimate unit effects in the copolymerization of acrylonitrile with itaconic acid.* European Polymer Journal, 2002. **38**(10): p. 2003-2010.

24. Devasia, R., C.P.R. Nair, and K.N. Ninan, *The partition coefficient of itaconic acid in two phase system of acrylonitrile and water.* Indian Journal of Chemistry Section a-Inorganic Bio-Inorganic Physical Theoretical & Analytical Chemistry, 2001. **40**(7): p. 738-741.

25. Fritzsche, P., et al., *Synthesis and Coagulation Behavior of Hydrophilic Acrylonitrile Copolymers.* Angewandte Makromolekulare Chemie, 1992. **195**: p. 171-190.

26. Oishi, T., et al., *Synthesis and polymerization of N-[4-(cholesteroxycarbonyl)phenyl]itaconimide.* Polymer, 1996. **37**(14): p. 3131-3139.

27. Otsu, T. and J.Z. Yang, *Radical Polymerization of Itaconic Anhydride and Reactions of the Resulting Polymers with Amines and Alcohols.* Polymer International, 1991. **25**(4): p. 245-251.

28. Abbott, A.P., et al., *Solubility of unsaturated carboxylic acids in supercritical 1,1,1,2-tetrafluoroethane (HFC 134a) and a methodology for the separation of ternary mixtures.* Green Chemistry, 2005. **7**(4): p. 210-216.

29. Huang, Y.Q., et al., *Synthesis of poly(acrylic acid-co-itaconic acid) in carbon dioxide-methanol mixtures.* Journal of Macromolecular Science-Pure and Applied Chemistry, 2002. **39**(1-2): p. 27-38.

30. Yang, C.Q. and X.H. Gu, *Polymerization of maleic acid and itaconic acid studied by FT-Raman spectroscopy.* Journal of Applied Polymer Science, 2001. **81**(1): p. 223-228.

31. Erbil, C. and N. Uyanik, *Interactions between poly(acrylamide)poly(itaconic acid) and cerium(IV)-nitrilotriacetic acid redox pair in the synthesis of acrylamide and itaconic acid homo- and copolymers.* Polymer International, 2001. **50**(7): p. 792-795.

32. Nakamoto, H., Y. Ogo, and T. Imoto, *Polymerization of Itaconic Acid under High Pressure.* Makromolekulare Chemie-Macromolecular Chemistry and Physics, 1968. **111**(Feb): p. 104-&.

33. Munoz, O., et al., *Tropane alkaloids from Schizanthus litoralis.* Phytochemistry, 1996. **43**(3): p. 709-713.

34. Sankhe, A.Y., S.M. Husson, and S.M. Kilbey, *Direct polymerization of surface-tethered polyelectrolyte layers in aqueous solution via surface-confined atom transfer radical polymerization.* Journal of Polymer Science Part a-Polymer Chemistry, 2007. **45**(4): p. 566-575.

35. Bakhtiyarova, Y.V., et al., *Carboxylate phosphabetaines based on tertiary phosphines and unsaturated dicarboxylic acids.* Russian Journal of Organic Chemistry, 2007. **43**(2): p. 207-213.

36. Carlsson, M., et al., *Study of the Sequential Conversion of Citric to Itaconic to Methacrylic-Acid in near-Critical and Supercritical Water.* Industrial & Engineering Chemistry Research, 1994. **33**(8): p. 1989-1996.

37. Cody, G.D., et al., *Geochemical roots of autotrophic carbon fixation: Hydrothermal experiments in the system citric acid, H2O-(+/- FeS)-(+/- NiS).* Geochimica Et Cosmochimica Acta, 2001. **65**(20): p. 3557-3576.

38. Li, J. and T.B. Brill, *Spectroscopy of hydrothermal solutions 18: pH-dependent kinetics of itaconic acid reactions in real time.* Journal of Physical Chemistry A, 2001. **105**(48): p. 10839-10845.

39. Sepulchre, M.O. and M. Sepulchre, *Synthesis of unsaturated polyesters from dipotassium salts of cis-aconitic, itaconic and mesaconic acids and 1,4-dibromobutane.* Macromolecular Symposia, 1997. **122**: p. 291-296.

40. Tate, B.E., *Decarboxylation of Itaconic Acid Polymers.* Makromolekulare Chemie, 1967. **109**(Nov): p. 176-&.

41. Gibbs, P.A., R.J. Seviour, and F. Schmid, *Growth of filamentous fungi in submerged culture: Problems and possible solutions.* Critical Reviews in Biotechnology, 2000. **20**(1): p. 17-48.

42. Joo, F., E. Papp, and A. Katho, *Molecular catalysis in liquid multiphase systems.* Topics in Catalysis, 1998. **5**(1-4): p. 113-124.

43. Shekhawat, D., et al., *Formation of citraconic anhydride via condensation of dialkyl succinates and formaldehyde.* Applied Catalysis a-General, 2002. **223**(1-2): p. 261-273.

44. Runeman, B., *Skin interaction with absorbent hygiene products.* Clinics in Dermatology, 2008. **26**(1): p. 45-51.

45. [Anon], *Superabsorbent fights fire.* Chemical & Engineering News, 2005. **83**(17): p. 11-11.

46. Buchholz, F.L., *Polymerization Methods of Superabsorbent Polyacrylates.* Abstracts of Papers of the American Chemical Society, 1993. **206**: p. 247-PMSE.

47. Buchholz, F.L., *Keeping Dry with Superabsorbent Polymers.* Chemtech, 1994. **24**(9): p. 38-43.

48. Buchholz, F.L., *Preparation Methods of Superabsorbent Polyacrylates.* Superabsorbent Polymers, 1994. **573**: p. 27-38.

49. Buchholz, F.L., S.R. Pesce, and C.L. Powell, *Deswelling stresses and reduced swelling of superabsorbent polymer in composites of fiber and superabsorbent polymers.* Journal of Applied Polymer Science, 2005. **98**(6): p. 2493-2507.

50. Burr, R.C., G.F. Fanta, and W.M. Doane, *Graft-Polymerization of Starch with Mixtures of Acrylonitrile and 2-Acrylamido-2-Methylpropanesulfonic Acid.* Journal of Applied Polymer Science, 1979. **24**(5): p. 1387-1390.

51. Burr, R.C., et al., *Graft Copolymers of Starch and Mixtures of Acrylamide and Acrylic-Acid.* Journal of Applied Polymer Science, 1976. **20**(11): p. 3201-3204.

52. Burr, R.C., et al., *Starch Graft Copolymers for Water Treatment.* Starke, 1975. **27**(5): p. 155-159.

53. Kazanskii, K.S. and S.A. Dubrovskii, *Chemistry and Physics of Agricultural Hydrogels.* Advances in Polymer Science, 1992. **104**: p. 97-133.

54. Kiatkamjornwong, S. and P. Suwanmala, *Partially hydrolyzed polyacrylamide-poly(N-vinylpyrrolidone) copolymers as superabsorbents synthesized by gamma irradiation.* Journal of Applied Polymer Science, 1998. **68**(2): p. 191-203.

55. Kiatkamjornwong, S. and R. Wongwatthanasatien, *Superabsorbent polymer of poly[acrylamide-co-(acrylic acid)] by foamed polymerization. I. Synthesis and water swelling properties.* Macromolecular Symposia, 2004. **207**: p. 229-240.

56. Kidwell, D.A., *Superabsorbent Polymers - Media for the Enzymatic Detection of Ethyl-Alcohol in Urine.* Analytical Biochemistry, 1989. **182**(2): p. 257-261.

57. Kilian, W. and J. Fanta, *Degradation of forest sites and possibilities for their recovery.* Ecological Engineering, 1998. **10**(1): p. 1-3.

58. Kim, J.H., J.H. Lee, and S.W. Yoon, *Preparation and swelling behavior of biodegradable superabsorbent gels based on polyaspartic acid.* Journal of Industrial and Engineering Chemistry, 2002. **8**(2): p. 138-142.

59. Kimura, T. and S. Hikichi, *pH-Dependence of the lower critical solution temperatures of random copolymers of N-isopropylacrylamide and itaconic acid.* Kobunshi Ronbunshu, 2000. **57**(11): p. 730-733.

60. Kitch, B.T., B.D. Levy, and C.H. Fanta, *Late onset asthma - Epidemiology, diagnosis and treatment.* Drugs & Aging, 2000. **17**(5): p. 385-397.

61. Knaebel, A., S.R. Rebre, and F. Lequeux, *Determination of the elastic modulus of superabsorbent gel beads.* Polymer Gels and Networks, 1997. **5**(2): p. 107-121.

62. [Anon], *Superabsorbent Substances for Utilization in Agriculture.* Agricultura De Las Americas, 1980. **29**(6): p. 16-17.

63. Buchholz, F.L., *A Swell Idea - Superabsorbent Polymers.* Chemistry in Britain, 1994. **30**(8): p. 652-656.

64. Zhao, Y., L. Fang, and T.W. Tan, *Optimization of the preparation of a poly(aspartic acid) superabsorbent resin with response surface methodology.* Journal of Applied Polymer Science, 2006. **102**(3): p. 2616-2622.

65. Wang, X.X., J.L. Zhao, and X.H. Wang, *Synthesis of poly (acrylic acid-co-itaconic acid) and its dispersing effect for barium titanate aqueous suspension.* High-Performance Ceramics Iii, Pts 1 and 2, 2005. **280-283**: p. 735-738.

66. Zheng, Y., et al., *Study on superabsorbent composite XVI. Synthesis, characterization and swelling behaviors of poly(sodium acrylate)/vermiculite superabsorbent composites.* European Polymer Journal, 2007. **43**(5): p. 1691-1698.

67. Zheng, Y. and A. Wang, *Preparation, characterization and swelling behaviours of a novel multifunctional superabsorbent composite based on Ca-montmorillonite and sodium humate.* E-Polymers, 2007: p. -.

68. Zhou, W.J., K.J. Yao, and M.J. Kurth, *Synthesis and swelling properties of the copolymer of acrylamide with anionic monomers.* Journal of Applied Polymer Science, 1996. **62**(6): p. 911-915.

69. Zohuriaan-Mehr, M.J., et al., *New super-absorbing hydrogel hybrids from gum arabic and acrylic monomers.* Journal of Macromolecular Science-Pure and Applied Chemistry, 2005. **A42**(12): p. 1655-1666.

70. Zohuriaan-Mehr, M.J. and A. Pourjavadi, *Superabsorbent hydrogels from starch-g-PAN: Effect of some reaction variables on swelling behavior.* Journal of Polymer Materials, 2003. **20**(1): p. 113-120.

71. Higuchi, A. and T. Iijima, *Permeation of Solutes in Water-Swollen Polyvinyl Alcohol-Co-Itaconic Acid) Membranes.* Journal of Applied Polymer Science, 1986. **32**(1): p. 3229-3237.

72. El-Maghraby, H.F., O. Gedeon, and A.A.A. Khalil, *Formation and characterization of poly(vinyl alcohol-co-vinyl acetate-co-itaconic acid)/plaster composites - Part 2. Composite formation and characteristics.* Ceramics-Silikaty, 2007. **51**(3): p. 168-172.

73. Doane, W.M., C.L. Swanson, and G.F. Fanta, *Emerging Polymeric Materials Based on Starch.* Acs Symposium Series, 1992. **476**: p. 197-230.

74. Fanta, G.F., G.E. Babcock, and R.C. Burr, *Copolymers of Starch and Polyacrylonitrile - Soluble Fraction.* Journal of Polymer Science Part a-1-Polymer Chemistry, 1969. **7**(3Pa1): p. 980-&.

75. Caykara, T. and I. Aycicek, *pH-responsive ionic poly(N,N-diethylaminoethyl methacrylate-co-N-vinyl-2-pyrrolidone) hydrogels: Synthesis and swelling properties.* Journal of Polymer Science Part B-Polymer Physics, 2005. **43**(19): p. 2819-2828.

76. Shakkthivel, P. and T. Vasudevan, *Newly developed itaconic acid copolymers for gypsum and calcium carbonate scale control.* Journal of Applied Polymer Science, 2007. **103**(5): p. 3206-3213.

77. Sun, Y.P., et al., *A method for the preparation of stable dispersion of zero-valent iron nanoparticles.* Colloids and Surfaces a-Physicochemical and Engineering Aspects, 2007. **308**(1-3): p. 60-66.

78. Chen, X.P., et al., *Synthesis and properties of acrylic-based superabsorbent.* Journal of Applied Polymer Science, 2004. **92**(1): p. 619-624.

79. MuralidharaRao, D., et al., *Fermentatative production of itaconic acid by Aspergillus terreus using Jatropha seed cake.* African Journal of Biotechnology, 2007. **6**(18): p. 2140-2142.

80. Dubrovskii, S.A., M.A. Lagutina, and K.S. Kazanskii, *Method of Measuring the Swelling Pressure of Superabsorbent Gels.* Polymer Gels and Networks, 1994. **2**(1): p. 49-58.

81. Favaro, S.L., et al., *Superabsorbent hydrogel composed of covalently crosslinked gum arabic with fast swelling dynamics.* Journal of Applied Polymer Science, 2008. **107**(3): p. 1500-1506.

82. Lionetto, F., A. Sannino, and A. Maffezzoli, *Ultrasonic monitoring of the network formation in superabsorbent cellulose based hydrogels.* Polymer, 2005. **46**(6): p. 1796-1803.

83. Chang, S.J. and F.C. Chang, *Synthesis and characterization of copolyesters containing the phosphorus linking pendent groups.* Journal of Applied Polymer Science, 1999. **72**(1): p. 109-122.

84. Chen, J.W. and Y.M. Zhao, *An efficient preparation method for superabsorbent polymers.* Journal of Applied Polymer Science, 1999. **74**(1): p. 119-124.

85. Fanta, C.H., *Fatal asthma and the environment.* Immunology and Allergy Clinics of North America, 2002. **22**(4): p. 911-+.

86. Ozdemir, S., et al., *In vivo biocompatibility studies of poly(n-vinyl 2-pyrrolidone/itaconic acid) hydrogels synthesized by gamma-rays.* Nuclear Instruments & Methods in Physics Research Section B-Beam Interactions with Materials and Atoms, 2003. **208**: p. 395-399.

87. Stahl, J.D., et al., *Biodegradation of superabsorbent polymers in soil.* Environmental Science and Pollution Research, 2000. **7**(2): p. 83-88.

88. Sahoo, P.K., P.K. Rana, and A. Sahoo, *Biodegradation studies of starch based composite superabsorbents.* Polymers & Polymer Composites, 2004. **12**(7): p. 627-635.

89. Chen, J. and K. Park, *Synthesis and characterization of superporous hydrogel composites.* Journal of Controlled Release, 2000. **65**(1-2): p. 73-82.

90. Bajpai, S.K. and S. Johnson, *Superabsorbent hydrogels for removal of divalent toxic ions. Part I: Synthesis and swelling characterization.* Reactive & Functional Polymers, 2005. **62**(3): p. 271-283.

91. Bohn, R., et al., *Submicron-grained multiphase TiAlSi alloys: Processing, characterization, and microstructural design.* Journal of Materials Research, 2001. **16**(6): p. 1850-1861.

92. Bonventre, P.F., *Relationship of Superabsorbent Tampons and the Toxic Shock Syndrome.* American Journal of Obstetrics and Gynecology, 1984. **149**(8): p. 915-915.

93. Fanta, G.F., F.C. Felker, and J.H. Salch, *Graft polymerization of acrylonitrile onto starch-coated polyethylene film surfaces.* Journal of Applied Polymer

Science, 2003. **89**(12): p. 3323-3328.

94. Fanta, G.F., F.C. Felker, and R.L. Shogren, *Graft polymerization of acrylonitrile onto spherocrystals formed from jet cooked cornstarch.* Carbohydrate Polymers, 2004. **56**(1): p. 77-84.

95. Fanta, G.F. and R.L. Shogren, *Modification of starch-poly(methyl acrylate) graft copolymers by steam jet cooking.* Journal of Applied Polymer Science, 1997. **65**(5): p. 1021-1029.

96. Finkenstadt, V.L. and J.L. Willett, *Reactive extrusion of starch-polyacrylamide graft copolymers: Effects of monomer/starch ratio and moisture content.* Macromolecular Chemistry and Physics, 2005. **206**(16): p. 1648-1652.

97. Kiatkamjornwong, S., K. Mongkolsawat, and M. Sonsuk, *Synthesis and property characterization of cassava starch grafted poly [acrylamide-co-(maleic acid)] superabsorbent via gamma-irradiation.* Polymer, 2002. **43**(14): p. 3915-3924.

98. Lee, W.F. and Y.C. Chen, *Preparation of reactive mineral powders used for poly(sodium acrylate) composite superabsorbents.* Journal of Applied Polymer Science, 2005. **97**(3): p. 855-861.

99. Luo, W., et al., *Synthesis and properties of starch grafted poly[acrylamide-co-(acrylic acid)]/montmorillonite nanosuperabsorbent via gamma-ray irradiation technique.* Journal of Applied Polymer Science, 2005. **96**(4): p. 1341-1346.

100. Bruna, J., et al., *Melt grafting of itaconic acid and its derivatives onto an ethylene-propylene copolymer.* Reactive & Functional Polymers, 2005. **64**(3): p. 169-178.

101. Yazdani-Pedram, M., H. Vega, and R. Quijada, *Melt functionalization of polypropylene with methyl esters of itaconic acid.* Polymer, 2001. **42**(10): p. 4751-4758.

102. Rodriguez, R., C. Alvarez-Lorenzo, and A. Concheiro, *Cationic cellulose hydrogels: kinetics of the cross-linking process and characterization as pH-/ion-sensitive drug delivery systems.* Journal of Controlled Release, 2003. **86**(2-3): p. 253-265.

103. Li, A., Y.G. Zhao, and A.Q. Wang, *Study on superabsorbent composite. - XII. - Effect of ion-exchanged attapulgite on water absorbency of poly(acrylic acid)/attapulgite superabsorbent composites.* Journal of Applied Polymer Science, 2007. **105**(6): p. 3476-3482.

104. Pourjavadi, A., M.S. Amini-Fazl, and H. Hosseinzadeh, *Partially hydrolyzed crosslinked alginate-graft-polymethacrylamide as a novel biopolymer-based superabsorbent hydrogel having pH-responsive properties.* Macromolecular Research, 2005. **13**(1): p. 45-53.

105. Pourjavadi, A., H. Hosseinzadeh, and M. Sadeghi, *Synthesis, characterization*

and swelling behavior of gelatin-g-poly(sodium acrylate)/kaolin superabsorbent hydrogel composites. Journal of Composite Materials, 2007. **41**(17): p. 2057-2069.

106. Zhang, J.P., H. Chen, and A.Q. Wang, *Study on superabsorbent composite. III. Swelling behaviors of polyacrylamide/attapulgite composite based on acidified attapulgite and organo-attapulgite.* European Polymer Journal, 2005. **41**(10): p. 2434-2442.

107. Chen, J.W. and J.R. Shen, *Swelling behaviors of polyacrylate superabsorbent in the mixtures of water and hydrophilic solvents.* Journal of Applied Polymer Science, 2000. **75**(11): p. 1331-1338.

108. Lawton, J.W. and G.F. Fanta, *Glycerol-Plasticized Films Prepared from Starch Poly(Vinyl Alcohol) Mixtures - Effect of Poly(Ethylene-Co-Acrylic Acid).* Carbohydrate Polymers, 1994. **23**(4): p. 275-280.

109. Ruan, W.Q., et al., *Synthesis of superabsorbent resin by ultraviolet photopolymerization.* Journal of Applied Polymer Science, 2004. **92**(3): p. 1618-1624.

110. Zohuriaan-Mehr, M.J., et al., *Gum arabic-acrylic superabsorbing hydrogel hybrids: Studies on swelling rate and environmental responsiveness.* Journal of Applied Polymer Science, 2006. **102**(6): p. 5667-5674.

111. Chen, Z.B., et al., *Conductance method study on the swelling kinetics of the superabsorbent.* Electrochimica Acta, 2007. **52**(5): p. 1839-1846.

112. Yoshimura, T., F. Tokunaga, and R. Fujioka, *Evaluation of carrageenans as superabsorbent polymers.* Kobunshi Ronbunshu, 2005. **62**(7): p. 331-334.

113. Bakass, M., et al., *The adsorption of water vapor an super absorbent product at low temperatures and low mass.* Journal of Applied Polymer Science, 2006. **100**(2): p. 1450-1456.

114. Bakass, M., A. Mokhlisse, and M. Lallemant, *Water absorption and desorption by a superabsorbent polymer - Drying a swollen polymer by conventional heating and in a microwave field.* Thermochimica Acta, 2000. **356**(1-2): p. 159-171.

115. Bakass, M., A. Mokhlisse, and M. Lallemant, *Absorption and desorption of liquid water by a superabsorbent polyelectrolyte: Role of polymer on the capacity for absorption of a ground.* Journal of Applied Polymer Science, 2001. **82**(6): p. 1541-1548.

116. Bakass, M., A. Mokhlisse, and M. Lallemant, *Absorption and desorption of liquid water by a superabsorbent polymer: Effect of polymer in the drying of the soil and the quality of certain plants.* Journal of Applied Polymer Science, 2002. **83**(2): p. 234-243.

117. Abd El-Mohdy, H.L., E.S.A. Hegazy, and H.A. Abd El-Rehim, *Characterization of starch/acrylic acid super-absorbent hydrogels prepared by*

ionizing radiation. Journal of Macromolecular Science Part a-Pure and Applied Chemistry, 2006. **43**(7): p. 1051-1063.

118. Bajpai, S.K. and S.S. Saggu, *Insulin release behavior of poly(methacrylamide-co-N-vinyl-2-pyrrolidone-co-itaconic acid) hydrogel: An interesting probe. Part II.* Journal of Macromolecular Science Part a-Pure and Applied Chemistry, 2007. **44**(2): p. 153-157.

119. Bakass, M., J.P. Bellat, and G. Bertrand, *Characterization of a superabsorbent polymer.* Journal of Applied Polymer Science, 2007. **104**(2): p. 782-786.

120. Ni, C.H. and X.X. Zhu, *Synthesis and swelling behavior of thermosensitive hydrogels based on N-substituted acrylamides and sodium acrylate.* European Polymer Journal, 2004. **40**(6): p. 1075-1080.

121. Philippova, O.E., et al., *Polyacrylamide hydrogels with trapped polyelectrolyte rods.* Macromolecules, 1998. **31**(4): p. 1168-1179.

122. Yan, Q.Z., et al., *Preparation of starch-g-sodium acrylate/acrylamide superabsorbent via frontal polymerization.* Chemical Journal of Chinese Universities-Chinese, 2005. **26**(7): p. 1363-1365.

123. Bajpai, S.K., M. Bajpai, and L. Sharma, *Investigation of water uptake behavior of superabsorbent polymers composed of N-vinyl-2-pyrrolidone and partially neutralized acrylic acid.* Journal of Macromolecular Science Part a-Pure and Applied Chemistry, 2006. **43**(9): p. 1323-1337.

124. Chu, M., et al., *Synthesis of poly(acrylic acid)/sodium humate superabsorbent composite for agricultural use.* Journal of Applied Polymer Science, 2006. **102**(6): p. 5137-5143.

125. Huang, J., et al., *Synthesis and properties of acrylic-based superabsorbents with enhanced crosslinking on particle surface.* Chinese Journal of Polymer Science, 2005. **23**(5): p. 463-469.

126. Kabiri, K., et al., *Concise synthesis of fast-swelling superabsorbent hydrogels: Effect of initiator concentration on porosity and absorption rate.* Journal of Polymer Materials, 2003. **20**(1): p. 17-22.

127. Kabiri, K. and M.M. Zohuriaan-Mehr, *Superabsorbent hydrogels from concentrated solution terpolymerization.* Iranian Polymer Journal, 2004. **13**(5): p. 423-430.

128. Arriola, D.J., et al., *Crosslinker reactivity and the structure of superabsorbent gels.* Journal of Applied Polymer Science, 1997. **63**(4): p. 439-451.

129. Goon, A.T.J., R.J.G. Rycroft, and J.P. McFadden, *Allergic contact dermatitis from trimethylolpropane triacrylate and pentaerythritol triacrylate.* Contact Dermatitis, 2002. **47**(4): p. 249-249.

130. Karadag, E. and D. Saraydin, *Swelling of superabsorbent acrylamide/sodium acrylate hydrogels prepared using multifunctional crosslinkers.* Turkish

Journal of Chemistry, 2002. **26**(6): p. 863-875.

131. Karadag, E., O.B. Uzum, and D. Saraydin, *Swelling equilibria and dye adsorption studies of chemically crosslinked superabsorbent acrylamide/maleic acid hydrogels.* European Polymer Journal, 2002. **38**(11): p. 2133-2141.

132. Kabiri, K., et al., *Synthesis of fast-swelling superabsorbent hydrogels: effect of crosslinker type and concentration on porosity and absorption rate.* European Polymer Journal, 2003. **39**(7): p. 1341-1348.

133. Kundakci, S., O.B. Uzum, and E. Karadag, *Swelling and dye sorption studies of acrylamide/2-acrylamido-2-methyl-l-propanesulfonic acid/bentonite highly swollen composite hydrogels.* Reactive & Functional Polymers, 2008. **68**(2): p. 458-473.

134. Sohn, O. and D. Kim, *Theoretical and experimental investigation of the swelling behavior of sodium polyacrylate superabsorbent particles.* Journal of Applied Polymer Science, 2003. **87**(2): p. 252-257.

135. An, L., A.Q. Wang, and J.M. Chen, *Studies on poly(acrylic acid)/attapulgite superabsorbent composites. II. Swelling behaviors of superabsorbent composites in saline solutions and hydrophilic solvent-water mixtures.* Journal of Applied Polymer Science, 2004. **94**(5): p. 1869-1876.

136. Cutie, S.S., et al., *Acrylic acid polymerization kinetics.* Journal of Polymer Science Part B-Polymer Physics, 1997. **35**(13): p. 2029-2047.

137. Fei, J.Q. and L.X. Gu, *Swelling/deswelling behavior of thermally induced PVA/PAA hydrogel fiber in aqueous salt solutions.* Journal of Polymer Materials, 2002. **19**(1): p. 103-112.

138. Freddi, G., M. Tsukada, and H. Shiozaki, *Chemical modification of wool fibers with acid anhydrides.* Journal of Applied Polymer Science, 1999. **71**(10): p. 1573-1579.

139. Quintana, J.R., N.E. Valderruten, and I. Katime, *Mechanical properties of poly(N-isopropyl-acrylamide- co-itaconic acid) hydrogels.* Journal of Applied Polymer Science, 2002. **85**(12): p. 2540-2545.

140. Caykara, T. and I. Akcakaya, *Synthesis and network structure of ionic poly(N,N-dimethylacrylamide-co-acrylamide) hydrogels: Comparison of swelling degree with theory.* European Polymer Journal, 2006. **42**(6): p. 1437-1445.

141. Chen, J., et al., *Effect of coagulation temperature on the properties of poly(acrylonitrile-itaconic acid) fibers in wet spinning.* Journal of Polymer Research, 2007. **14**(3): p. 223-228.

142. Klassen, T., et al., *Tailoring nanocrystalline materials towards potential applications.* Zeitschrift Fur Metallkunde, 2003. **94**(5): p. 610-614.

143. Blanco, M.D., et al., *Transdermal application of bupivacaine-loaded poly (acrylamide(A)-co-monomethyl itaconate) hydrogels.* International Journal of Pharmaceutics, 2003. **255**(1-2): p. 99-107.

144. Blanco, M.D., et al., *5-fluorouracil release from copolymeric hydrogels of itaconic acid monoester .1. Acrylamide-co-monomethyl itaconate.* Biomaterials, 1996. **17**(11): p. 1061-1067.

145. Ge, H.Y., et al., *The skin-core structure of poly(acrylonitrile-itaconic acid) precursor fibers in wet-spinning.* Journal of Applied Polymer Science, 2008. **108**(2): p. 947-952.

146. Kacarevic-Popovic, Z., et al., *Radiolytic synthesis of Ag-poly(BIS-co-HEMA-co-IA) nanocomposites.* Radiation Physics and Chemistry, 2007. **76**(8-9): p. 1333-1336.

147. Briens, C., et al., *Development of an ultra-rapid reactor for superabsorbent polymer.* Industrial & Engineering Chemistry Research, 2001. **40**(23): p. 5386-5390.

148. Aoki, S. and A. Fukui, *Poly(itaconic acid) derivatives as thermal stabilizers for polystyrene and poly(methyl methacrylate).* Polymer Journal, 1998. **30**(4): p. 295-299.

149. Radic, D., et al., *Thermal stability of aromatic poly(monoitaconates).* International Journal of Polymeric Materials, 1996. **33**(1-2): p. 25-30.

150. Ma, L., et al., *Improvement in the water-absorbing properties of superabsorbent polymers (acrylic acid-co-acrylamide) in supercritical CO2.* Journal of Applied Polymer Science, 2002. **86**(9): p. 2272-2278.

151. Argade, A.B. and N.A. Peppas, *Poly(acrylic acid) poly(vinyl alcohol) copolymers with superabsorbent properties.* Journal of Applied Polymer Science, 1998. **70**(4): p. 817-829.

152. Lanthong, P., R. Nuisin, and S. Kiatkamjornwong, *Graft copolymerization, characterization, and degradation of cassava starch-g-acrylamide/itaconic acid superabsorbents.* Carbohydrate Polymers, 2006. **66**(2): p. 229-245.

153. Sutherland, G.R.J., J. Haselbach, and S.D. Aust, *Biodegradation of crosslinked acrylic polymers by a white-rot fungus.* Environmental Science and Pollution Research, 1997. **4**(1): p. 16-20.

154. Swanson, C.L., G.F. Fanta, and J.H. Salch, *Skin and Layer Formation in Films Prepared from Carbohydrates, Poly(Ethylene-Co-Acrylic Acid), and Polyethylene.* Journal of Applied Polymer Science, 1993. **49**(10): p. 1683-1693.

155. Wolter, M., et al., *Biological degradability of syntetic superabsorbent soil conditioners.* Landbauforschung Volkenrode, 2002. **52**(1): p. 43-52.

156. Yoshimura, T., et al., *Synthesis and characterization of biodegradable*

hydrogels based on starch and succinic anhydride. Carbohydrate Polymers, 2006. **64**(2): p. 345-349.

157. Buzanowski, W.C., et al., *Determination of Sodium Polyacrylate by Pyrolysis-Gas Chromatography.* Journal of Chromatography A, 1994. **677**(2): p. 355-364.

158. Cutie, S.S. and S.J. Martin, *Size-Exclusion Chromatography of Cross-Linked Superabsorbent Polymers.* Journal of Applied Polymer Science, 1995. **55**(4): p. 605-609.

159. Gourmand, M. and J.M. Corpart, *Superabsorbent revolution in hygiene.* Actualite Chimique, 1999(11): p. 46-50.

160. Nuutinen, M., N.P. Huttunen, and M. Uhari, *Type of nappy and nursing habits in acquiring acute urinary tract infection.* Acta Paediatrica, 1996. **85**(9): p. 1039-1041.

161. Breskin, I., *Overcapacity Leads to Superabsorbent Discounting.* Chemical Week, 1995. **156**(5): p. 14-14.

APPENDICES

APPENDIX A: Polymerization of itaconic acid with large quantity of initiator

Materials

Itaconic Acid; 2,2'-azodiisobytyronitrile(AIBN); hydrogen peroxide; Tertiary Butyl Hydroperoxide; ferric ammonium sulfate; toluene; Span 80; hydrochloric acid were used without further purification.

Synthesis A for Poly(itaconic acid) in aqueous solution (PIA A)

50g (0.385 mol) of itaconic acid was half neutralized with 15.4g (0.385 mol) sodium hydroxide, and was dissolved in 25ml deionized water into a flask, and 8 mg ferric ammonium sulfate was added. The mixture was heated to 80°C and 25ml tBHP (70wt% in water); 50ml H_2O_2 (35wt% in water) were fed by syringe pump for 2 hours, and heat was maintained for an additional 4 hours. The product was dried at 25°C under vacuum for 10 hours. Conversion is 100%

Synthesis B for poly(itaconic acid) by inverse emulsion polymerization (PIA B)

Mixture of 10g of itaconic acid, 40ml of deionized water, 0.0146g hydrochloric acid was placed in 500ml reactor, and then 2.5 g of Span 80 and 250ml toluene were added. The mixture was heated to 90°C to give a clear solution. 0.5g AIBN in 15ml acetone was fed by syringe pump over 24 hours. A sample was precipitated in acetone twice and dried for 10h at 25°C under vacuum. Conversion is 33%

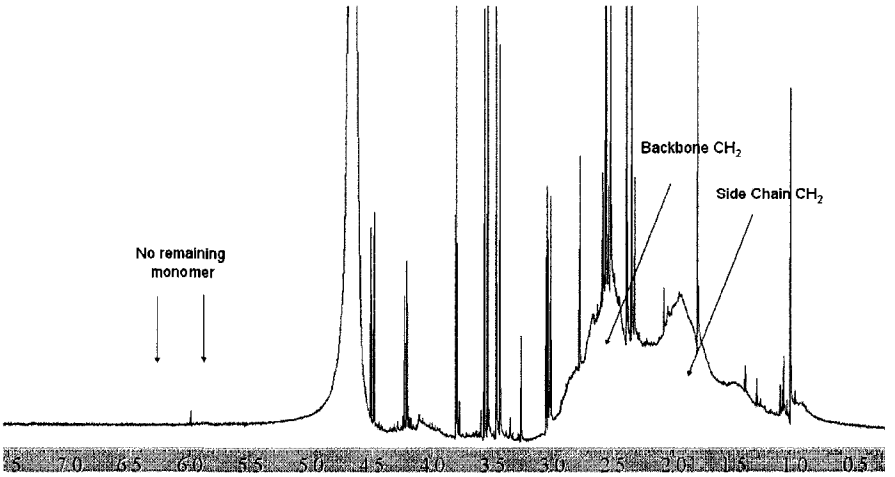

Figure 62 400-MHz ^1H NMR spectra of poly(itaconic acid) of D_2O solution(synthesis A).

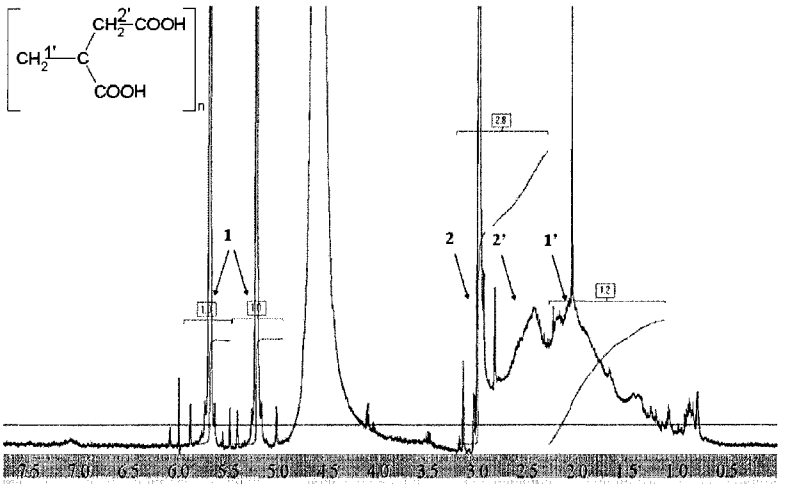

Chemical shift/ppm

Figure 63 400-MHz ^{1}H NMR spectra of poly(itaconic acid) of D_2O solution(synthesis B).

Synthesis C: for Poly(itaconic acid) in aqueous solution

50g (0.385 mol) of itaconic acid was half neutralized with 15.4g (0.385 mol) sodium hydroxide, and was dissolved in 25ml deionized water into a flask, and 8 mg ferric ammonium sulfate was added. The mixture was heated to 80°C and 25ml tBHP (70wt% in water) were fed by syringe pump for 2 hours, and heat was maintained for additional 2 hours. The product was dried at 25°C under vacuum for 10 hours. Conversion is 78%.

Synthesis D for poly(itaconic acid) by inverse emulsion polymerization

10g of Itaconic acid was half neutralized. Mixture of half neutralized itaconic acid, 40ml of deionized water and 2 mg ferric ammonium sulfate was placed in 500ml reactor, and then 2 g of Span 80 and 250ml toluene were added. The mixture was heated to 80°C to give a clear solution. 4g of tBHP in 8.54ml toluene solution was fed by syringe pump over 2 hours and heat was maintained for additional 2 hours. A sample was precipitated in acetone twice and dried for 10h at 25°C under vacuum. Conversion is 65%

Synthesis E for poly(itaconic acid) in aqueous solution

Itaconic acid was half neutralized with NaOH in DI-water with cooling by ice water, forming a concentrated solution, which was deoxygenized by purging with N_2, 4 mg ferric ammonium sulfate was added and then heated to the 100°C. 1ml 70wt% tBHP water solution was fed for 2 hrs and heat was maintained for additional 2 hrs. The final products were dried at 40 °C under vacuum (5mm Hg) for 10 hours. Yield is 58.2%.

APPENDIX B: Low conversion reaction for polyitaconic acid

1. Inverse emulsion polymerization

Mixture of 100ml toluene, 17.4g IA, 5ml water, 3.48ml 0.5g/mol water solution and 5.35g NaOH was placed into 250ml reactor. 1g of span80 was added. The mixture was heated to 60°C for 6hrs. 0% conversion was obtained.

2. Solution polymerization

Mixture of 50g IA and 250ml DI-water, 210microliter HCl was placed into 500ml reactor equipped with nitrogen feed and condenser. Redox initiator: 2.5g KPS and 1.7g Na2S2O5 was added at 90°C for 2 hrs. 0% conversion was obtained.

3. Solution polymerization

100g itaconic acid was totally neutralized with NaOH in DI-water with cooling by ice water. Solution was purged by nitrogen gas for 10 minutes and placed to 250 ml 3 neck reactor equipped with nitrogen feed and condenser. Then the mixture was heated to 100°C. 1ml tBHP was fed in 2 hours and 1 hour additional heat was applied. The conversion for final sample is 42.3%.

APPENDIX C: Elementary Analysis

Elementary analysis was preformed in Perkin Elmer 2400 to analyze carbon, hydrogen and oxygen percentage.

Sample No.	%C	%H
PIA-5	37.69	4.33
PIA-3	36.96	5.05
PIA-7	38.42	4.72
Perfect PIA	39.47	3.29

Table 10 Elementary analysis of PIA

APPENDIX D: Structure of Diaper

Above 90% of SAPs was applied in disposable diapers. Superabsorbent can be added into baby diaper with two methods[157-160]: layered and blended. As the figure shows, the superabsorbent beads are scattered in the fluff pulp. Fluff pulp was used to overcome the problem of slow absorbency generally for every kind of superabsorbents. Two layers of non-woven covered the top and bottom. Also, superabsorbent can be blended homogeneously with the fluff pulp.[147, 161]

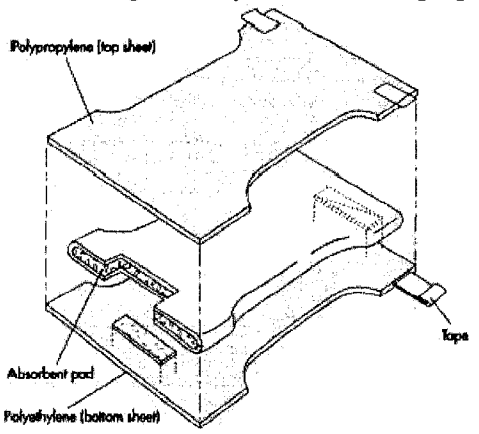

Figure 64 structure of commercial diapers

For the early baby diaper in 1980s, the SAP used in diaper was about 1-2 gram. Now, the amount of superabsorbent is 10-15 grams in each diaper. The bigger amount of superabsorbent is a compensate for thinner fluff pulp. The cost percentage of the SAP among diaper materials is about 30%.